

---

Masters

Engineering

---

2005-01-01

## Adequacy Assessment of the Irish Generation System Including Wind Capacity

William Carr  
*Technological University Dublin*

Follow this and additional works at: <https://arrow.tudublin.ie/engmas>



Part of the [Electrical and Computer Engineering Commons](#)

---

### Recommended Citation

Carr, W. (2005). *Adequacy assessment of the Irish generation system including wind capacity*. Masters dissertation. Technological University Dublin. doi:10.21427/D77W4V

This Theses, Masters is brought to you for free and open access by the Engineering at ARROW@TU Dublin. It has been accepted for inclusion in Masters by an authorized administrator of ARROW@TU Dublin. For more information, please contact [yvonne.desmond@tudublin.ie](mailto:yvonne.desmond@tudublin.ie), [arrow.admin@tudublin.ie](mailto:arrow.admin@tudublin.ie), [brian.widdis@tudublin.ie](mailto:brian.widdis@tudublin.ie).



This work is licensed under a [Creative Commons Attribution-Noncommercial-Share Alike 3.0 License](#)



# Adequacy Assessment Of the Irish Generation System Including Wind capacity

William Carr BEng  
School of Control Systems and Electrical Engineering,  
Dublin Institute of Technology

A thesis presented to Dublin Institute of Technology,  
Faculty of Engineering  
For the degree of  
Master of Philosophy

2005

Research Supervisor:

Dr. Michael Conlon

## Abstract

Adequacy assessment of generation capacity is a statistical measure of the ability of existing or planned generation plant to meet predicted levels of electrical demand. Complications arise in this calculation because at any point in time the exact level of capacity available is variable due to planned and forced outages. Planned outages is a term used to describe the period during the year when a generation unit is required to be shut down to allow for maintenance work to be carried out. The duration of this outage is normally known and its timing can be chosen. Forced outages describe the random failure that can occur that lead to a unit being shut down for repair. Due to the random nature of forced outages, regardless of the level of capacity in a system, 100% reliability cannot be guaranteed. The goal of this work is to investigate generation adequacy assessment in an Irish context. In this thesis the literature review in the area that was undertaken is outlined. Details of how the information gathered by this process allowed for the development of the data sets used in the investigation of generation adequacy are discussed. One of the principle sources of the information used in this process was the Generation Adequacy Report (GAR) that is published by Eirgrid each year.

The developed analytical and numerical methods were first applied to the IEEE reliability test system and then extended to the Irish generation system. Another of the principle aims of the project is to investigate the inclusion of wind capacity into generation adequacy assessment. To achieve this, a series of wind capacity models have been developed using data sets that have been acquired from Met Eireann and wind capacity production data from several Airtricity wind farms. The methodology behind and the various results from applying these different models are detailed.

## Declaration

I hereby declare that this submission is my own work and that, to the best of my knowledge and belief, it contains no material previously published or written by another person nor material which to a substantial extent has been accepted for the award of any other degree or diploma of a university or other institute of higher learning, except where due acknowledgement is made in the text

A handwritten signature in blue ink, appearing to read "William Lee", is written over a dotted line.

November 2005

## **Acknowledgements**

I would like to thank the following people without whom writing this thesis would not have been as enjoyable an undertaking. Firstly Dr. Michael Colon, my project supervisor, for his constant energy and drive over the course of the project and helpful criticism during the writing of this thesis. Michael Kelly and the other members of the adequacy assessment team in Eirgrid, Brian Hurley and Paul Hughes from Airtricity and Prof. Peter Lynch from the Dept. of Meteorology in UCD for generously donating their time to contribute their expertise and experience to the project. Also I would like to thank the other research students in the department namely Dan, Eileen, Jim, Mark, Niall, Owen, Pauline and Sharon for always being happy to discuss to a problem even when they didn't know the solution.

## TABLE OF CONTENTS

1	INTRODUCTION .....	1
1.1	PROJECT BACKGROUND.....	1
1.2	Thesis Outline .....	2
2	LITERATURE SURVEY .....	6
2.1	INTRODUCTION .....	6
2.2	HISTORICAL DEVELOPMENT .....	6
2.3	INCORPORATION OF WIND CAPACITY INTO GENERATION ADEQUACY ASSESSMENT.....	7
2.4	SIMULATION OF WIND SPEED DATA FOR ADEQUACY ASSESSMENT CALCULATIONS .....	11
2.5	CONCLUSION.....	12
3	INTRODUCTION TO ANALYSIS TECHNIQUES .....	14
3.1	INTRODUCTION .....	14
3.2	LOAD MODELS .....	15
3.3	CAPACITY MODELS .....	16
3.4	IEEE RELIABILITY TEST SYSTEM.....	19
3.4.1	IEEE-RTS Load Model.....	19
3.4.2	IEEE-RTS Capacity Model.....	20
3.4.3	LOLE and LOEE calculation for the IEEE-RTS.....	21
3.5	MAINTENANCE SCHEDULING.....	22
3.6	MONTE CARLO METHODS.....	32
3.6.1	Monte Carlo Simulation.....	32
3.6.2	Maintenance Scheduling .....	34
3.7	CONCLUSION.....	36
4	EXTENSION OF ANALYSIS TO THE IRISH SYSTEM.....	38
4.1	INTRODUCTION .....	38
4.2	LOAD MODEL .....	40
4.3	CAPACITY MODELS .....	44
4.3.1	Deterministic Capacity Model .....	44
4.3.2	Monte Carlo Capacity Model.....	46

4.4	RESULTS OF ADEQUACY CALCULATIONS ON THE IRISH SYSTEM EXCLUDING WIND CAPACITY.....	48
4.5	MODEL VERIFICATION.....	51
4.6	INCLUSION OF WIND CAPACITY .....	55
4.6.1	Elevated FOR Wind Capacity Model .....	55
4.6.2	Wiebull Load Modifier Wind Capacity Model.....	57
4.7	CONCLUSION.....	59
5	INVESTIGATION OF WIND DATA.....	61
5.1	INTRODUCTION .....	61
5.2	WIND SPEED DATA .....	61
5.2.1	Mean And Standard Deviation Of Wind Speed Data .....	61
5.2.2	Probability Distribution.....	66
5.2.3	Variation Analysis.....	66
5.2.4	Auto- And Cross-Correlation.....	67
5.2.5	Frequency Domain Analysis.....	70
5.3	WIND PRODUCTION DATA.....	75
5.4	CONCLUSION.....	77
6	TIME SERIES METHODS .....	78
6.1	INTRODUCTION .....	78
6.2	INTRODUCTION TO TIMES SERIES MODELS .....	78
6.3	PURPOSED DEVELOPMENT OF WIND MODELS .....	83
6.3.1	Data Normalisation .....	84
6.3.2	Separating the Data Components.....	85
6.3.2.1	Time domain removal of dominant elements over total sample .....	86
6.3.2.2	Time domain removal of dominant elements by frequent analysis ...	90
6.3.3	Modelling Stochastic Elements.....	93
6.3.4	Generation Of Simulated Series.....	96
6.4	SIMULATED WIND SPEED SERIES .....	97
6.5	INTER SITE CORRELATION .....	101
6.6	CONCLUSION.....	104
7	EVALUATION AND APPLICATION OF WIND SPEED MODELS .....	105
7.1	INTRODUCTION .....	105

7.2	WIND SPEED TO WIND POWER CONVERSION.....	105
7.2.1	Wind Height Adjustment .....	105
7.2.2	Association Of Wind Capacity To Wind Speed Series.....	107
7.2.3	Wind Turbine Model.....	109
7.3	APPLICATION OF TIME SERIES WIND CAPACITY MODEL .....	111
7.3.1	Comparison of various wind capacity models .....	112
7.3.2	Calculation of Risk-Based Capacity Credit .....	114
7.3.3	Effect of inter-annual variations on LOLE calculations .....	115
7.4	CONCLUSION .....	117
8	CONCLUSIONS AND FUTURE WORK .....	119
8.1	CONCLUSIONS.....	119
8.2	FUTURE WORK.....	122
	REFERENCES.....	123
	Appendix A UPEC Bristol 2004.....	128
	Appendix B UPEC Cork 2005 .....	135
	Appendix C: Generation Capacity Predictions 2005-.....	142
	Appendix D: Ten-Year Periodograms of Normalised Data.....	144
	Appendix E: Fitted ARMA models .....	145



## TABLE OF FIGURES

Figure 1: Hierarchical diagram of electrical system .....	1
Figure 2: Daily peak loads of the IEEE-RTS load model.....	19
Figure 3: Calculated cumulative probability of the IEEE-RTS .....	21
Figure 4: Change in the capacity reserve before and after maintenance.....	25
Figure 5: Plot of the weekly capacity on maintenance outage.....	26
Figure 6: Weekly contribution to the LOLE .....	28
Figure 7: Change in the calculated LOLE before and after the maintenance correction .....	29
Figure 8: Weekly capacity outage due to scheduled maintenance.....	30
Figure 9: Contrast of the weekly contributions made to LOLE.....	31
Figure 10: Two state model of generation unit .....	33
Figure 11: LOLE calculated over the sample period .....	34
Figure 12: 3-state model of generation unit .....	35
Figure 13: Plot of the four applied load shapes.....	40
Figure 14: Top 5% of the LDC of the recorded load data .....	41
Figure 15: Hourly percentage LOLE contribution.....	43
Figure 16: Running total of percentage LOLE contributions .....	43
Figure 17: GAR 04-10 predictions.....	44
Figure 18: Recorded data .....	44
Figure 19 Comparison of results .....	49
Figure 20: 2005 results with extended sampling period .....	50
Figure 21: Plot of the LOLE values calculated from scenario one .....	52
Figure 22: Plot of the LOLE values calculated from scenario two.....	53
Figure 23: Plot of the result from Table 6.....	56
Figure 24: Plot of results found for the different variations in wind capacity model ....	57
Figure 25: PV characteristic of a generic wind turbine.....	58
Figure 26: Comparison of Elevated FOR and Weibull load modifying methods.....	59
Figure 27: Annual mean wind speed values .....	62
Figure 28: Percentage annual variation from mean .....	63
Figure 29: Monthly mean wind speed values .....	63
Figure 30: Probability distributions calculated for the six sites.....	66
Figure 31: Plot of the percentage variation on three different time horizons from the Malin Head data .....	67

Figure 32: Annual cross correlation coefficients .....	69
Figure 33: Auto-correlation functions of the six sites.....	70
Figure 34: Normalised version of the original data .....	71
Figure 35: Periodogram of the normalised sample data.....	71
Figure 36: Adjusted periodogram of the normalised sample data .....	72
Figure 37: Periodogram of normalised data from Nov. 95 to Oct. 96 .....	72
Figure 38: Periodogram of normalised data from Nov. 98 to Oct. 99 .....	73
Figure 39: Periodogram of normalised data from Nov. 94 to Oct. 04 .....	73
Figure 40: Periodogram of normalised Valentia data from Nov. 94 to Oct. 95.....	74
Figure 41: Periodogram of normalised Valentia data from Nov. 95 to Oct. 96.....	74
Figure 42: Periodogram of normalised Valentia data from Nov. 99 to Oct. 04.....	75
Figure 43: Duration of the available wind power series .....	76
Figure 44: Diurnal patterns in wind production data .....	77
Figure 45: Plot of the original recorded wind speed.....	84
Figure 46: Probability density function of data .....	84
Figure 47: Normalised version of the original data .....	85
Figure 48: Periodogram of sample data .....	86
Figure 49: Effect of method on the periodogram.....	87
Figure 50: Closer view on the target frequency .....	88
Figure 51: Average terms.....	88
Figure 52: Resulting periodogram after averaging method was applied .....	89
Figure 53: A closer view of the resulting periodogram after averaging method was applied .....	89
Figure 54: Plot of the resulting series after averaging method was applied .....	90
Figure 55: Level of reduction seen in the dominant peak .....	91
Figure 56: Closer view of the level of reduction seen in the dominant peak.....	91
Figure 57: Resulting periodogram after Fourier method was applied .....	92
Figure 58: Closer view of the periodogram after Fourier method was applied .....	92
Figure 59: Comparison of auto correlation functions .....	93
Figure 60: Comparison of observed and model generated auto-correlation functions ..	95
Figure 61: Probability distribution of the residuals.....	95
Figure 62: Correlogram of the residuals .....	96
Figure 63: Comparison of recorded and simulated series inter-annual.....	98
Figure 64: Comparison of recorded and simulated series seasonal indicator .....	99

Figure 65: Comparison of recorded and simulated series periodograms.....	101
Figure 66: Comparison of recorded and simulated inter-annual variation in correlation coefficient.....	104
Figure 67: Map of the regional divides and the location of each of the weather stations courtesy of Sustainable Energy Ireland.....	108
Figure 68: Contrast of single and multi-turbine PV characteristics.....	110
Figure 69: Contrast calculated power series using a single and multi-turbine method	111
Figure 70 Plot of results from various wind capacity models.....	112
Figure 71: Convergence path of Monte Carlo calculations including upper and lower boundaries .....	116
Figure 72: Results of extending calculation over the period to 2011 .....	117
Figure 73: Result of applying increasing wind penetration under the same conditions .....	117

## TABLE OF TABLES

Table 1: COPT for the above example.....	17
Table 2: Details of the IEEE-RTS generation unit's capacities and FOR .....	21
Table 3: Calculated and published figures of the IEEE-RTS and the percentage error.	22
Table 4: Maintenance requirements of the units in the IEEE-RTS.....	23
Table 5: Weekly breakdown of when each unit is out on scheduled maintenance.....	26
Table 6: Calculated and published results and the percentage error between them.....	28
Table 7: Weekly breakdown of when each unit is out on scheduled maintenance.....	29
Table 8: Comparison of results from analytical and Monte Carlo methods .....	34
Table 9: Comparison of results between published and Monte Carlo simulation .....	36
Table 10 Comparison of results from analytical and Monte Carlo methods .....	36
Table 11: Recorded load data TER and peak values.....	41
Table 12: GAR 04-10 predicted growth rate and model peak and total demand.....	42
Table 13: Predicted availability and calculated FOR.....	46
Table 14: Calculated values of LOLE for the Irish system using deterministic method	48
Table 15: Calculated values of LOLE for the Irish system using Monte Carlo method	49
Table 16: Comparison of results .....	49
Table 17 Plot of the LOLE values calculated from scenario one .....	51
Table 18: Values of LOLE calculated for scenario two.....	52
Table 19: Comparison of Calculated LOLE values to GAR 05-11 in capacity terms...	54
Table 20: Values calculated using elevated FOR wind capacity model .....	55
Table 21: Results from the application of the elevated FOR and Weibull load modifying methods .....	58
Table 22: Annual mean wind speed values.....	62
Table 23: Calculated value of seasonality indicated.....	64
Table 24: Standard deviations found in data set .....	65
Table 25: Calculated standard deviations divided by the mean for the same period.....	66
Table 26: Mean cross correlations coefficient calculated .....	68
Table 27: Wind farm information .....	76
Table 28: Calculated statistical data.....	85
Table 29: Comparison of recorded and simulated series annual mean wind speed.....	97
Table 30: Comparison of recorded and simulated series standard deviations .....	100

Table 31: Comparison of recorded and simulated series correlation coefficient matrices ..... 103

Table 32: Roughness length classification definitions..... 106

Table 33: Breakdown of predicted wind capacity associated with each weather station ..... 109

Table 34: Result of various wind capacity models ..... 112

Table 35: Comparison of results with and without correlation relationship..... 114

Table 36: Risk-based capacity credit estimates calculated ..... 115

# 1 INTRODUCTION

## 1.1 PROJECT BACKGROUND

An electrical system for the purposes of quantitative reliability assessment can be considered as a three level hierarchical structure as in Figure 1 [1]. The functional zones within this structure are generation, transmission and distribution. In hierarchical level one (HLI) reliability evaluation the total system generation is compared to the total system load. This type of calculation is also termed generation adequacy assessment. In hierarchical level two (HLII) calculations the ability of the transmission system to transport the generated energy to the customer load centres are factored into the reliability calculation. For hierarchical level three (HLIII) as the distribution system is also under consideration a system-wide reliability calculation is not normally attempted due to the complexity and scale of the distribution system.

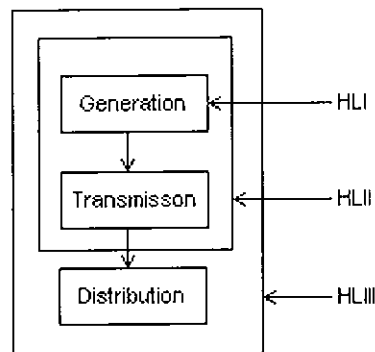


Figure 1: Hierarchical diagram of electrical system

Adequacy assessment of generation capacity is a statistical measure of the ability of existing or planned generation plant to meet predicted levels of electrical demand. Complications arise in this calculation because at any point in time the exact level of capacity available is variable due to planned and forced outages. Planned outages is a term used to describe the period during the year when a generation unit is required to be shut down to allow for maintenance work to be carried out. The duration of this outage is normally known and its timing can be chosen. Forced outages describe the random failure that can occur that lead to a unit being shut down for repair. The duration and timing of forced outages cannot be exactly predicted but from the age, type and outage

history of a unit, approximate values of the mean time to failure (i.e. average number of hours that a unit will operate before it is expected to go on forced outage and the mean time to repair i.e. average number of hours taken to bring the unit back online) can be derived.

It is normal practise the mean time to failure and repair is expressed as one figure. This figure describes a unit's probability of being on forced outage at any time and is known as the unit forced outage rate or FOR. Due to the random nature of forced outages, regardless of the level of capacity in a system, 100% reliability cannot be guaranteed. From experience the electricity industry has developed a generation adequacy standard. If generation adequacy is outside this standard then there is considered to be an unacceptable level of risk that supply will be unable to meet demand. It is possible to use adequacy assessment techniques to calculate the level of future generation required to maintain the system within standard.

## **1.2 Thesis Outline**

The overall goal of the project is to investigate generation adequacy assessment in the context of the generation system of the Republic of Ireland (R.O.I.). Initially the scope of the project was investigated through a review of the current generation adequacy methods being used in the generation system of the R.O.I. and using this, the aims of the project was mapped out. There is a wide range of different methods used in the assessment of generation adequacy. These methods can be divided into two groups: analytical methods and numerical or Monte Carlo methods. Analytical methods use mathematical models to enumerate and combine the probabilities of the system's states to form the required reliability indices. Monte Carlo methods operate by attempting to simulate the operating characteristics of the system's components so that the required reliability indices can be calculated by experimentation. Currently, analytical methods are the predominant tools used to assess the level of generation adequacy in the generation system of the R.O.I. The initial goal of this project is to develop and apply analytical methods, which would serve as a benchmark for future work. The next step in doing this was to review the literature in the area and the information gathered by the literature review allowed for the development of the data sets required to make this calculation. The outcome of this literature survey is given in Chapter 2.

The analytical and Monte Carlo methods were first applied to the IEEE reliability test system and then extended to the generation system of the R.O.I. One of the principle sources of information used in extending the developed methods to the generation system of the R.O.I, were the Generation Adequacy Reports which are published by Eirgrid each year. The development of adequacy calculations on the IEEE-RTS is detailed in Chapter 3.

Analytical calculations of generation adequacy assessment can be seen as the combination of two statistical models. The first is a model of the system's expected load and this model is constructed normally by taking the recorded values of the system levels of demand from previous years. By averaging these values on an hourly basis the average load shape of the system is modelled. Predictions for the year on year growth in demand are based on economic forecasts, as there is a long established relationship between the levels of energy demands and economic growth. In Republic of Ireland (R.O.I.) these forecasts are produced by the ESRI. These levels of year on year growth are used to scale up the average load shape to the predicted levels of electrical demand.

The second model is of the expected levels of generation capacity. The current and planned electrical plant is expected to provide. As discussed above each unit can be defined by two properties, its capacity and FOR. Using these two properties for a system of  $n$  units it is possible to define the probability of the system capacity being at any of its possible levels at any time. This forms the basis of the model of system capacity and the resulting table is known as the capacity outage probability table or COPT. Once these two models are developed they are combined and used to derive statistical indices upon which the assessment of the adequacy of the system is made. There are two principal indices named the loss of load expectation or LOLE and the loss of energy expectation or LOEE. The LOLE is a statistical measure of the likelihood of failure of supply to match demand i.e. the expected number of hours that the available plant will be unable to match the load. The unit of LOLE is hours/year. The generation adequacy standard that was mentioned earlier is quoted to terms of the LOLE and is 8 (hrs/yr) in the generation system of the R.O.I. The LOEE is a similar index that records the quantity of energy that is expected to be unsupplied to the load, it has units of (kW-hr/year).



With the analytical method established the focus of the project shifted to the development of Monte Carlo methods. Again, a model of the system's expected load is created as before but the capacity of the system is not calculated on a basis of probability. Instead, initially all the units are considered to be operating and random draws are made from an exponential distribution that is centred on the mean time to failure of the unit. The result of this is the number of hours until the unit will fail. Once the unit does fail another random draw, this time centred on the unit mean time to repair is made. This process is repeated for each unit over the course of the year and in this way the capacity of the system at anytime is the sum the units that are operating. This capacity model is then compared to the load model and the adequacy indices calculated directly with the LOLE being equal to the number hours in the year that the capacity was less then the load and the LOEE being the summation of the difference between the load and the capacity in these hours. The values the adequacy indices calculated for a year will depend on the results from the random draws taken over the course of that year but it is found that by looping the program so that the calculation is repeated (so that the final state for one becomes the initial state of the next) that the mean values of the adequacy indices calculated convergence to the analytically calculated value as the number of iterations is increased. In Chapter 4 the extension of the developed adequacy calculation methods to the Irish system is addressed.

From the beginning of the project one of the key areas of interest was to assess wind capacity models used in generation adequacy calculations. Several different simplistic wind modelling methods were developed. However by applying these methods to adequacy calculations under a variety of different scenarios it became clear that these wind modelling methods where not adequate to capture the full impact of wind capacity on the adequacy of a system. In order to do this it would be necessary to form a model that would combine the ability to capture both the stochastic and periodic elements of the wind resource. To do this a data set of wind speed data was acquired from Met Eireann. In Chapter 5 the properties of this data set are investigated. The wind modelling method developed uses the assumption that wind can be characterised by its periodic and stochastic element. The development of this model is discussed in Chapter 6. The objective of this model is to form possible wind series that could occur at the site where the original is recorded. This model is then incorporated into a Monte Carlo

based calculation. The wind modelling methods are applied to the Irish system and the results then calculated are discussed in Chapter 7. In Chapter 8 some conclusions are drawn from the work and areas of future work are outlined. During the course of this project the models and calculations have been performed using MATLAB version 6.5 release 12 with secondary calculations and plotting made using Microsoft Excel 2000.

The project was undertaken against the background of rapidly increasing wind capacity penetration into the Irish generation system. This rapid increase in wind penetration has resulted in fears that the inherent variability of the wind regime will result in a threat to the security of supply if its growth continues unfettered. In this project the impact of wind capacity on the adequacy of the generation system is independently explored and quantified. The models and methodologies applied and developed in the course of this project have been reported in two conference papers which can be seen Appendix A and B.

## **2 LITERATURE SURVEY**

### **2.1 INTRODUCTION**

This chapter presents the results of a survey of the literature relating to the adequacy assessment of generation capacity. The first section deals with the early development of the area of adequacy assessment. The second section looks at the different methods that have been developed to incorporate wind capacity into adequacy assessment and the third section discusses the simulation of wind speed data for adequacy assessment calculations. These three sections are representative of the logical and chronological progression of the project. The first section arose from the start of the project when a general review of adequacy assessment and its development was undertaken. The second section came from a similar undertaking when the question of including wind capacity in adequacy assessment calculations was first considered. While the third section resulted from research into a specific area covered in section two. None of the sections below can claim to be a complete review of the work done in their specific areas. But it is felt that references chosen are representative of the literature that exists in each area.

### **2.2 HISTORICAL DEVELOPMENT**

The application of probability based analysis to generation capacity problems can be traced back as far as the 1930's when the concept was first introduced by [2] and then later by [3] where probability theory was applied to determine the level of reserve capacity that a system should maintain given the make up of its generation portfolio. In 1947 a group of papers were published which discussed reliability as the probability that an outage of generating capacity would exceed the reserve available at the time of peak load. This problem was complicated by a variety of factors such as the effect of daily and seasonal load shapes, of maintenance outages, of interconnections and of uncertainties in load forecasts.

These complications and the criteria for reliability applied differed between authors. In [4] reliability was determined by the computation of the interval in years between outages of various magnitudes. While [5] presents a short-cut method for computing

probability of outages of any given magnitude, [6], [7] discuss the combined probability of outage with peak durations to determine the probability that the load might exceed the available capacity. In [6] the calculations were extended to determine the kilowatt-hours of load that might be interrupted and then to provide an index of the possible loss of energy which is related to some dimension representative of the system size. In [7] also considered are the calculation of the probable duration and interval of multiple outages.

The increasing availability of digital computers reduced the manual burden in making probability calculations and lead to their increased use. In 1958 another group of papers in the area were published. The methods presented in [8], [9] had several similarities to [4] in that the interval between outages rather than the probability of these outages occurring that is the focus of the calculations. In [10], [11], [12],[13] the probability that the load would exceed the available capacity is the measure of reliability calculated while in [14] a kilowatt-hours measure of reliability is used similar to [6].

This three set of papers represent the foundations for the three principle approaches taken in generation reliability. They are termed frequency and duration for power system reliability calculations, loss of load probability expectation and loss of energy probability or expectation. Each of these three types of methods have been continually expanded and developed to incorporate all the facets of generation systems. An extremely extensive bibliography exists of the work that has been done in the development and application of probabilistic techniques for power system reliability evaluation. A subsection within this bibliography deals with the area of generating capacity reliability evaluation. The bibliography has been developed in a series of papers [15], [16], [17], [18] by a group under the leadership of Billinton.

### **2.3 INCORPORATION OF WIND CAPACITY INTO GENERATION ADEQUACY ASSESSMENT**

For many years wind capacity was not considered to have any impact on system adequacy. In general wind capacity was ascribed an energy credit but no capacity credit. The reasons for this being that wind capacity installations were relatively small and

connected at distribution level. In recent years the rate of growth in the scale of wind capacity seen in many electricity networks around the world and the increasing trend for connection at transmission level has led many authors to consider methods of determining the level of capacity credit that should be given to wind capacity and its inclusion into traditional adequacy assessment calculations.

In [19] two methods of including wind capacity into adequacy assessment calculations are outlined; the multi-state unit and load adjustment approach. In the multi-state approach wind capacity is represented as a supply-side unit containing partial capacity states. In the load adjustment approach wind capacity is accounted for by subtracting the energy it produces from the load model using a generation capacity distribution. Also in [19] the multi-state method is applied to a numerical example using the IEEE reliability test system and a number of sensitivity tests are performed. In [20] the capacity credit that should be attributed to wind capacity is discussed. Capacity credit is a term that is used to describe the reliability of a conventional unit but in terms of renewable capacity it is the amount of conventional generation that can be offset by the renewable production, without making the system less reliable. In [20] the author suggests two methods to calculate capacity credit. The first uses capacity factor as an approximation to capacity credit, with capacity being defined as the ratio of the sum of energy production for a given period to the ideal energy production for the same period, where capacity factor is arbitrarily calculated over only the first 50% of the load duration curve. The reason given for only using the first 50% of the load duration curve is that power is only as valuable as it is available when it is required. Therefore it is decided that only the peak load hour should be included in the calculation. The second method calculates capacity credit, as the difference in the conventional capacity before and after the capacity is included so that the probability of the system capacity being greater than the load remains the same. Both methods are applied to case studies and in [20] the author concludes that the first method is suited to post installation evaluation for system operation purposes whereas the second is suited to system planners to calculate the amount of conventional generation that wind capacity could offset.

In [21], two risk based indices are introduced. These indices are used as an indication of the effect of wind capacity on the system in terms of peak load carrying capability. The two indices are termed load carrying capacity benefit ratio (LCCBR) and equivalent

capacity rate (ECR). The LCCBR indicates the per unit incremented peak load that the system can carry due to the addition of wind capacity. ECR provides a risk-based equivalence between conventional and wind capacity. In [21] the simulation methods required to form these statistics are explained and highlighted by numerical example. In [22] the effects of various wind turbine parameters including cut in, cut out and rated wind speed on the system adequacy are investigated in terms of the load carrying capacity benefit ratio. The analysis is done using a method that is discussed in [23]. This method uses an auto-regressive moving average (ARMA) model fitted to a recorded wind series to generate simulated wind series that are similar to the recorded wind series in terms of chronological wind velocity characteristics. The simulated wind series are converted into power series by applying them to a typical wind turbine power-velocity curve, the parameters of which are specified by the author. Each of the wind power series is used as a load modifier in one year of a Monte Carlo generation adequacy calculation. This method is used by the author to assess the contribution of wind capacity to the system reliability in terms of its effect on LOLE levels calculated.

The capacity value of wind capacity and methods to evaluate it are considered in [24]. The methods discussed are based on comparing the wind capacity to another unit that is used as a standard of measure. The author suggests incorporating wind capacity into loss of load probability (LOLP) calculations using either an elevated forced outage rate (FOR) representation or a chronological load modifying method. The LOLP calculated forms the basis of finding the effective load carrying capacity (ELCC), which is used as an approximate measure of capacity credit in terms of an ideally reliable unit. A caveat of this approach is the dependence of LOLP calculations on the systems peak load hours. If the wind capacity model is based on a single year of records then the results may be biased. Therefore the author concludes that there is a need to differentiate between operational and planning capacity credit. For the planning horizon the LOLP/ELCC gives a good indication of average values but on the operational horizon, capacity credit should be more closely related to weather forecasts.

In [25] modelling wind capacity as supply side units is investigated and a method of calculating a time varying equivalent forced outage rate for wind capacity is discussed. The approach uses an hourly wind power series. The equivalent forced outage rate for each hour is found by centring a window, the length of which is user-defined, on that

hour and subtracting for one the ratio of the sum of the output inside the window by the ideal output for the period. When this calculation is complete, an FOR figure is available for each hour. When the LOLE is being calculated these values are folded into the capacity outage probability table similar to the conventional units. The benefit of this method is that it simultaneously represents the stochastic nature and the variance of the wind resource. An addition to this technique is to allow the wind to be represented as a multi-state unit. In [25], the author suggests that to do this the sliding window could be reformed into a frequency distribution table and each hour convolving with each row of the table containing the relative frequency and the wind power output into the capacity outage table. The author does not specify a optimal length for the sliding window but does note that if the sliding window is reduced to one hour then applying this method to an LOLE calculation would give the same result as applying the wind power series as a load modifier. Similarly if the window was extended to the length of the year the result would be the same as making the FOR equal one minus the capacity factor.

In [26] the effect of the load duration curve (LDC) modelling in a typical production cost calculation on the value attributed to intermittent generation by comparison to a chronological model. In drawing this comparison the author introduces a wind capacity model that considers wind capacity as a supply side unit with a time dependent probability distribution. After applying the method to two case studies, the author concludes that LDC model can offer similar measurements of the value of wind generation to the chronological model but that some questions cannot be answered due to the lack of time resolution. Similar conclusions are drawn in [27] where more extensive case studies are used to investigate the same questions.

The variance of the capacity credit values that arise from calculations based on single year wind records using the ELCC method are investigated in [28]. To do this the author uses a Markov process to generate the required wind power series from a year of recorded data. The Markov process is designed to capture some of the time scale properties and an estimate of the variance in the recorded data. The simulated data is then applied to an ELCC calculation that is used as an approximation of capacity credit attributed to wind capacity vary reasonably widely year on year. In [29] this approach is again taken to the same question but this paper the simulated data is based on a 13-year

wind record. In this paper it is concluded that while the simulated data results in a considerable improvement over single year estimate techniques, the inter-annual variation in capacity credit is still understated by the simulated data.

In [30] and [31] the author introduces a reduced enumerated probabilistic approach (REPA) to long-term wind capacity credit calculation. The basic technique uses simulated wind speed data generated by a Markov process applied to an ELCC calculation. However in this case the generated wind series are sorted into representative groups in terms of the energy that they would produce so that the variation in the grouped data closely represents the variation seen in the ungrouped data. The method is applied to a case study, which allows the author to conclude that the REPA is a computationally efficient way to find estimates of the wind capacity credit.

The ELCC method is compared with less computationally intense methods such as approximating capacity credit to capacity factor in [32]. Different methods of choosing the hours on which the capacity factor is calculated are investigated. From the results obtained it is concluded that capacity factor tends to underestimate the ELCC value and also is very sensitive to the number of hours used and the method used to select them.

## **2.4 SIMULATION OF WIND SPEED DATA FOR ADEQUACY ASSESSMENT CALCULATIONS**

As mentioned above in [28] and [29] the author is attempting to extrapolate multiple years of wind speed series from a single year of data by applying a Markov process. A Markov process is a discrete time stochastic process that adheres to the Markov principle, which requires that the conditional probability distribution of the future of the process given the present state depends only on the current state i.e. that it is conditionally independent. The matrix of the transitional probabilities is formed by counting the number of transitions from state  $i$  to state  $j$  and then dividing by the total number of transitions from state  $i$ . To generate simulated wind speed there are a number of methods suggested, all of which involve assuming an initial state. Then the drawing of a random and using this in comparison to the state transition matrix to determine the next state. In [28], [29] the authors suggest that once the transitional matrix has been



developed an initial  $i$  state is selected and then a random number between zero and one is drawn. If this number is less than the first element of the  $i^{\text{th}}$  row then the next state is State1. If the number drawn is greater than the first element in the  $i^{\text{th}}$  row and lower than the sum of the first two elements then the next state chosen is State2. If the number chosen is greater than the sum of the first two elements but less than the first three elements then the next state is State3, etc. The process is repeated to find further states using the latest as the initial state.

Another method which is applied to this problem is detailed in [33] uses a time series model to generate hourly wind speed estimates. The author suggests the use of an auto-regressive moving average (ARMA) model. The auto-regressive element of the model considers the degree to which each hour of the data is dependent on previous values while the moving average element is a type of random walk where in each hour a number is chosen randomly and combined with previously chosen values.

This type of model presents two different challenges. The first is to decide the order of the model's two component elements and secondly to estimate the parameters of these elements. To reduce the complication in determining the order of the model the authors in [33] consider the wind to be a stationary stochastic process. This means that the underlying process can be closely approximated by a model of the order ARMA ( $n, n-1$ ). This means the order the auto-regressive element has  $n$  terms and therefore  $n$  parameters to be chosen and likewise the moving average element has  $n-1$  terms and therefore  $n-1$  parameters. The order of the model can be found by determining the most appropriate value of  $n$ . To do this  $n$  is set to two and the parameters for that order of model chosen using non-linear least squares methods. Then the residual sum of squared errors is calculated, this process is repeated for  $n$  equal to three. The F-criterion is then applied to investigate if increasing the order of the model from two to three has improved its performance significantly. If not then the order of the model is set to two, otherwise  $n$  is set to four and the process repeats until the optimal value of  $n$  is found.

## **2.5 CONCLUSION**

From the survey of the literature it was seen that three methods of estimating the adequacy of a generation system have evolved namely: the loss of load expectation, the

loss of energy expectation and the frequency and duration method. It is felt the combined application of the first two of these methods gives the best insight into the adequacy of a generation system and for this reason these methods will be applied in the following work. The different methods outlined for the incorporation of wind capacity into generation adequacy assessment calculation arise when the wind resource is considered as a probabilistic or stochastic process. A case can be made for both of these positions depending on the time horizon applied. For this reason methods to include wind capacity into generation adequacy assessments that are based on both sides of this consideration will be examined further during the course of this work. Depending on the data set available and the type of calculation being undertaken it can be necessary to attempt to extrapolate multiple years of wind speed data from a single year of data. Two methods of approaching this problem have been discussed. The Markov method does offer an effective method to generate simulated wind data. However, as the nature of the Markov method enforces the conditional probabilities of the source data onto all of the simulated data, the time series approach using ARMA models will be applied in the following work.

## 3 INTRODUCTION TO ANALYSIS TECHNIQUES

### 3.1 INTRODUCTION

The two principal indices that form the main focus of adequacy calculations are the loss of load expectation (LOLE) and the loss of energy expectation (LOEE). The LOLE is a statistical measure of the likelihood of failure of supply to match demand i.e. the expected number of hours that the available plant will be unable to match the load. The LOEE is a similar index that records the quantity of energy that is expected to be unsupplied. These indices can be defined as:

$$LOLE = \sum_{d=1}^D \sum_{h=1}^H \text{Prob}(G_{hd} < L_{hd}) \quad (3.1.1)$$

$$LOEE = \sum_{d=1}^D \sum_{h=1}^H (L_{hd} - G_{hd}) \quad (3.1.2)$$

where:  $L_{hd}$  = the load at hour  $h$  on day  $d$

$G_{hd}$  = the generation plant available at hour  $h$  on day  $d$

$H$  = the number of loads/day to be examined

$D$  = the number of days/year to be examined

From these formulae it can be seen that there are two aspects of the system that need to be modelled in order to calculate both the LOLE and LOEE; the first is the system load model, which is used to specify load requirements characteristic of the system. This model is generally based on recorded load levels. The model can be one of two different types, either representative or chronological. The formation of these different types of load models and the different effects that they have on the adequacy calculation will be discussed in Section 3.2.

The second aspect of the system that needs to be modelled is the ability of the system to match the level of capacity requirement specified by the load model. Ideally the system's capacity model would be constant i.e. at any time the available production

level would be equal to the installed capacity but this situation is complicated as it is not possible to know if or when a generation unit will break down or go on forced outage. But through experience it is possible to estimate the rate at which a particular unit will go on forced outage by considering the units outage history and also its type and age. This rate is normally calculated as in Equation (3.1.3) and is called the forced outage rate (FOR).

$$FOR = \frac{MTTR}{MTTR + MTTF} \quad (3.1.3)$$

where: MTTR = mean time to repair

MTTF = mean time to failure

A table is drawn up which combines the FOR and the capacity of all the units operating in the system to specify all of the possible capacity states the system can be in and probability of their occurring. This table is known as the cumulative outage probability table or COPT and can be calculated by a range of different methods. The COPT forms the basis for the capacity model of the system. The different methods of developing the COPT are discussed in Section 3.3.

### **3.2 LOAD MODELS**

As mentioned above, the two types of load models used in adequacy calculation are chronological and representative. The chronological model is the more straightforward of the two; a chronological model is based on forming hourly load predictions for the duration of the calculation, the time period used is typically one year. The most common method of developing a chronological model is to use hourly loads records to develop a typical load shape characteristic of the system. This can then be developed depending on the type of scenario that is being considered in the adequacy calculation. For example if the adequacy calculation is being used to investigate the adequacy of a system in the upcoming years then each hour of the developed load shape can be scaled by the expected growth factor for the system energy requirement. If there is a clear linear relationship between the total energy requirement (TER) of the system and the

peak load in the system, the load model can be made to reflect this by setting the scaling factor to be a function of the value of the load shape.

The second type of load model is a representative model. Representative models are based on forming load duration curves using records of hourly loads by sorting the load by demand levels. Typically two load duration curves would be generated representing both a peak and off peak period for the system. These load duration curves could be based on as little as a week of data. The adequacy calculation would then be applied to these load duration curves. Each week in the year would then be categorised as either being a peak or off peak week, in this way the results found from the calculation being applied to the load duration curves allowing results for the whole year to be extrapolated. The application of representative load model to different types of scenarios is similar to chronological models. The advantage of representative models is that the computational effort required to perform adequacy calculations is much less than with chronological models. There is also a relatively small reduction in the overall accuracy of the calculation reported [34]. While at the time of their development this represented a significant advantage, the developments since that time in the availability of processor power has led to a reduction in their application.

### **3.3 CAPACITY MODELS**

The objective of the capacity model is to define the probability of the system being in any of its possible capacity states. To do this each of the units are considered to have a discrete probability distribution associated with its FOR. It is also generally assumed that outages of different units are independent. This assumption can be called into question. For example failure of gas turbine plant due to a disruption in gas supplies. However the strength of the conditional probability linking the failures of conventional plant is considered to be weak enough to disregard. Also it is assumed that if a unit is operational that it will be available if required. It is possible that a unit could be operational but not available i.e. if it had not been dispatched in many hours a unit may have been allowed to cool and so would take several hour notice to be made available. These distributions are convolved to form the COPT. To do this, several different methods (both direct and approximate) have been developed.

The recursive method [35] uses a recursive formula to perform the convolution integral on the individual distributions. Initially there are no units in the system and therefore the probability of producing zero energy is equal to unity. As units are added to the system the probability in the table is redistributed, e.g. if the first unit to be added to the system is a 100 MW unit which has a FOR of 0.25 then the possible levels of output are 0 and 100 MW and the probabilities associated with these levels are 0.25 and 0.75 respectively. As more units are added the number of possible levels increases and the probability of any one individual level decreases so that the sum of all the probabilities in the table remains equal to unity. To order the table and to implement the recursive method, the COPT is split into  $N+1$  states where  $N$  is the installed capacity of the system divided by the highest common denominator in MW terms ( $\Delta$ ) of the installed units

The  $N+1$  state corresponds to the probability of there being zero outage capacity i.e. all the units working. Therefore the COPT has the structure  $0, \Delta, 2\Delta, \dots, N\Delta$  and individual state probability  $k\Delta$  can be referred to as  $p(k)$ . Adopting this structure means that some of the entries will be redundant.

For example if there are two units in a system both having FOR rates of 0.6 and 0.75 and capacities of 20 and 30 MW respectively, then  $\Delta=10$ ,  $N=5$ , therefore the COPT will have six entries as shown in Table 1.

Table 1: COPT for the above example

	Equiv. MW outage	Probability Calculation	Probability
0	0	$(0.6 \times 0.75)$	0.45
$\Delta$	10	Not possible	0
$2\Delta$	20	$(0.4 \times 0.75)$	0.3
$3\Delta$	30	$(0.6 \times 0.25)$	0.15
$4\Delta$	40	Not possible	0
$5\Delta$	50	$(0.4 \times 0.25)$	0.1

The entries at  $\Delta$  and  $4\Delta$  represent outage levels that are not possible with the installed units and so will have zero possibility of outage.

In general terms the recursive formula for the individual state probabilities after the unit  $i$  which has  $m$  discrete states has been added to the system [36] can be given as in Equation (3.3.1).

$$p(k) = \sum_{j=1}^m p_{ij} p'(k - C_{ij}/\Delta) \quad (3.3.1)$$

where  $p_{ij}$  is the individual probabilities such that  $p_{ij} = p(C_{ij})$   $j = 1, 2, \dots, m$ ,  $C_{ij}$  is the outage capacity at levels  $j = 1, 2, \dots, m$  and  $p'(k - C_{ij}/\Delta)$  refers to the probability at the outage level  $(k - C_{ij}/\Delta)$  before the unit  $i$  was added

As before the recursive process starts with the initial conditions  $p(0) = 1$  and  $p(k) = 0$ ,  $k = 1, 2, \dots, N$  and also  $p(k) = 0$  if  $k < 0$ . The main advantages of the recursive method are that it delivers the exact probabilities of the capacity states of the system but if the system being studied contains a large number of units then the amount of calculations needed to generate the COPT can be laborious.

When the system is large the discrete distribution of the system's capacity outages can be approximated by a continuous distribution. This approximation can lead to errors being introduced into the calculation and several different methods have been developed to minimise this error. The central limit theorem tells us that the summation of random variables tend to a normal distribution. Therefore as the number of units in a system increases the distribution of the system's capacity outages tends to a normal distribution. It was shown in [37] that the typical power system has a distribution that is positively skewed for the capacity available. To incorporate skewness into the normal distribution approximation a Gram-Charlier series can be used to modify the normal distribution [38]. Other approaches include the distribution fitting technique, which attempts to fit a non-normal distribution to the data on system capacity outage, and estimating the probabilities from the fitted distribution. In [39] the authors found that Beta distributions provide the best approximation. Also some methods consider different ways to perform the convolution of the discrete distributions. In [40] the Fast Fourier Transform of the discrete distributions is taken and they are multiplied in the

frequency domain. Then the convoluted distribution is derived by taking the inverse Fast Fourier Transform of the result. While in [41] a z-transform procedure is proposed, where the unit distributions are transformed into the z-domain and multiplied. The result of this multiplication can be transformed back by interpreting all powers of  $z$  as delayed impulses in the MW domain.

### 3.4 IEEE RELIABILITY TEST SYSTEM

The IEEE reliability test system (RTS) [42] defines a load model, a generation system and a transmission network. The goal of the system is to present a platform where different methodologies and analysis techniques can be implemented and compared. In developing the analysis tools required to perform adequacy calculations, the IEEE-RTS represents a benchmark system for which the adequacy indices have been calculated and published which is helpful in the process of error checking.

#### 3.4.1 IEEE-RTS Load Model

The IEEE reliability test system includes a load model, the hourly annual peak load of which is 2850 MW. It presents a typical load pattern, with two seasonal peaks. The first of the peaks occurs in week 23 and is 90% of the annual peak, which occurs in week 51. The valleys between these seasonal peaks are at about 70% of the annual peak. If the week 1 is taken as the start of January then the model describes a winter peaking system. Figure 2 shows the peak daily load plotted against time.

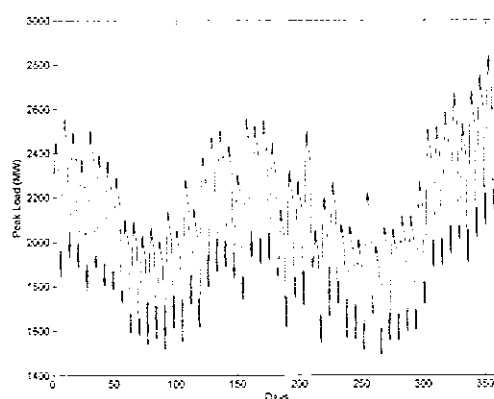


Figure 2: Daily peak loads of the IEEE-RTS load model



### 3.4.2 IEEE-RTS Capacity Model

To draw the COPT for the IEEE-RTS generation system the recursive convolution method was applied. In Table 2 the size and FOR rate of all of the units in the IEEE-RTS are detailed. The total installed capacity is 3405 MW and  $\Delta$  equals 1. Therefore there were 3406 entries in the COPT. The cumulative distribution, which is plotted below in Figure 3, helps to verify the implementation of the recursive method applied to draw the COPT. On the left of the figure the probability of all of the possible capacity states are summed and are seen to sum to one. Moving to the right the number of possible capacity states included in the summation are reduced incrementally and the plot is seen to reduce to zero. For example a cumulative probability of 0.35 at 200Mw indicates that the probability of an outage of 200MW or greater is 0.35.

Table 2: Details of the IEEE-RTS generation unit's capacities and FOR

Unit Number	Unit Capacity (MW)	Unit FOR	Unit Number	Unit Capacity (MW)	Unit FOR
1	12	0.02	17	76	0.02
2	12	0.02	18	76	0.02
3	12	0.02	19	76	0.02
4	12	0.02	20	100	0.04
5	12	0.02	21	100	0.04
6	20	0.1	22	100	0.04
7	20	0.1	23	155	0.04
8	20	0.1	24	155	0.04
9	20	0.1	25	155	0.04
10	50	0.01	26	155	0.04
11	50	0.01	27	197	0.05
12	50	0.01	28	197	0.05
13	50	0.01	29	197	0.05
14	50	0.01	30	350	0.08
15	50	0.01	31	400	0.12
16	76	0.02	32	400	0.12

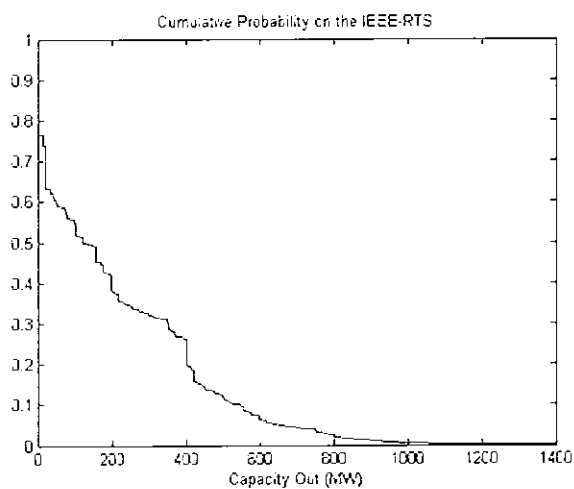


Figure 3: Calculated cumulative probability of the IEEE-RTS

### 3.4.3 LOLE and LOEE calculation for the IEEE-RTS

Once the capacity model had been developed using the recursive method it was compared with the load model on a chronological basis to produce the adequacy indices as described by Equations (3.4.1) to (3.4.4).

$$LOLE = \sum_{i=1}^T P_i \quad (3.4.1)$$

$$LOEE = \sum_{i=1}^T E_i \quad (3.4.2)$$

where: T is the length study period in hours.

$P_i$  is the loss of load probability in hour  $i$ .

$E_i$  is the energy not supplied in hour  $i$ .

$$P_i = \sum_{s=k_i}^N p(s) = P(k) \quad (3.4.3)$$

$$E_i = \sum_{s=k_i}^N p(s)[L_i - IC + s\Delta] \quad (3.4.4)$$

where:  $L_i$  is the load in hour  $i$ .

$k_i$  is the lowest outage capacity that would lead to a loss of load.

IC is the installed capacity

$\Delta$  is the highest common denominator of the installed units

The results obtained for the LOLE and LOEE indices are compared in Table 3 to results found in [36] where the same calculations were applied to the IEEE-RTS. The two sets of results are very similar with a less than one percent error between the two. This difference can most likely be attributed to different rounding errors as opposed to a difference in the applied methods.

Table 3: Calculated and published figures of the IEEE-RTS and the percentage error

	Calculated	Published	% error
LOLE (hrs./yr.)	9.41	9.37	0.426894
LOEE (MWh/yr.)	1185	1176	0.765306

### 3.5 MAINTENANCE SCHEDULING

Up to this point it has been assumed that all the generating units will be available at all times apart for forced outages. However all units require on an annual basis several

weeks of scheduled maintenance. It is likely that the maintenance cycles of some components of a generation unit would be longer than one year but for the purpose of the following calculations it is assumed that the maintenance requirement is constant from year to year. This scheduled maintenance or planned outage is used to perform inspections and general overhaul on the unit and to help prevent forced outages and so decrease FOR rates.

In this way scheduling maintenance is necessary and cannot be cancelled in order to improve adequacy assessment indices. But it is the timing of this maintenance that is important and it will depend on seasonal variations in the load i.e. scheduling maintenance for one or more large base units during a winter week in a winter peaking system will have a much greater impact on system reliability than if the same maintenance were scheduled during spring or autumn. Therefore the timing of scheduled maintenance should be such that as far as is possible system reliability is unaffected. The maintenance requirements of the units in the IEEE-RTS are detailed in Table 4.

Table 4: Maintenance requirements of the units in the IEEE-RTS

Unit No.	Unit Capacity (MW)	Maintenance (weeks)	Unit No.	Unit Capacity (MW)	Maintenance (weeks)
1	12	2	17	76	3
2	12	2	18	76	3
3	12	2	19	76	3
4	12	2	20	100	3
5	12	2	21	100	3
6	20	2	22	100	3
7	20	2	23	155	4
8	20	2	24	155	4
9	20	2	25	155	4
10	50	2	26	155	4
11	50	2	27	197	4
12	50	2	28	197	4
13	50	2	29	197	4
14	50	2	30	350	5
15	50	2	31	400	6
16	76	3	32	400	6

There are two well-developed methods employed to schedule the maintenance requirements; levelling the reserve and levelling the risk [43]. The levelling the reserve method is a direct method, which as far as is possible equalizes the net capacity reserve

of the system over the course of the year. This objective function is given in Equation (3.5.1).

$$\Delta P_i = \Delta P_j \quad i, j \in t, t = 1, 2, \dots, T \quad (3.5.1)$$

where  $\Delta P$  is the net capacity reserve in any stage  $t$ .

The objective of the levelling the risk method is to make the probability of loss of load throughout the year constant. This can be expressed in Equation (3.5.2)

$$LOLP_i = LOLP_j \quad i, j \in t, t = 1, 2, \dots, T \quad (3.5.2)$$

where LOLP is the system risk at any time period  $t$ .

Both methods were applied to the IEEE-RTS. The first scheduling maintenance implemented followed the objective of the levelized reserve method. As the maintenance requirement of each unit in the IEEE-RTS is given in weeks, the year was broken into 52 blocks of one-week duration and the capacity reserve of each block is then calculated by subtracting the load curve from an idealized production curve. The maintenance was then scheduled. By beginning with the largest unit, the required maintenance ( $y$  weeks) for this unit was used to divide the year into sets of blocks that were  $y$  weeks long as detailed in Equation(3.5.3).

$$\begin{aligned} \text{Set 1} &= \text{weeks}(1 \rightarrow y), \text{ Set 2} = \text{weeks}(2 \rightarrow y+1) \dots \\ \text{Set N} &= \text{weeks}(52-y \rightarrow 52) \end{aligned} \quad (3.5.3)$$

Then for each element of each set the capacity of the unit was taken from the weekly reserve and the result of this used to calculate an average capacity reserve figure after maintenance for each set. The unit's maintenance was then scheduled to the set that has the highest average. The weekly capacity reserve for the appropriate weeks were then updated to the previous calculated capacity reserve figure after maintenance. This process was then repeated for each of the units and where possible, the capacity reserve is levelized. The Figure 4 shows a before and after plot of the calculated weekly reserve

capacity. Table 5 below shows the units whose maintenance were scheduled in each week and Figure 5 shows the equivalent weekly capacity outage due to the scheduled maintenance.

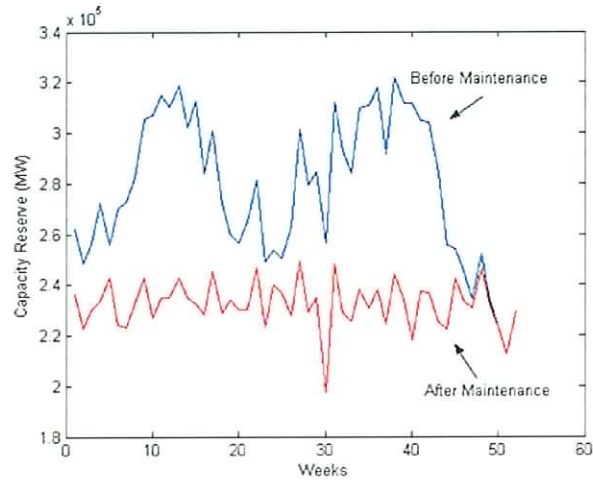


Figure 4: Change in the capacity reserve before and after maintenance

Table 5: Weekly breakdown of when each unit is out on scheduled maintenance

Week No.	Unit out on maintenance	Weeks No.	Unit out on maintenance
1	24	27	27, 21, 3
2	24	28	27, 21
3	24	29	27, 21
4	24, 16	30	30
5	16	31	30, 8, 1
6	28, 16	32	30, 8, 1
7	28, 20	33	30
8	28, 20	34	30, 19
9	28, 20, 17	35	32, 19
10	31, 17	36	32, 19
11	31, 17	37	32
12	31, 12	38	32, 13, 4
13	31, 12	39	32, 13, 4
14	31	40	32, 23
15	31, 18	41	29, 23, 10
16	26, 22, 18	42	29, 23, 10
17	26, 22, 18	43	29, 23
18	26, 22	44	29
19	26	45	14, 6
20	25	46	14, 6
21	25, 11	47	7
22	25, 11	48	7, 5
23	25	49	5
24	15, 9, 2	50	0
25	15, 9, 2	51	0
26	27, 3	52	0

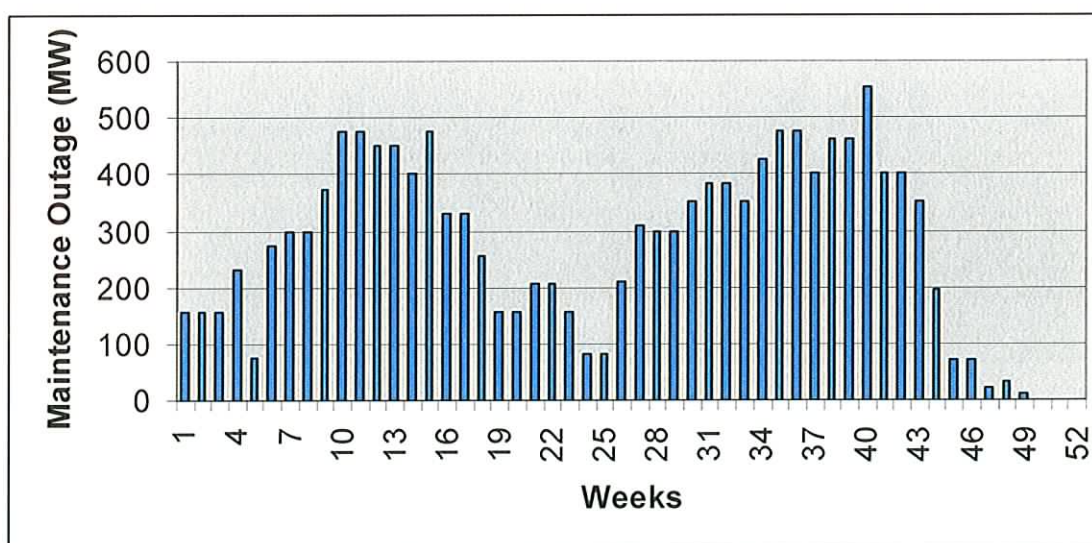


Figure 5: Plot of the weekly capacity on maintenance outage

Using this table, the LOLE and LOEE were recalculated by generating a COPT on a weekly basis leaving out the units that are due for maintenance that week. The indices are then calculated as before for each week and the summation of which gives the annual figure. The result from this process is given in the Table 6. Also shown are the

published values found in [36] where the method of maintenance scheduling applied was the levelised reserve method. It can be seen that while the two set of figures are broadly in-line there is significant percentage variation between them. The one possible reason for this is that the published figures were calculated on a daily basis while the initial results below were derived on using a weekly basis. Alternatively it is possible that a different application of the levelized reserve method principle was applied. In Figure 6 there is a weekly breakdown of the contributions made to the final LOLE value. From Figure 6 it can be seen that there is a significant contribution to the total LOLE made in the period from week 49 to week 52. In this period the contribution to total LOLE was driven purely by the load as it can be seen from Figure 4 that the amount of capacity scheduled for maintenance over that period is very low. An opposing situation occurs in week 30 where from Figure 4 it can be seen that after the maintenance has been scheduled there is a large reduction in the capacity reserve for that week. This results in a corresponding spike in the level of LOLE for that week in Figure 6. This highlights the weakness of the levelised reserve methods to be unable to reflect the difference between removing a large reliable unit so opposed to several smaller less reliable units.



Table 6: Calculated and published results and the percentage error between them

	Published	Weekly Calculation		Daily Calculation	
		Leveli. Risk	Level. Reserve	Level Risk	Level. Reserve
LOLE (hrs./yr.)	20.07	18.86	22.25	18.28	21.26
% difference from published		6.03	10.86	8.92	5.93
LOEE (MWh/yr.)	2350	2202	2738	2231	2607
% difference from published		6.30	16.51	5.06	10.94

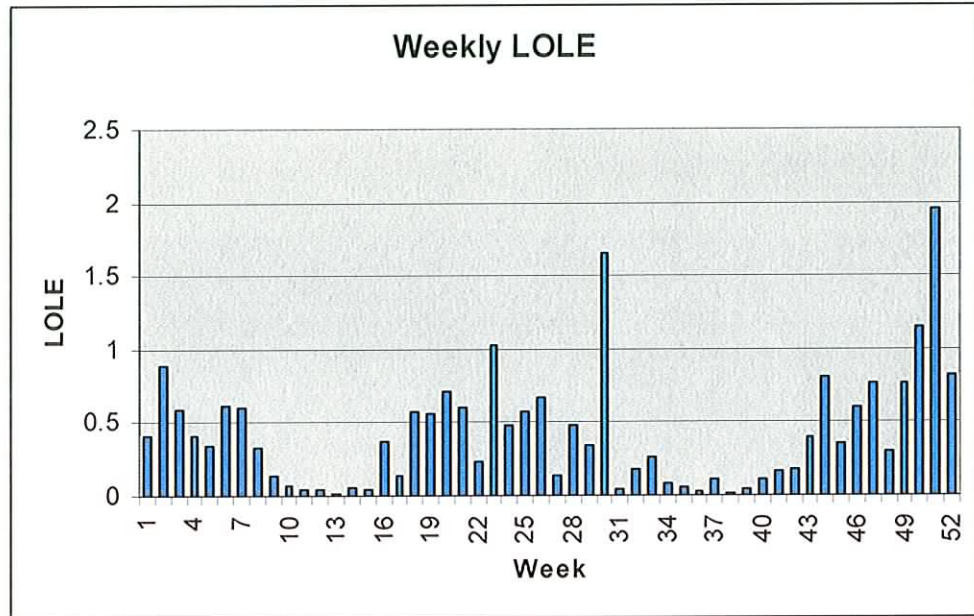


Figure 6: Weekly contribution to the LOLE

The second scheduling maintenance implemented followed the objective of the leveled risk method. Again the year was broken into 52 weeklong blocks but in this case the weekly LOLE with no maintenance was calculated. Then a similar approach was followed as before, beginning with the largest unit. The year was divided into sets of weeks that could accommodate the maintenance required by this unit. For each set of weeks the average LOLE was calculated and the maintenance allotted to the set that had the lowest average. The LOLE for these weeks was then re-calculated with the unit removed. These figures were used to update the weekly LOLE array after each allocation. In this way the maintenance was then scheduled in a way that conserved and where possible leveled the risk of loss of load. Figure 7 shows a before and after plot of the calculated weekly LOLE values. Table 7 below shows the units whose maintenance was scheduled in each week and Figure 8 shows the equivalent weekly capacity outage due to scheduled maintenance.

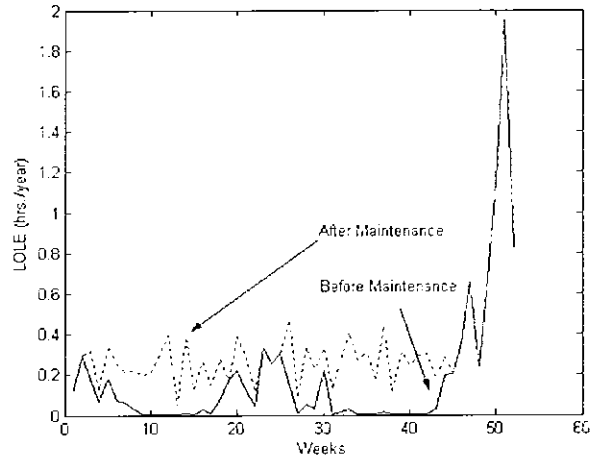


Figure 7: Change in the calculated LOLE before and after the maintenance correction

Table 7: Weekly breakdown of when each unit is out on scheduled maintenance

Week No.	Units on maintenance	Week No.	Units on maintenance
1	0	27	24, 19, 1
2	0	28	24, 19, 1
3	16	29	24, 19
4	16	30	11
5	16	31	29, 23, 11, 6
6	25	32	29, 23, 6
7	25	33	29, 23
8	25, 14, 5, 3	34	29, 26, 23
9	28, 25, 14, 5, 3	35	31, 26, 15, 12
10	32, 28	36	31, 26, 15, 12
11	32, 28, 20	37	31, 26
12	32, 28, 20	38	31, 30, 7
13	32, 20, 8, 2	39	31, 30, 7
14	32, 27, 8, 2	40	31, 30
15	32, 27	41	30, 22, 18
16	27, 21	42	30, 22, 18
17	27, 21, 13	43	22, 18, 10
18	21, 13	44	10
19	0	45	0
20	17	46	0
21	17, 9, 4	47	0
22	17, 9, 4	48	0
23	0	49	0
24	0	50	0
25	0	51	0
26	24	52	0

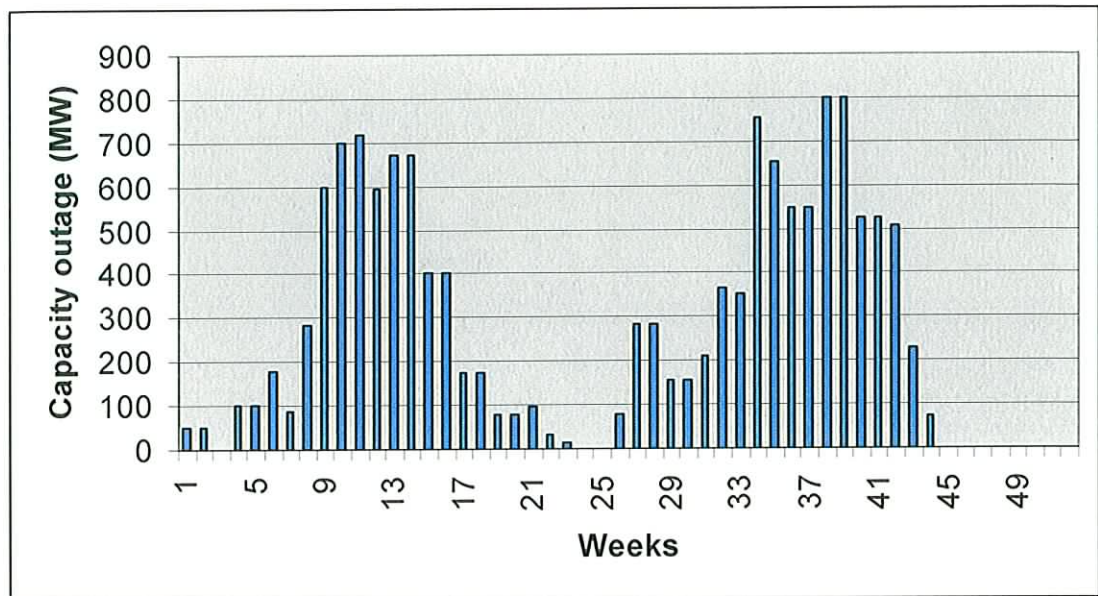


Figure 8: Weekly capacity outage due to scheduled maintenance

Again using Table 7 the LOLE and LOEE were recalculated by generating a COPT on a weekly basis, leaving out the units that are due for maintenance that week. The adequacy indices are then calculated as before for each week, the summation of which gives the annual figure. The results from this process are given in Table 6. It can be seen that results above represent an improvement in the indices over both the previously calculated result and that published for the levelized reserve. This is to be expected as the levelized reserve method has no way of assessing if the unit that is taken out in any week has high or low FOR rates. This could lead to several units with high reliability being taken out at the same time and therefore increasing the probability of loss of load. To highlight this problem in Figure 9 below the weekly LOLE figures for both methods are shown.

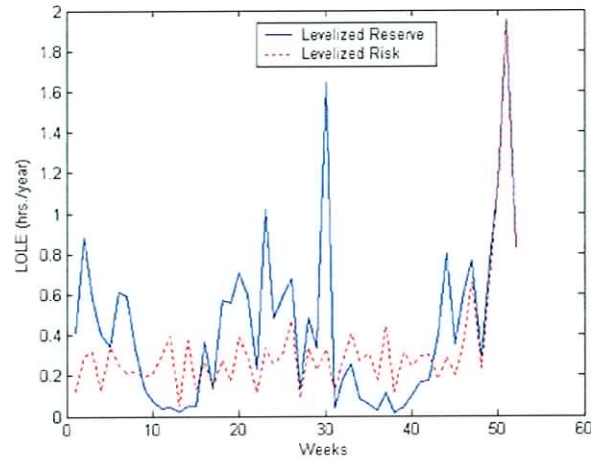


Figure 9: Contrast of the weekly contributions made to LOLE

In Figure 9 the benefit of the levelized risk is highlighted, for example, in week 30. The levelized reserve makes a contribution of over 1.6 hrs/yr or 7.2% to the calculated LOLE of 22.25 hrs/yr while the levelized risk contribution is approximately 0.3 hrs/yr or 1.6% to the calculated LOLE of 18.86 hrs/yr. This is caused by the levelized reserve's inability to predict the effects of removing units with varying levels of FOR from the system. Also it can be seen that in the final weeks of the year the contributions for both methods are the same. This happens because the winter peak in the load model which cause both methods to avoid scheduling any maintenance in this period. In fact the contribution to the total LOLE in this three-week period is 21% and 24% for the levelised risk and reserve methods respectively, which shows that regardless of the maintenance scheduling method employed there is a base level of LOLE that is unavoidable.

To address the question of whether calculating the maintenance scheduling over a daily rather than weekly bases would have a large effect on the resulting indices, the process of calculation was reconfigured to operate on a daily basis for both the levelized reserve and risk methods. The results of this calculation can be seen in Table 6. It can be seen that percentage error between the published results and the levelised reserve method has been reduced significantly but not altogether. This implies that there remains some difference in the application of the method. In order to chase down this difference the reference that is given by [36] as the source of the method of maintenance scheduling used was sourced. In this paper [44] it is suggests representing a unit withdrawn for

maintenance as an addition to the load so as to avoid have to redraw the COPT for each maintenance period but this approximation ignores the FOR of the unit and treats it as if it has 100% reliability. This paper was published in 1979 and it is likely that the approximation was seen as acceptable in order to reduce the computational burden of the calculations. This is supported by the relatively small error that is seen between results published in [36] and the calculated results. The results for the levelised risk method also show a slight decrease in the calculated LOLE in percentage terms. The reduction is approximately 3%, which is in line with the percentage reduction of approximately 4% for the calculated LOLE figure using the levelized reserve method. More interestingly there can be seen a slight increase in the LOEE figure which suggests that there may be a trade off between the time duration of loss of load and its severity.

### **3.6 MONTE CARLO METHODS**

In previous sections the generation adequacy assessment indices LOLE and LOEE were calculated based on the IEEE-RTS using analytical methods and the results of these calculations then compared with published results. In this section the same calculations are made using Monte Carlo simulation. A Monte Carlo simulation requires the system under study be modelled and then the variables on which the model of the system depends are randomly chosen. In this way Monte Carlo simulation represents a numerical alternative to the deterministic method discussed earlier.

#### **3.6.1 Monte Carlo Simulation**

To apply a Monte Carlo simulation to the calculation the LOLE and LOEE the capacity of the system was modelled so that the failure and repair cycle of the individual generation could be simulated over a series of years. In order to do this it was assumed that the time to failure and repair followed an exponential distribution [35], [45]]. The equation of the exponential probability distribution function is given in Equation(3.6.1) the lifetime parameter  $\mu$  is set to the mean time to failure of the unit.

$$y = f(x | \mu) = \frac{1}{\mu} e^{-x/\mu} \quad (3.6.1)$$

With this assumption in place a two state model can be used for each unit as shown in Figure 10. The up-state represents the unit operating. The time that the unit will remain in this state is determined by picking a random number and then translating it through an exponential distribution that is centred on the mean time to failure of the unit. The down-state represents the unit being on forced outage. The time that the unit will remain in this state is determined similarly except that the exponential distribution is centred on the mean time to repair of the unit.

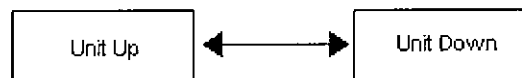


Figure 10: Two state model of generation unit

All the units in the IEE-RTS had this model applied to them and in this way the generation capacity of the system was modelled. As an initial condition it was assumed that at the beginning of the first year all the units began operating i.e. in the up state. This model was then used to track the capacity of the system on an hourly basis by summing the capacities of the unit that are in the up-state. This figure was then compared to the load model and if the capacity was less than the load, a loss of load and the capacity shortfall for that hour was recorded. Over a series of  $i$  years the LOLE and LOEE indices can be calculated from Equation (3.6.2) and Equation (3.6.3).

$$LOLE(\text{hrs./yr.}) = \frac{\sum_{i=1}^N r_i}{N} \quad (3.6.2)$$

$$LOEE(\text{MWh./yr.}) = \frac{\sum_{i=1}^N E_i}{N} \quad (3.6.3)$$

where:  $r_i$  is the number of loss of load occurrences in year  $i$ .

$E_i$  is the total capacity shortfall in year  $i$ .

$N$  is the sample period in years.

On this basis the LOLE and LOEE were calculated using a sample period of 500 years. In Table 8 the results of the application of the Monte Carlo method, the previously calculated results shown in Table 3 and the percentage error between them are shown. From this table it can be seen that the error between the two methods was of the order of ten to fifteen percent, this error could be reduced by increasing the length of the sampling period. In Figure 11, a running average of the LOLE over the sample period is shown.

Table 8: Comparison of results from analytical and Monte Carlo methods

No maintenance	Monte Carlo simulation	Analytical methods	% error
LOLE (hrs./yr.)	10.18	9.41	8.14
LOEE (MWh/yr.)	1342.80	1185.00	13.32

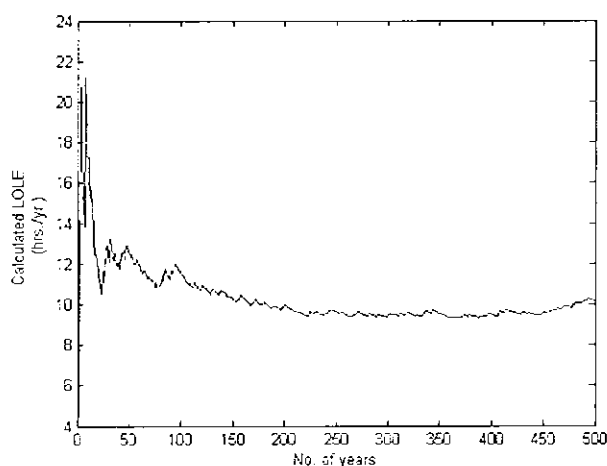


Figure 11: LOLE calculated over the sample period

### 3.6.2 Maintenance Scheduling

To introduce the maintenance scheduling required by the units into the unit model a third state was added as shown in Figure 12.

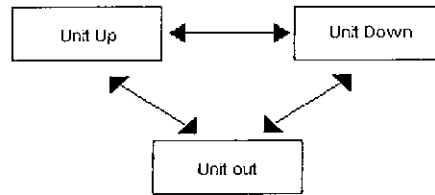


Figure 12: 3-state model of generation unit

The out-state represents a unit when it is out due to scheduled maintenance, the duration of a unit scheduled maintenance is pre-determined in the IEEE-RTS data Table 4 and the timing is determined by the previously developed scheduling routines. In implementing the model it was assumed that, whether a unit was operating (in the up-state) or on forced outage (in the down-state), once the time that had been determined by the maintenance scheduling routine was reached, the unit would switch to the out-state. The number of hours that the unit had remaining in its previous state (up or down) would be stored. For example if a unit goes on maintenance with ten operating hours remaining, when it returns from maintenance it continues for those ten hours of operation. It was found by experimentation that this procedure had the effect of slightly positively distorting the overall equivalent FOR rates of the units. The equivalent FOR rate of a unit is defined as one minus the ratio of the total operating hours to the total number of hours in the sample period. In the ideal case this value would be equal to the FOR but due to the random nature of the process this rarely occurs. To resolve this issue the process that controls the failure and repair cycle of the units continues while they are on maintenance outage. Then once the scheduled maintenance is complete the unit returns to its original state for the number of stored hours. This approach was taken so that the long term simulated FOR of each unit converged to the level set out by in the IEEE-RTS data With this model established the calculation of the LOLE and LOEE was repeated as before for the different scheduling routines. In Table 9 a comparison is shown between the results for the Monte Carlo simulation and the published results. In Table 10 the results from the Monte Carlo and analytical methods are shown and also the percentage difference between them.



Table 9: Comparison of results between published and Monte Carlo simulation

Weekly Calculation		Published	Level. Risk	Level. Reserve
	LOLE (hrs./yr.)		20.07	19.166
% difference from published			4.50	-15.67
LOEE (MWh/yr.)		2350	2243.3	2894.9
% difference from published			4.54	-29.05
Daily Calculation				
	LOLE (hrs./yr.)	20.07	18.976	20.656
	% difference from published		5.45	-8.85
	LOEE (MWh/yr.)	2350	2455.3	2576.8
% difference from published		-4.48	-4.95	

Table 10 Comparison of results from analytical and Monte Carlo methods

	Level. Risk		Level. Reserve	
	Analytical	Monte Carlo	Analytical	Monte Carlo
<b>Weekly Calculation</b>				
LOLE (hrs./yr.)	18.86	19.166	22.25	22.17
% difference	1.60		-0.36	
LOEE (MWh/yr.)	2202	2243.3	2738	2894.9
% difference	1.84		5.42	
<b>Daily Calculation</b>				
LOLE (hrs./yr.)	18.28	18.976	21.26	20.656
% difference	3.67		-2.92	
LOEE (MWh/yr.)	2231	2455.3	2607	2576.8
% difference	9.14		-1.17	

### 3.7 CONCLUSION

The required modelling and calculations to evaluate both the LOLE and the LOEE for the IEEE-RTS and also maintenance scheduling techniques based on both the levelised reserve and levelised risk methods have been developed. The results gained from these calculations were then compared to previous published results. It was found that when maintenance is excluded from the calculation the results found using the analytical method are within one percent of previously published values. A Monte Carlo simulation of the IEEE-RTS has been developed and used to derive values for both the LOLE and the LOEE. Using a sampling period of 500 years the Monte Carlo methods was seen to converge to within 10% of the analytically calculated values. Also maintenance scheduling was incorporated into the Monte Carlo model based on both the levelized reserve and levelized risk methods. The percentage difference seen between the calculated LOLE when the different maintenance scheduling methods were applied was of the order of fifteen percent and the improvement found when the calculation was

made on a daily rather than a weekly basis was of the order of 4%. The results from the deterministic calculation became a reference point for the expected results when the methodology used to calculate the adequacy indices was switched to a numerical methods based on Monte Carlo simulation

## **4 EXTENSION OF ANALYSIS TO THE IRISH SYSTEM**

### **4.1 INTRODUCTION**

The electricity supply system of the Republic of Ireland (R.O.I.) is a relatively small and isolated system that is continuing to experience strong rates of growth. In 2004 there were 32 conventional generation units supplying 4871 MW. Also in addition to this, 570 MW of non-conventional generation existed on the system. Of this 416 MW was from renewable sources with the remainder coming from combined heat and power and from industrial back-up systems. Currently in the generation system of the R.O.I., the level of wind capacity is projected to grow to 756 MW before the end of 2005. This will represent a wind capacity penetration of approximately 11.75%. Under the targets set down in the EU directive on the promotion of the electricity from renewable energy, the R.O.I. should by 2010 produce 13.2% of its gross electricity requirement from renewable sources. Given the extent of the wind resource that exists in the R.O.I. and the relatively slow growth potential from other renewable sources, wind energy is expected to make up the bulk of this requirement. Current predictions estimate approximately 974 MW of wind capacity being required to meet this target, representing a wind capacity penetration of approximately 13.36% [46].

The only interconnection to the generation system of the R.O.I. at transmission level is to Northern Ireland, having a transfer capacity of 300 MW. In the following analysis the assumption is made that the interconnection to Northern Ireland has no impact on the adequacy of the generation system in the R.O.I. This assumption was made as the adequacy standard is planned to be realised by generation capacity dedicated to the load requirements of the R.O.I. This high level of isolation and the relatively small size of the generation system of the R.O.I. have raised concerns over the costs associated with the integration of wind capacity for both the consumer. Due to the cost for extra reserves being required, and also for other producers in the system, due to increased number of start-ups, increased levels of ramping requirement and increased gas prices associated with CCGT units having reduced capacity factors and being irregularly loaded. This problem is compounded by the continuing deregulation, which makes future policy and trading arrangements less clear. Currently a plan for the development

of an All-island wholesale electricity market is being formulated by the regulatory authorities north and south at the request of their respective governments. The goals of an All-Island energy market are to deliver a larger single market with more competitive energy prices, to improve the security of supply and to increase the diversity of the energy mix. If the all island market is implemented it is likely that there will be an increase in the level of interconnection between the two systems [47].

The construction of the capacity and load models in the generation system of the R.O.I. used in this study, were based on the information contained in the Generation Adequacy Report [46]. This report is a public document, published by the transmission system operator (TSO) in the Republic of Ireland on an annual basis. It contains the TSO's predictions in terms of load and capacity growth and overall system availability over a seven-year period. The statement also details the existing capacity in terms of individual unit capacities. The adequacy assessment predictions of the TSO over the period are outlined. Taking in all cases the median forecasts made by the TSO in the period 2005–2011, the total energy requirement is expected to grow from 26.1 to 33.5 TWh. This represents an average year on year growth rate of 3.9%. This is accompanied by an expected growth in the peak demand from 4608 to 5755 MW. The overall system availability is expected to improve over the period from approximately 83.5% to 85.5% due to the replacement of older plant. At the time of the publication of this forecast some concerns existed over its validity as the system availability was running at approximately 77%, which is significantly below the predicted levels. Since that time these concerns have been alleviated by the continual improvement of the system performance, such that currently the availability is running at approximately 83% on a 52 week rolling average.

In this chapter the approach taken in modelling the generation system of the R.O.I. was such as to allow the calculation of the adequacy indices is discussed. Initially wind capacity was excluded from the LOLE calculations so that the required modelling could be investigated without this complication. Two different methodologies of LOLE calculation were investigated; deterministic methods, which is currently the method used by the TSO and Monte Carlo methods. The deterministic methods offer a computationally efficient way of calculating the LOLE for a given system while Monte

Carlo methods involve a higher computational burden. The structure of the Monte Carlo model is such that it allows for a more detailed analysis of the system's operation.

## 4.2 LOAD MODEL

To develop a load model that would reflect the variability on a year-to-year basis in the generation system of the R.O.I, the recorded demand levels from five different years were scaled to the predicted load level of each of the years being investigated. In this way, for each forecast year, there are five different load shapes. The total energy requirement of each of the load profiles is the same but the levels of peak demand vary. The weekly peak values of the five load shapes are plotted, in Figure 13. From this figure the clear winter peaking nature of the generation system of the R.O.I. can be seen with the annual peak demand occurring either before or after Christmas. The lowest annual loads occur consistently around the last week of July or the first week of August.

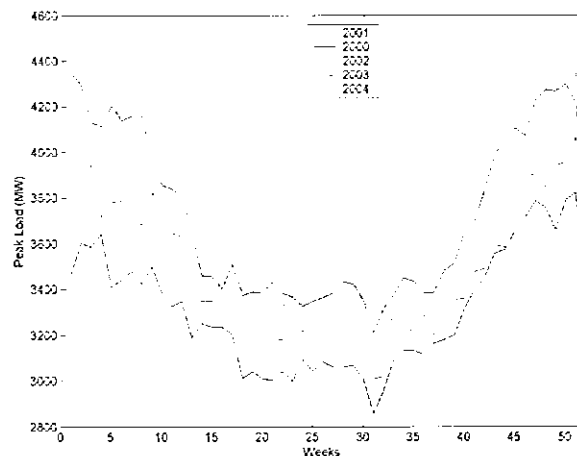


Figure 13: Plot of the four applied load shapes

In Table 11, the original peak load values and total energy requirements are shown, highlighting the differences in the five load shapes. When the effect of year-on-year growth is eliminated by scaling all of the load curves to the 2004 energy level it is found that the five load shapes are very similar. This is as would be expected and the variation

that does exist occurs mostly in the top 5% of the load duration curve. To investigate this further, the top 5% of the load duration curve was plotted in Figure 14.

Table 11: Recorded load data TER and peak values

Year	Total Energy (GWh)	Peak (MW)
2000	22,505	3823.5
2001	23,576	4068.7
2002	24,350	4344.5
2003	25,049	4350.7
2004	25,678	4435

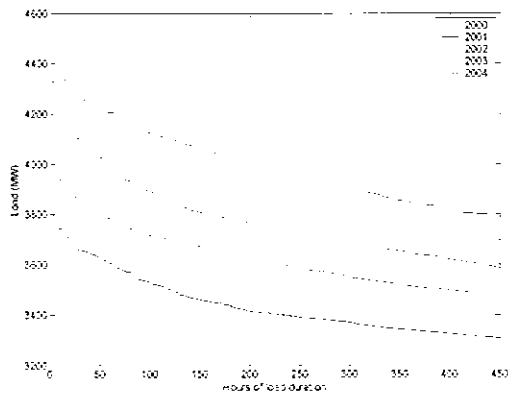


Figure 14: Top 5% of the LDC of the recorded load data

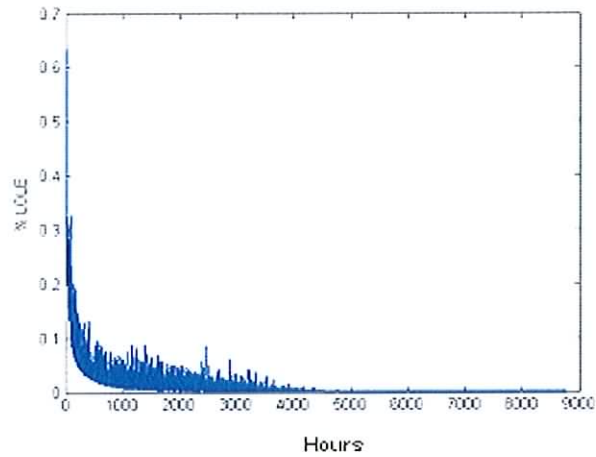
While it is difficult to determine which of the load curves will result in the highest LOLE figures as the curves are so similar, it can be seen that just because one year has the highest peak it does not necessarily follow that year will have the highest LOLE figure. With these load shapes in place it was possible to generate a load model by scaling up each of the load shapes to the median growth levels predicted by [46]. These are shown in summary in Table 12. This table was formed by scaling the load shapes seen in Figure 13 by calculating the total energy requirements for each of the load shapes and then finding the percentage difference between this and the predicted energy requirement. Each of the hourly-recorded load levels that make the load shapes are then scaled up by this amount. In the table the predicted peak load and the peak load derived from scaling each of the load shapes are detailed. Also shown are the total energy requirement and the peak load of each of the load models.

Table 12: GAR 04-10 predicted growth rate and model peak and total demand

Year	% Growth	Energy	Peak	Peak '00	Peak '01	Peak '02	Peak '03	Peak '04
		(GWh)	(MW)					
2004	-	25,678	4448	4296	4401	4569	4457	4435
2005	3.77	26,647	4608	4458	4567	4741	4625	4602
2006	4.44	27,829	4803	4656	4770	4952	4830	4807
2007	4.16	28,987	4994	4850	4968	5158	5031	5007
2008	4.14	30,188	5193	5051	5174	5371	5240	5214
2009	3.95	31,381	5391	5250	5378	5584	5447	5420
2010	3.78	32,568	5590	5449	5582	5795	5653	5625
2011	3.04	33,559	5755	5615	5752	5971	5825	5796

While this method is intended to give a reflection of the year on year variability of the load shape of the generation system of the R.O.I, it is not able to account for the changing relationship between peak demand and the total energy requirement. To understand the importance of this relationship it should be understood that the hours of peak and near peak demand contribution to the adequacy indices is much higher than hours of lesser demand.

This relationship can be seen in Figure 15 where the hourly loads placed on the system were arranged in descending order of magnitude and then the percentage contribution of each hour to the total LOLE value calculated. It can be seen that these values follow an exponential function with peaks occurring on the curve caused by various units being taken in and out of service for scheduled maintenance. The importance of this relationship is further highlighted in Figure 16. The results used in this plot were derived when calculating the system LOLE for the year 2005. In this plot a running total of the sorted percentage hourly LOLE values are shown. From this plot it is possible to see that approximately 55% of the total LOLE value is generated by the top 5% of peak hours.



**Figure 15: Hourly percentage LOLE contribution**

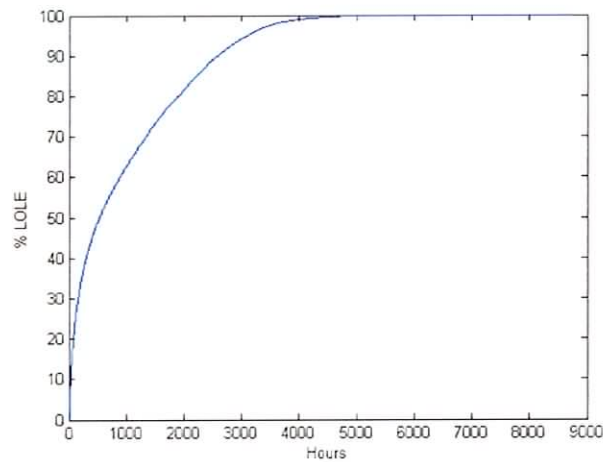


**Figure 16: Running total of percentage LOLE contributions**

While the predictions for this relationship are not explicitly detailed in the [46], in Figure 17 the ratio of total energy requirement to peak of each year is plotted. It can be seen from the figure that this ratio is predicted to increase steadily over a small range during the lifetime of the report, this implies that the level of dominance of the peak value on the LOLE figure is predicted to fall slightly over the coming years. For comparison, the same ratio is plotted in Figure 18 based on the recorded data for the period 2000 to 2004. It seems that from this plot that the year-on-year variations in the ratio in question are much more volatile than the prediction suggests but, based on the last set of recorded data, the trend of the predictions appears correct. This relationship has also been changed in recent years as a result of demand management schemes.



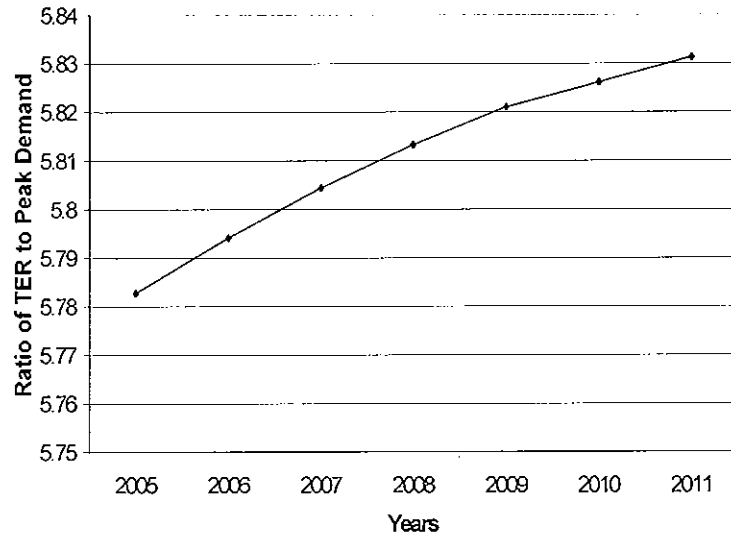


Figure 17: GAR 04-10 predictions

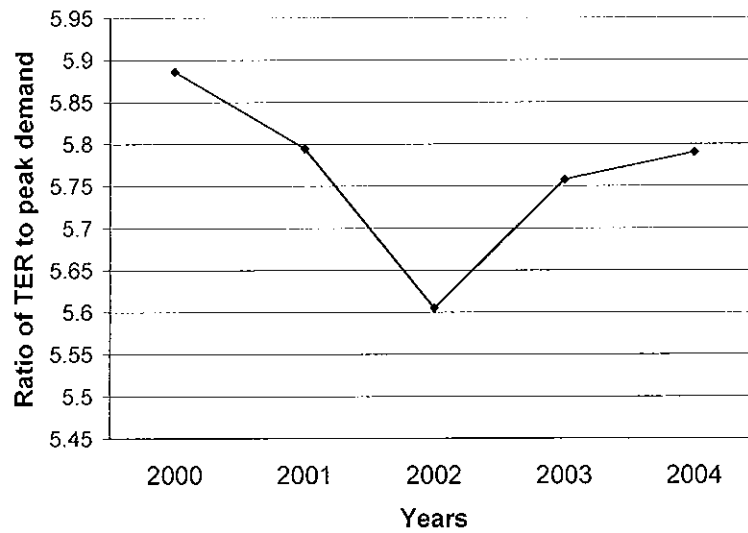


Figure 18: Recorded data

## 4.3 CAPACITY MODELS

### 4.3.1 Deterministic Capacity Model

The capacity model was developed by applying the regression method [48] to the information given in the [46] regarding the number, size and type of units in operation and also the commissioning/decommissioning schedule for the coming years, for details see Appendix C to generate a capacity outage probability table for the system. To do

this it was necessary to find approximate values for both the FOR and scheduled maintenance requirement of the unit as this information is considered to be commercially sensitive and is therefore not published. Overall system availability rates were found in [49] and, by assuming a twenty-day scheduled maintenance requirement for all the units, and then applying Equation (4.3.1), it was possible to estimate a FOR for all the units. While it is clear that it is very unlikely that all units will share a common FOR and scheduled maintenance requirement, and that this approximation is likely to cause some degree of error, in the absence of further information this assumption was necessary.

$$\text{System\_Availability} = \frac{\sum_{i=1,n} A_i \cdot C_i}{\sum_{i=1,n} C_i} \quad (4.3.1)$$

where  $n$  = number of generation units in the system

$$A_i = (1 - SOD_i) * (1 - FOP_i) \quad (4.3.2)$$

where  $A_i$  = Availability of generation unit  $i$

$SOD_i$  = Scheduled outage duration of unit  $i$

$FOP_i$  = Forced outage probability of unit  $i$

$C_i$  = Capacity of unit  $i$

It was decided to exclude wind capacity from the initial set of calculations as initially efforts were focused on investigating the degree of accuracy with which the conventional elements of the system could be modelled and with ensuring that convergence could be established between the deterministic and Monte Carlo methods being applied. In Table 13 the availability rates taken from the median availability predictions of [46] are shown, as well as the derived FOR found when the method described above was applied.

Table 13: Predicted availability and calculated FOR

Year	Availability	Maintenance (Days)	FOR
2005	83.20%	20	12.00%
2006	83.90%	20	11.30%
2007	85.00%	20	10.00%
2008	86.00%	20	9.00%
2009	86.00%	20	9.00%
2010	86.60%	20	8.40%
2011	85.40%	20	9.50%

### 4.3.2 Monte Carlo Capacity Model

Previously in Section 3.6 the generation adequacy indices of the IEEE-RTS [50] were calculated using Monte Carlo methods. The same methods were extended to the generation system of the R.O.I, initially excluding wind capacity. The sourcing of the data used and the necessary approximations made to allow for the construction of capacity models have been previously discussed Section 4.3. As mentioned before the process of Monte Carlo modelling involves the generation of an analytical model of a system, the goal of which is to be able to predict the outcome of the system for a given set of input conditions, where these inputs are randomly selected from the input parameter underlining the probability distribution by a process of repeated random draws. The model output settles to its most probable state after multiple simulation years.

To apply Monte Carlo simulation to the calculation of adequacy indices requires the chronological convolution of a load and capacity model. The development of the load model has already been discussed and is simply the hourly predictions for the system load. The details of the generation of the capacity model for a Monte Carlo based calculation [51], [52] can be summarised as drawing random operating and repair times from an exponential distribution centred on each unit's mean time to failure and repair repeatedly. These times are then used to specify which units are available on each hour and this then allows the hourly capacity of the system to be calculated.

A complication arises when the effect of scheduled maintenance is considered. The solution to this is to introduce a third possible state of the units (i.e. operating, under

repair, out for maintenance) as discussed in Section 3.6.2. A further complication arises if the opportunity that the chronological nature of Monte Carlo model is exploited to model peaking units separately from base load units. In order to implement this idea it is necessary initially to separate the base units from the peaking units. The base units are modelled by the three state model previously implemented while for the peaking units a fourth state is needed i.e. a state where the unit is available but not required. A peaking is put into this state when the load for a given hour can be met without the capacity it supplies and is equivalent to the unit being turned off. When a peaking unit is required the probability of the unit failing on start up is modelled by drawing a random number and comparing it to the units starting probability. If the unit starts up successfully then the time to failure is found in the usual way. Likewise if the unit fails to start up, then time to repair is found similarly. This method of modelling these units is intuitively appealing as it follows closely the actual operating pattern of peaking units. Also this model can allow for the calculation of the capacity factor of each of the units. In this way the effects of various parameters such as the ratio of base to peaking capacity or wind capacity in a system could be investigated.

The model could be expanded further to incorporate other effects such as maximum ramping rates and minimum loading levels and in this way to reflect more closely the underlying generation system. There are two principle difficulties in doing this. Firstly, the more complicated the model the higher the computational burden but while this is a concern it is not the principle limiting factor. Secondly, and more importantly, the closer a model is designed to approximate a system the more information about the system is required. For example, for the model used in the calculation of the results detailed below, the starting probabilities of the peaking units were not known and so in order to allow the model to operate a value of starting probability was chosen so that the resulting LOLE values calculated were the same as if all units were considered to be base units. This situation in effect reduces the model to the position where all of the unit are considered to be base units and negates the extra effort required to include peaking capacity as a separate element in the model

Regardless of the model that was used to calculate the capacity of the system, in any hour when the load is greater then the capacity of the system, a loss of load is recorded

along with the capacity shortfall for that hour. Over a series of  $i$  years the LOLE and LOEE indices can be calculated by Equation (3.6.1) and Equation (3.6.2).

#### **4.4 RESULTS OF ADEQUACY CALCULATIONS ON THE IRISH SYSTEM EXCLUDING WIND CAPACITY**

Using the load model and the capacity models that have been developed, the LOLE and LOEE of the generation system of the R.O.I. were calculated for the period 2005 to 2011. For each year of the study, the five load shapes that were based on the recorded system demand curves from 2000 to 2004 were applied. In Table 14 and Table 15 the values of LOLE found from these calculations are detailed. In all of the Monte Carlo calculations a sample period of 200 years was applied. These two sets of results show the Irish generation system being outside the adequacy standard in 2005. From 2006 until 2008 the system is inside standard due largely to the addition of new generation capacity as detailed in Appendix C and also due to a slight improvement in the overall system availability as given in Table 13. Then from 2009 to 2011 the system again moves outside standard due to continued strong growth in the load requirement as shown in Table 12. In Table 16 the average results from the Monte Carlo and deterministic calculations are compared. Also shown are the percentage differences between the two sets of results.

**Table 14: Calculated values of LOLE for the Irish system using deterministic method**

Year	Load Shape					Average
	2000	2001	2002	2003	2004	
2005	14.41	15.28	17.77	16.30	16.60	16.07
2006	4.03	4.44	5.57	4.83	4.95	4.76
2007	2.68	3.06	3.95	3.32	3.42	3.29
2008	3.71	4.20	5.62	4.70	4.83	4.61
2009	8.72	9.80	12.42	10.92	11.14	10.60
2010	14.52	15.90	20.08	17.88	18.33	17.34
2011	45.13	48.45	56.79	52.48	52.97	51.16

Table 15: Calculated values of LOLE for the Irish system using Monte Carlo method

Year	Load Shape					Average
	2000	2001	2002	2003	2004	
2005	14.10	15.57	17.45	16.49	16.50	16.02
2006	3.64	4.15	5.32	4.39	4.64	4.43
2007	2.60	3.86	3.99	3.45	3.64	3.51
2008	3.93	4.01	6.39	4.79	5.37	4.90
2009	8.87	9.76	12.93	11.86	11.55	10.99
2010	13.49	15.64	20.88	18.42	18.29	17.34
2011	44.89	50.62	59.05	51.47	53.90	51.99

Table 16: Comparison of results

Year	Monte Carlo	Deterministic	Difference
2005	16.02	16.07	0.31%
2006	4.43	4.77	7.10%
2007	3.51	3.29	6.76%
2008	4.90	4.61	6.20%
2009	10.99	10.60	3.72%
2010	17.34	17.34	0.01%
2011	51.99	51.16	1.61%

To allow for clear comparison between the analytical and Monte Carlo results, Figure 19 presents both sets of results on a common axis. In this figure it can be seen the level of LOLE drops in the initial years of the study due to the introduction of new generation capacity but in the later years, the continuing strong growth in load results in the LOLE rising rapidly.

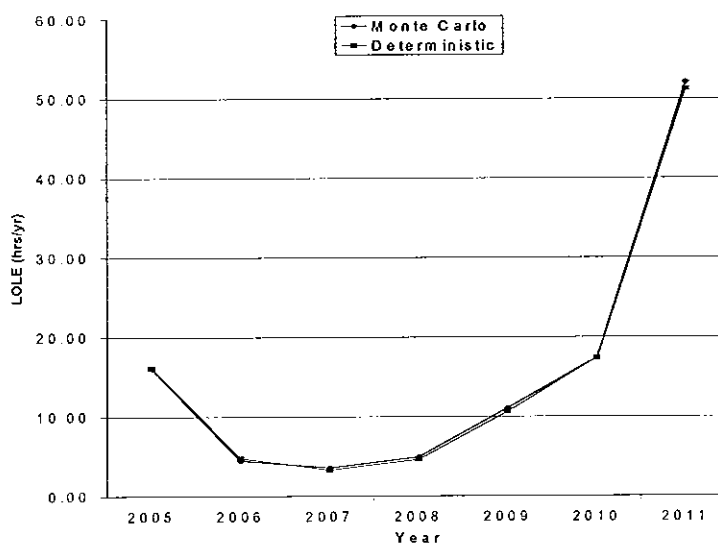


Figure 19 Comparison of results

From this set of results the convergence of the two methods has been well established but as a further check of their convergence the calculation of the year 2005 was re-simulated with an extended sampling period of 1000 years, the results of this are shown below in Figure 20. On the graph the Monte Carlo convergence path is shown in blue and the deterministic result shown in red as a constant line. The deterministic result is 14.41 hrs/yr, compared to the Monte Carlo result of 14.26 hrs/yr, representing a difference of less than 1%. This contrasts with a difference of 2.2% for a sample length of 200 years.

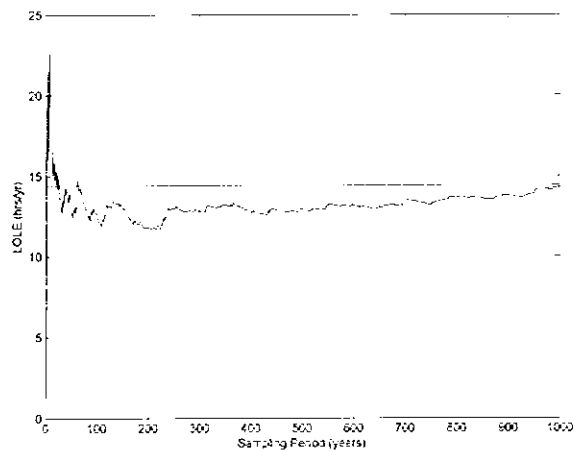


Figure 20: 2005 results with extended sampling period

It can be concluded that the results found using the modelling and calculations applied in the Monte Carlo method as described above are convergent to the results found when using deterministic methods. The degree of this convergence is an inverse function of the length of the sampling period applied. This result has two positive implications; firstly, each set of results serves to verify the other and in this way suggest that for the data available the results gained are accurate. Secondly the convergence in the results will allow for direct comparison between results gained from Monte Carlo simulations that include various representations of wind capacity and results gained using deterministic methods.

## 4.5 MODEL VERIFICATION

With the convergence of the methods established it is possible to calculate the adequacy indices in the generation system of the R.O.I. However, due to the approximations that were made in formulating the models it was difficult to assess the validity of results obtained. To tackle this problem, a set of simplified scenarios was implemented, the effects of which would be clear so that these expected trends could be compared easily with those trends found in the results.

In the first scenario, the capacity of the system was held constant at the 2005 level and the load increased as predicted in order to allow the impact of growing load in the system to be assessed. In all calculations the wind capacity continued to be excluded from the system. The results are tabulated in Table 17 and plotted Figure 21. As expected the results show the value of LOLE will rise rapidly.

Table 17 Plot of the LOLE values calculated from scenario one

Year	LOLE		% Difference
	Monte Carlo	Analytical	
2005	16.02	16.07	0.31
2006	32.42	33.18	2.29
2007	75.08	73.34	2.37
2008	151.22	148.37	1.92
2009	281.26	276.2	1.83
2010	483.22	478.96	0.89
2011	727.58	721.02	0.91



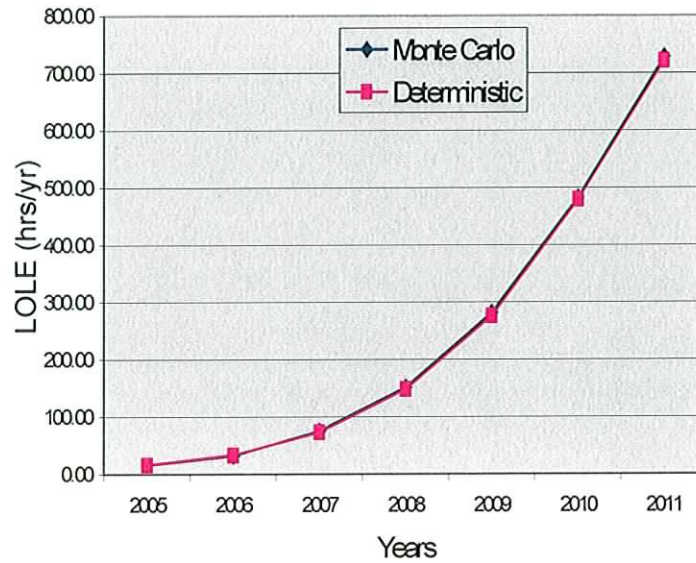


Figure 21: Plot of the LOLE values calculated from scenario one

In second scenario the situation was reversed in that the load requirement of the system was held constant at the 2005 level and the capacity of the system increased as predicted. This was in order to allow the impact of growing capacity in the system to be assessed. The results are tabulated in Table 18 and plotted Figure 21. As expected the results show the value of LOLE will falling rapidly.

Table 18: Values of LOLE calculated for scenario two

Year	LOLE		% Difference
	Monte Carlo	Analytical	
2005	16.02	16.07	0.31
2006	1.93	2.07	6.76
2007	0.56	0.53	5.66
2008	0.25	0.24	3.72
2009	0.28	0.27	3.65
2010	0.10	0.11	7.14
2011	0.31	0.34	8.21

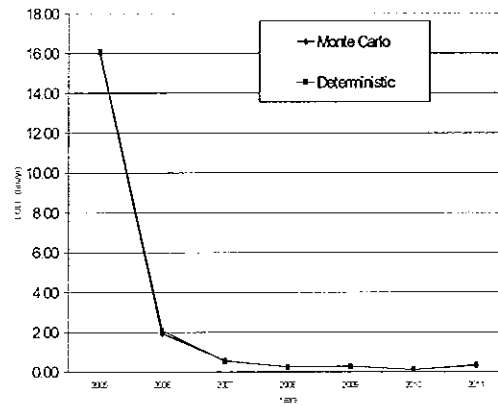


Figure 22: Plot of the LOLE values calculated from scenario two

A series of other scenarios were investigated such that the effect of varying the level of availability and increasing / decreasing the proportion of the total expected level of outage that is considered due to scheduled outages. In this way the level of FOR attributed to each of the units is varied. For each of these scenarios the trends that were observed in the results mirrored the expected trend. While this process demonstrates that the models that have constructed behave in the manner that would be expected, it fails to show the degree of accuracy to which the results produced relate the generation system of the R.O.I. The figures produced by the TSO in [46] represent a benchmark for the calculations that are being made. However, two difficulties arise in using these figures for comparative purposes. The first is that the values produced by the TSO include wind capacity; the second difficulty is that the figures presented by the TSO are given in capacity terms calculated by finding the peak carrying capability (PCC).

In the generation system of the R.O.I. the adequacy standard is set at 8 hrs/yr. This figure suggests that in a typical year the total amount of time that any degree of load will have to be curtailed will be 8 hours. This standard is used to judge whether there is a surplus or deficit of capacity on the system. When the LOLE is calculated to be less than 8 hours/yr then it is expected that there is a surplus of capacity on the system. Likewise when the LOLE is calculated to be greater than 8 hours then it is expected that there is a deficit of capacity on the system. The PCC is calculated by using a scaling factor to adjust the level of load over the course of the year such that after the scaling factor has been applied the LOLE calculated will be equal to the standard. The PCC value is the peak load value multiplied by scaling factor and the difference between the

original peak and the PCC is the value used as an indicator for the surplus or deficit on the system.

While the PCC offers a good indicator for the level for the surplus or deficit on the system it is heavily dependent on the load shape and the corresponding level of peak demand that is used in the calculation. The nature of the input assumptions used in the formation of the capacity offers the possibility of using a different method of calculating the surplus or deficit on the system. Because of the input assumptions applied, each of the units in the system have a common level of scheduled maintenance and forced outage rate and in this way a typical unit for the system has been defined. Therefore if the calculated LOLE is outside the standard then the system can be forced to return to standard by the addition of a correctly sized fictional unit. The capacity of this unit represents the level of deficit on the system. To find the level of surplus on the system a unit with a negative capacity could be added but this is not an intuitive solution and therefore the same capacity can be systematically deducted from each of the other units on the system. In Table 19 the previously calculated LOLE values have been put into capacity value terms. Also shown are the values shown in [46] for the same set of base input conditions, the differences in the two sets of results are caused by assumptions required to form the capacity model due to the lack of data about individual units FOR and maintenance requirements and also by the exclusion of wind capacity from the calculation. In this and subsequent tables the values from [46] are not considered to represent a set of definitive values. However they do offer a useful reference point and it is consider important that trends reflected in these values be reflected in the calculated values.

Table 19: Comparison of Calculated LOLE values to GAR 05-11 in capacity terms

Year	Calculated value (MW)	GAR 05-11 (MW)
2005	-131	65
2006	166	221
2007	262	281
2008	188	200
2009	-20	19
2010	-131	-92
2011	-508	-292

## 4.6 INCLUSION OF WIND CAPACITY

In [49] the method used by the TSO for including wind capacity into adequacy calculations is outlined. This method involves combining historical wind power series from on-shore wind farms with offshore wind speed data to form a wind power series that is representative of a geographically diverse wind capacity resource. This wind power series is scaled to the level of wind capacity predicted of each for the years under examination. The scaled power series is applied to adequacy calculations by considering it as a load modifier i.e. the scaled wind power series that subtracted from the load before any other calculated is performed. The logic behind this is that as the fuel associated with wind energy is zero then in a least cost dispatch wind will always be used when available. This method has the benefits of being able to retain a lot of the chronological aspects of the wind resource i.e. the change of the mean wind speed/power over the course of the year, while also including the benefits of geographical dispersion. Initially for the purposes of the calculations being made the efficacy of using more simplistic models of wind capacity was investigated.

### 4.6.1 Elevated FOR Wind Capacity Model

In the first model considered wind capacity was treated as a single lumped unit with a FOR value of 0.7 (i.e. availability of 30%) [53]. The results of including this model for wind capacity are tabulated in Table 20 and plotted in Figure 23. Also included on the graph are the predictions in [46] and the values found when wind capacity is excluded from the calculations.

Table 20: Values calculated using elevated FOR wind capacity model

Year	Calculated value (MW)	GAR 05-11 (MW)
2005	-83	65
2006	219	221
2007	313	281
2008	236	200
2009	20	19
2010	-97	-92
2011	-439	-291

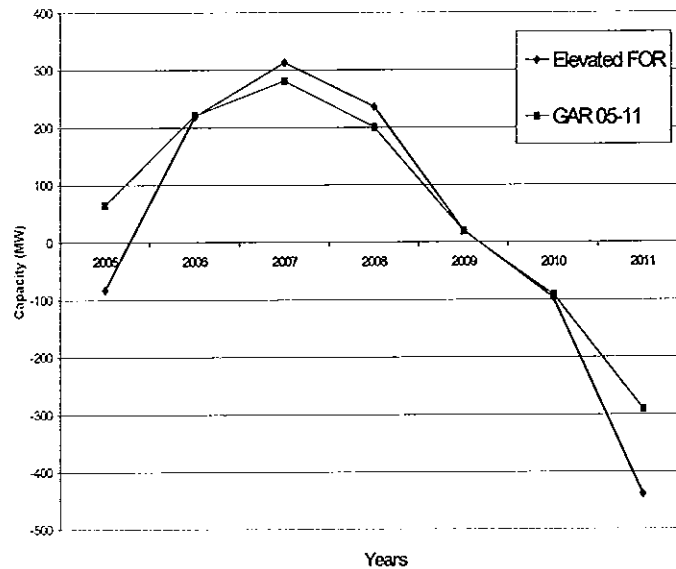


Figure 23: Plot of the result from Table 6

A number of different variations of the elevated FOR wind capacity model were tested. The first approach was to split the model into four units; the total capacity and availability of which equals the original lumped unit. The next variation returns the wind capacity model to a single lumped unit but increased its availability to 40%. The final variation combines the first two by modelling the wind capacity as four units with an availability of 40%. Gathering the results together from the four variations in Figure 24 it can be seen that increasing the reliability of the wind capacity model either by directly increasing the availability or by splitting the model into more units has the effect of reducing the calculated LOLE figures.

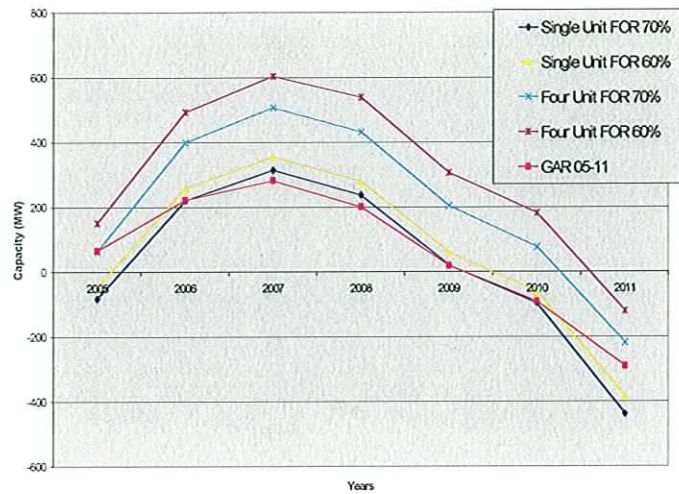


Figure 24: Plot of results found for the different variations in wind capacity model

#### 4.6.2 Weibull Load Modifier Wind Capacity Model

The second type of wind capacity model used generally assumes that an estimate of the mean and variance of the wind series at a location is known. Then the wind can be modelled by the construction of a Weibull distribution [54] based on these parameters and then taking random draws from the constructed distribution to form a hourly wind series. This series can be passed through the model of the wind turbine, which defines the relationship between wind speed and power output. If the mean and variance are known at multiple sites, then a distribution can be generated for each of them and the total capacity divided among them. While this process will capture the stochastic element that drives the wind capacity, it will ignore the chronological aspects mentioned earlier. Power outputs from 18 existing on-shore farms are combined with offshore recorded wind speed series to form a wind power series in a 67% on-shore to 33% offshore split. This is a high percentage to associate with offshore wind capacity as currently there only one offshore wind farm in operation in the R.O.I. Which is located on the Arklow Banks 10km off the coast of Co. Wicklow and has a capacity of 25MW. The overall capacity factor was calculated to be 34.7% [55].

The application of the Weibull based load modifier method suggests that the mean and variance of the wind at different locations be known and that the parameters of the wind turbines used at these locations also be known. As this information was not available it

was necessary to assume a set of generic wind turbine characteristics. Therefore values of 3,12 and 20 m/s were chosen for cut in, rated and cut out wind speeds. A plot of the power to wind velocity (PV) characteristic of this generic turbine is shown in Figure 25.

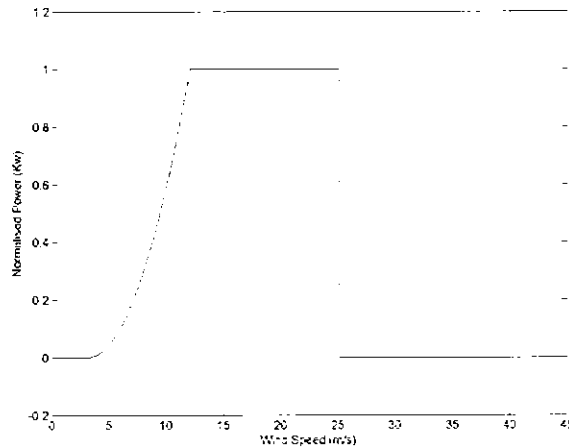


Figure 25: PV characteristic of a generic wind turbine

It was decided that in order to give a valid comparison of the methods, the characteristics of the wind series used to drive the turbine model would be chosen so that the average capacity factor over a one year period would be 34.7% approximately. Therefore a mean wind speed of 8.15 m/s and a variance of 6 m/s were used. The calculations over the period 2005-2011 were repeated using this wind capacity model and also by applying the elevated FOR method with the value of FOR set to one minus the established capacity factor. The results from these calculations are presented in Table 21 and plotted in Figure 26 along with predictions in [46] under the same set of input assumptions.

Table 21: Results from the application of the elevated FOR and Weibull load modifying methods

Year	Elevated FOR (MW)	Weibull load modifier (MW)	GAR 05-11 (MW)
2005	-67	129	65
2006	235	458	221
2007	331	561	281
2008	256	499	200
2009	37	273	19
2010	-82	156	-92
2011	-411	-133	-291

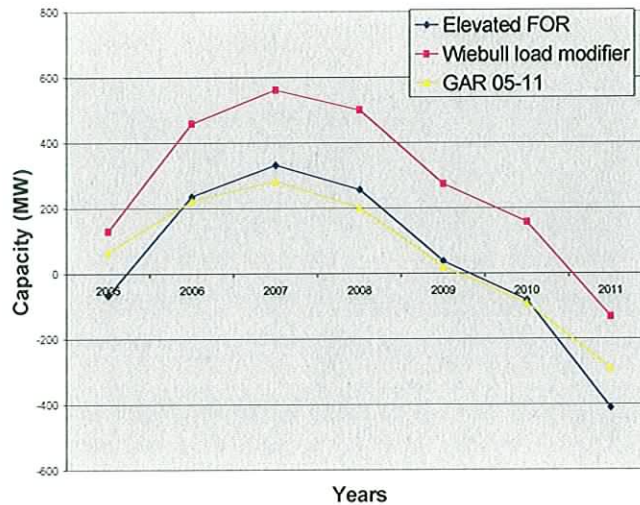


Figure 26: Comparison of Elevated FOR and Wiebull load modifying methods

## 4.7 CONCLUSION

It can be seen from the results presented in Table 17 and Table 18 the model of the system will track the expected behaviour of the LOLE but that the actual results obtained contain differences to those predicted in [46] due largely to the assumptions made to calculate the approximate FOR values and the wind capacity models applied. These approximations were necessary in the absence of further information on the predicted scheduled maintenance requirements and FOR values of the generation units. Also the wind capacity in [46] is treated as a load modifier and is based on both recorded on shore wind power series and offshore wind speed series. In this work it has been modelled as both a supply side unit with an elevated level of FOR and a load modifier based on a random draw from a Wiebull distribution. While both of these methods have been extensively tested, the appropriateness or accuracy of one over the other is dependent on a number of factors.

These include the level of wind penetration, the degree of variability in the wind power over an appropriate time period and the level of correlation between the wind series that drive the wind capacity and the system load. Each of the three wind capacity models discussed in this chapter represent different aspects of the nature wind capacity. The elevated FOR methods represent wind as being probabilistic and if considered over the



course of several years then wind capacity can be characterised quite well in this way but LOLE calculations are based on a hourly (or possibly less) comparison of the load and capacity models and in this time frame the probabilistic representation is less appropriate. Also this method has no way of incorporating other aspect of the wind capacity, such as it being to some extent stochastic in nature. The Weibull based load modifying methods has the ability to represent this aspect of wind capacity but in most wind regimes there is seasonal and diurnal aspect to the mean wind speeds which the random draws of the Weibull based load modifying methods has no way of incorporating. But these seasonal aspects can be preserved by basing the model of wind capacity of recorded wind series as in [46] but this then will ignore the stochastic elements. Also there are concerns around basing the model on a single year of data as this may lead to distorted results. Ideally a model of wind capacity would be able to combine the stochastic and seasonal elements of a wind regime to form hourly predictions in a ways that results in the long-term probability being preserved. But in order to model the wind capacity more closely, further information regarding the wind regimes and the parameters of the wind turbines at the various existing and proposed wind farm sites would be required.

## **5 INVESTIGATION OF WIND DATA**

### **5.1 INTRODUCTION**

In the previous chapter simplified representations of wind capacity were applied to generation adequacy assessment calculations. These simplified models were derived from general assumptions about wind capacity and the capacity credit that could be attributed based on recorded levels of energy production. The nature of the wind regime that acts as the prime mover of the wind capacity was ignored. To begin to incorporate this into the wind capacity model an appropriate data set is required. To address this wind speed data was gathered from six weather stations (Belmullet, Clones, Knock, Malin Head, Shannon and Valentia). The data consists of ten years of hourly recordings over the period November 1994 to October 2004 in all cases except Knock where the data was only available from 1996 onwards.

In this chapter this wind speed data set will be explored in terms of its statistical properties, the various auto and cross-correlation relationships that exist within the data and also in terms of the frequency components found. It is intended that this data will form the basis of a wind model. To investigate the appropriateness of this application the findings from the analysis of the wind data set described above will be compared to a similar analysis of recorded wind power series. The wind power data series are records from six Airtricity wind farms in R.O.I. The six sites are Culliagh and Cronalaght Co. Donegal, Corneen and Snugborough Co. Cavan, Kingsmountain Co. Sligo, Carnsore Co. Wexford. The duration of the records from these six sites varies from one to a few years and are made on a half hourly basis. Initially the wind speed data will be analysed and then the wind production data will be used to verify that the characteristics found in the wind speed data are reflected in the wind production data.

### **5.2 WIND SPEED DATA**

#### **5.2.1 Mean And Standard Deviation Of Wind Speed Data**

In Table 22 the annual mean wind speed of the data are tabulated and this data is plotted in Figure 27. One of the clearest results that can be seen from Figure 27 is that the

average wind speed found at Malin Head and to a lesser extent at Belmullet are much higher than those recorded at the other sites. The main reason for this is that the records at Malin Head are made using a 22 m mast and at Belmullet a 12 m mast was used while at the rest of the sites 10 m meter masts were used. The increase in mean wind speed with mast height is due to the reduced effect of friction with the surface as height increases.

Table 22: Annual mean wind speed values

Year	Belmullet	Clones	Knock	Malin Head	Shannon	Valentia
1995	7.30	4.22	N/A	8.52	4.80	4.82
1996	6.63	3.62	N/A	8.15	4.50	4.61
1997	6.86	3.72	4.95	7.88	4.51	4.26
1998	7.02	4.34	5.14	8.23	4.66	4.62
1999	7.34	4.39	5.34	8.49	4.89	4.81
2000	7.30	4.17	5.06	8.05	4.52	4.93
2001	5.65	3.96	4.92	7.87	4.45	4.55
2002	6.76	4.11	5.07	7.71	4.63	4.92
2003	6.25	4.03	4.93	7.56	4.63	4.74
2004	6.58	4.05	5.02	7.74	4.82	4.86
Mean	6.77	4.06	5.06	8.02	4.64	4.71

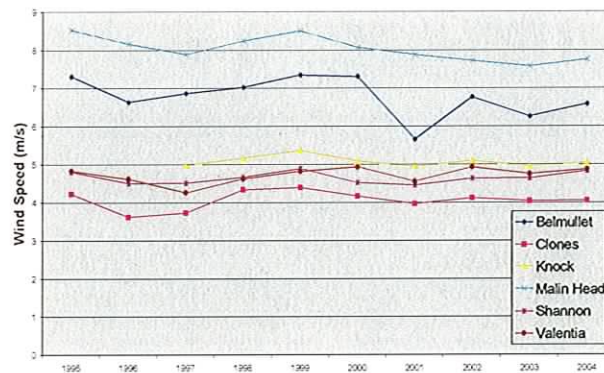


Figure 27: Annual mean wind speed values

The question of the significance of variations in annual wind energy capture due to the variation in mean wind speed and the effect this has on the calculation of capacity credit for wind capacity was considered in [28],[29]. This question can in more general terms be addressed by calculating the annual variation in mean wind speed as a percentage of the mean wind speed for the length of the data set. In Figure 28 the result of this process is shown.

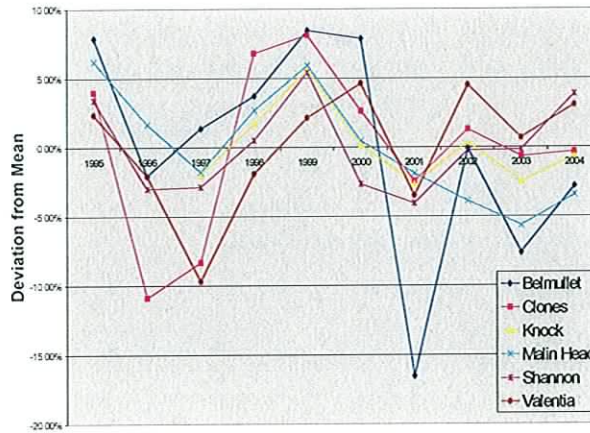


Figure 28: Percentage annual variation from mean

Figure 28 shows that the possibility exists for a large degree of inter-annual variation in mean wind speed with the largest variation shown to be in the order of 17% but that a typical value at least for the data set available would be 3% variation from the mean. Another important aspect in characterising a wind regime is the degree to which the wind speed is affected by a seasonal variation. To investigate this aspect, the monthly mean wind speed from each site over the length of the data set was calculated. In Figure 29 the results of this process for the Malin Head data is shown. Each line in the figure represents one year of data running from November to October

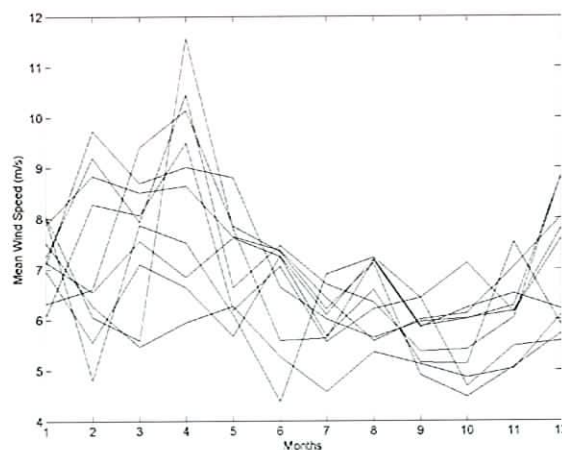


Figure 29: Monthly mean wind speed values

Although there is a large degree of variation between the different years, a general pattern emerges where the mean wind speed tends to be higher in the second to fourth month (December to February) and lower in the seventh to tenth month which corresponds to May to August. This result is intuitively correct, as it would be expected that the mean wind speed would be higher in winter than in summer. In order to quantify this effect the maximum monthly variation between winter and summer is expressed as a percentage of the maximum monthly mean for that year. By repeating this process over the ten-year period and then averaging the results a term is derived that is considered being reflective of the seasonal variation in the data. This seasonality indicator (S.I.) is defined in Equation (5.2.1)

$$S.I. = \frac{\sum_{y=1}^{10} \left[ \frac{SPM_y - WPM_y}{SPM_y} \right]}{10} \quad (5.2.1)$$

where  $SPM_y$  and  $WPM_y$  are the winter and summer peak monthly means for year  $y$

This process was implemented for each of the six sites. This seasonality indicator ranges from zero where there is no seasonal variation, to a hundred where the wind speeds vary from their peak to zero. From Table 23 it can be seen that the maximum seasonal variation occurs at the Valentia site but that the range of values across the six sites is small.

Table 23: Calculated value of seasonality indicated

Year	Belmullet	Clones	Knock	Malin Head	Shannon	Valentia
1995	42.06	57.85	N/A	44.22	40.86	57.09
1996	37.12	48.24	N/A	44.61	34.28	48.47
1997	51.73	57.91	48.35	50.50	52.09	70.21
1998	41.45	32.36	34.84	36.55	29.13	48.26
1999	36.86	33.05	32.17	36.40	28.95	34.37
2000	48.64	49.57	48.56	54.65	41.31	52.08
2001	39.25	36.82	32.27	46.48	35.22	46.47
2002	55.94	49.31	46.44	51.16	53.33	54.27
2003	45.58	41.68	42.55	45.98	39.52	47.87
2004	32.64	32.82	30.91	36.61	27.70	34.96
Average	43.13	43.96	39.51	44.71	38.24	49.40

The mean wind speed is an important indicator of the suitability of a particular site for the development of a wind capacity site with a direct correlation between mean wind speed and profitability existing over a certain range. But another important factor is the degree of variability in the wind speed on an hour-to-hour basis. The standard deviation of the data can be used to give an impression of the degree of variability that exists in the data. In Table 24 the standard deviations calculated on an annual basis and the average standard deviation over the whole period are shown.

Table 24: Standard deviations found in data set

Year	Belmullet	Clones	Knock	Malin Head	Shannon	Valentia
1995	3.54	2.76	N/A	3.93	2.74	3.23
1996	3.23	2.45	N/A	3.87	2.70	3.01
1997	3.79	2.51	2.68	4.15	2.71	3.26
1998	3.56	2.26	2.65	3.85	2.64	2.93
1999	3.73	2.39	2.82	4.01	2.78	2.87
2000	3.90	2.34	2.88	4.31	2.85	3.13
2001	3.28	2.26	2.54	3.82	2.61	2.95
2002	3.71	2.25	2.74	4.04	2.85	3.10
2003	3.46	2.08	2.47	3.93	2.51	2.69
2004	3.34	2.12	2.51	3.71	2.72	2.91
<b>Average</b>	3.55	2.34	2.66	3.96	2.71	3.01

The values in Table 24 in values given are in absolute terms and do not allow for direct comparison because, as mentioned above, there is a difference in the mast height used in recording the data between some of the sites. To overcome this, the standard deviations are divided by the mean wind speed calculated for the same period. In this way the values are relative to the means, which results in their being corrected for differences in the way they were recorded allowing for direct comparison. The results from this process are shown in Table 25, these figures suggest that Malin Head has the lowest degree of variability while Valentia has the highest.

Table 25: Calculated standard deviations divided by the mean for the same period

Year	Belmullet	Clones	Knock	Malin Head	Shannon	Valentia
1995	0.48	0.65	N/A	0.46	0.57	0.67
1996	0.49	0.68	N/A	0.48	0.60	0.65
1997	0.55	0.67	0.54	0.53	0.60	0.77
1998	0.51	0.52	0.51	0.47	0.57	0.63
1999	0.51	0.54	0.53	0.47	0.57	0.60
2000	0.53	0.56	0.57	0.53	0.63	0.64
2001	0.58	0.57	0.52	0.49	0.59	0.65
2002	0.55	0.55	0.54	0.52	0.62	0.63
2003	0.55	0.52	0.50	0.52	0.54	0.57
2004	0.51	0.52	0.50	0.48	0.57	0.60
Average	0.53	0.58	0.53	0.49	0.58	0.64

### 5.2.2 Probability Distribution

In Figure 30 the probability distributions calculated directly from the data from the six sites are shown. While some of the distributions are very similar to a typical Weibull distribution (Clones and Knock) others are closer to a bimodal distribution (Valentia).

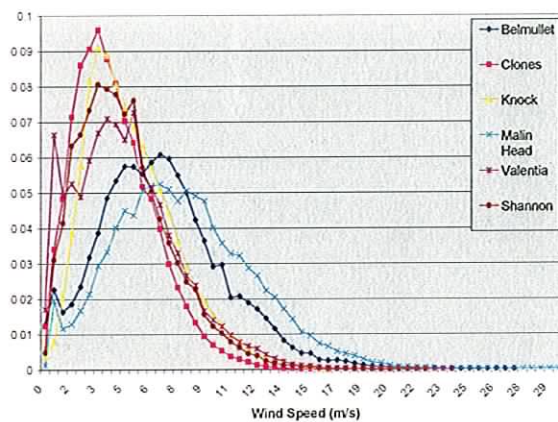
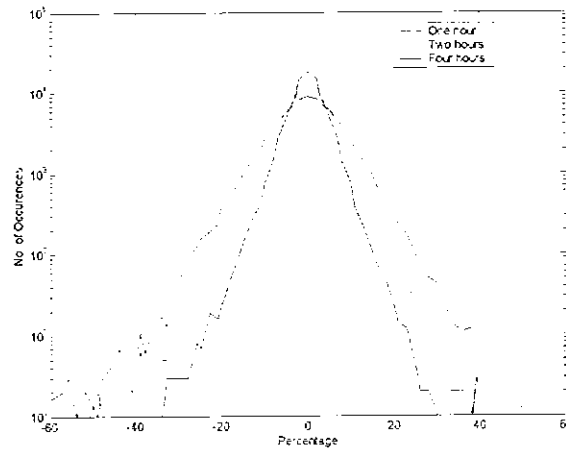


Figure 30: Probability distributions calculated for the six sites

### 5.2.3 Variation Analysis

Often in considering wind capacity, one of the key considerations is the persistence of the wind speed and consequentially the wind power at a particular site. In [56] this question was addressed by calculating the percentage change in wind power over three time horizons of one, two and four hours. For each of this time horizons the percentage changes were divided into bins i.e. 0%-10%, 10%-20% etc. The number of times that each percentage change bin occurred was found. This method was adapted to use wind

speed and results of applying this method to the data from Malin Head are presented in Figure 31.



**Figure 31: Plot of the percentage variation on three different time horizons from the Malin Head data**

From Figure 31 it can be seen that in the one hour time frame, the maximum percentage change over the course of the ten year period is approximately 40% and that this happened once, while there were approximately 2000 hours were less than a one percent change in the wind speed. The effect of increasing the time horizon from one to two and then to four hours was to increase the extreme values of percentage change found and a general increase in the number of large percent changes. Also there was a reduction in the number of hours that the percentage change was less than one percent. When this type of analysis was repeated for the other five sites similar results were found.

#### 5.2.4 Auto- And Cross-Correlation

Another important factor in the analysis of wind series is the degree of correlation that exists between the different sites. The importance of this aspect of wind is significant in the analysis of system adequacy. Conventional plant outages are considered to be independent events. That is, an outage at one unit does not effect the likelihood of an outage at any other unit i.e. they are uncorrelated. While the outages of wind capacity that are caused by a component failure (such as a turbine failure) can also be considered independent, this assumption of independence cannot be extended to wind capacity







when considering the effects of a reduction of wind speed resulting in a reduction of the energy output of the wind capacity.

To investigate the degree to which a drop in wind speed at one site is likely to occur at the same time as a drop in wind speed at a different site a cross correlation between the recorded wind speed from the two sites is calculated. The equation for cross correlation coefficient between two series is given in Equation (5.2.2).

$$X - Corr = \frac{\sum [(x - \bar{x})(y - \bar{y})]}{\sqrt{\sum (x - \bar{x})^2 \sum (y - \bar{y})^2}} \quad (5.2.2)$$

The cross correlation coefficient is an index that indicates the degree of linear independence. Therefore if there is strong linear relationship between two series there will be a large correlation between them with the maximum correlation of unity occurring when one series is a scaled version of the other. A low or zero correlation indicates that two series are linearly independent. A negative value occurs when there is an inverse correlation between two series. The various cross correlation coefficients between the different sites were calculated on an annual basis. In Table 26 the mean results of this calculation are tabulated, and in Figure 32 the correlations between Belmullet and the other sites over the ten-year period are shown.

Table 26: Mean cross correlations coefficient calculated

	Belmullet	Clones	Knock	Malin Head	Shannon	Valentia
Belmullet	1	0.67	0.77	0.64	0.65	0.60
Clones	0.67	1	0.80	0.70	0.70	0.61
Knock	0.77	0.80	1	0.65	0.77	0.68
Malin Head	0.64	0.70	0.65	1	0.52	0.47
Shannon	0.65	0.70	0.77	0.52	1	0.76
Valentia	0.64	0.60	0.68	0.47	0.76	1

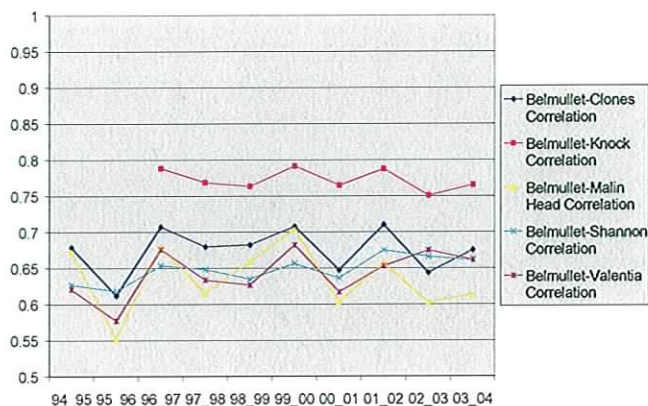


Figure 32: Annual cross correlation coefficients

In Table 26 the strongest correlation seen is between Knock and Clones and the weakest correlation is between Malin Head and Valentia. The reason for this the relative proximity of Knock to Clones while Malin Head and Valentia are the two sites with the greatest distance between them. In Figure 32 this relationship between correlation and distance between sites is borne out with the strongest correlation being between Belmullet and Clones and the weakest being between Belmullet and either Valentia or Malin Head.

The auto-correlation is calculated using the same formula as the cross correlation but in this case a series of calculations are made were a series is correlated to a time lagged version of itself. In the first iteration the time lag is set to zero and therefore the correlation coefficient calculated is unity. In the second iteration the second series lags the original series by one sample period. The calculation is repeated in this way the number of iterations will depend on the length and nature of the signals being investigated. The result of this process defines the auto-correlation function of the series. This offers a method to investigate the periodicity that exists in the series in Figure 33 the auto-correlation functions of the six sites for the year 1994-1995 are shown.

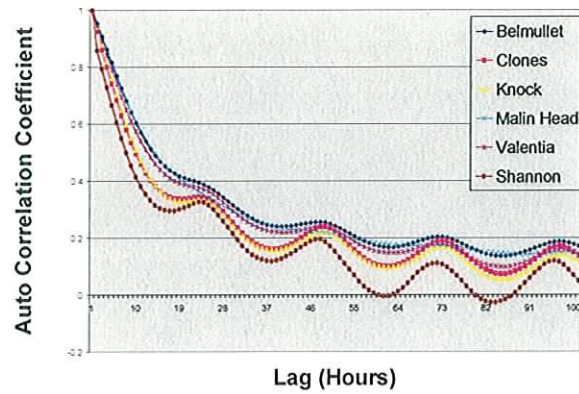


Figure 33: Auto-correlation functions of the six sites

All the sites produce a similarly shaped auto correlation function with the correlation coefficients in all cases dropping rapidly from unity in the form of a damped sinusoid.

### 5.2.5 Frequency Domain Analysis

The period of the damped sinusoid is 24 hours, which suggests the presence of a diurnal cycle in the wind speed series. To further investigate the frequency content of the wind speed data, Fourier analysis can be applied with a sampling rate of one sample per hour. To illustrate the proposed method it is applied to wind data recorded from Malin Head from October '95 to October '96. Before Fourier analysis is applied, the data is normalised. To normalise the data it is divided into appropriate sections i.e. weeks or months. The mean of each section is calculated and then subtracted from the data in each section so the data becomes zero centred. When this is done the standard deviation of each of the sections is calculated and the normalised data is found by dividing each section by its standard deviation. In Figure 34 the normalised version of the original data is shown.

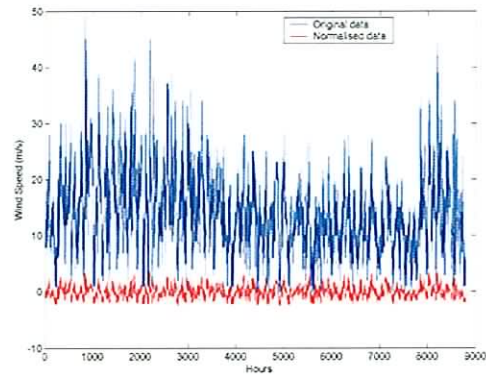


Figure 34: Normalised version of the original data

This normalisation process acts like a high pass filter on the data so that the dc and very low frequency components in the data are removed. The reason for doing this is to avoid these low frequency components, which have the high amplitudes from swamping the rest of the frequency spectrum of the series. Figure 35 shows a periodogram of the normalised data. The periodogram shows that there are some strong frequency components in the data. To make the periodogram easier to interpret the x-axis is inverted and scaled so that it denotes period in terms of days per cycle. Figure 36 shows this adjusted periodogram.

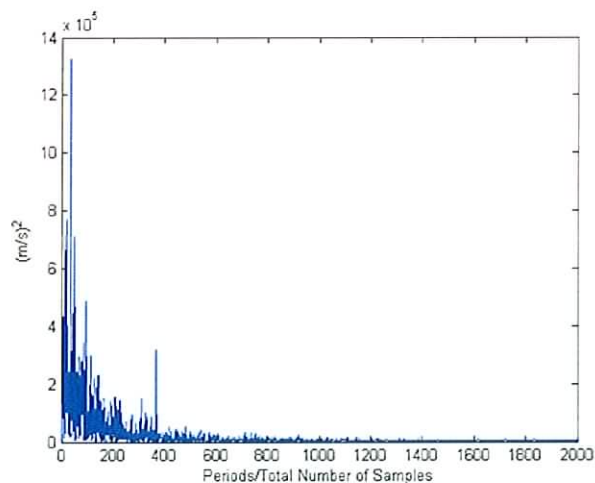
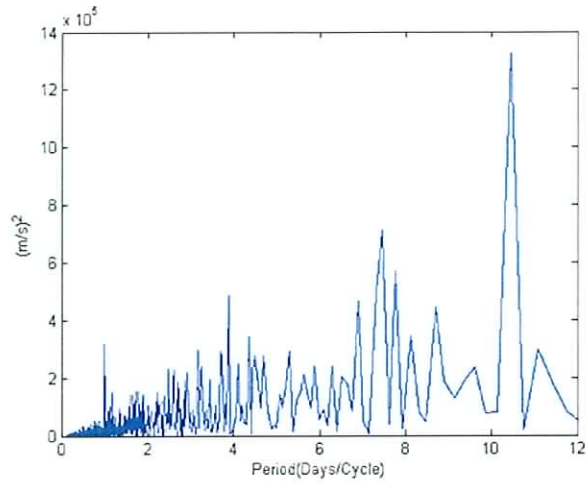
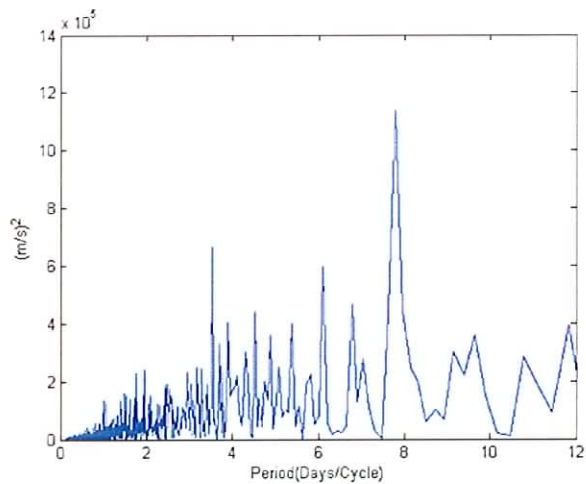


Figure 35: Periodogram of the normalised sample data



**Figure 36: Adjusted periodogram of the normalised sample data**

From Figure 36 four strong components can be picked out. The largest at approximately 11 days then 7 days, 4 days and finally 24-hours. The set of graphs from Figure 37 to Figure 38 show the same analysis applied to different years at the same site.



**Figure 37: Periodogram of normalised data from Nov. 95 to Oct. 96**

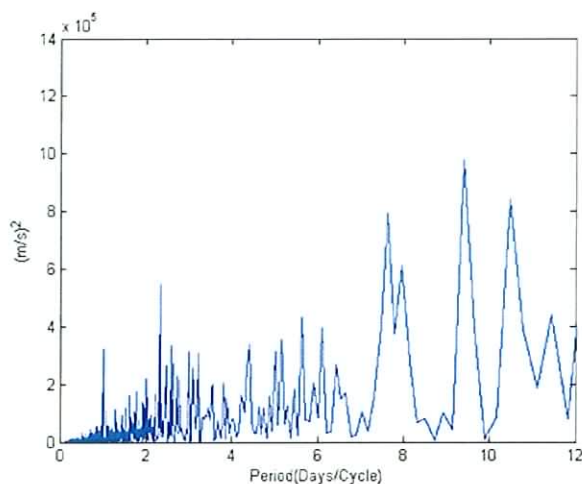


Figure 38: Periodogram of normalised data from Nov. 98 to Oct. 99

From the set of figures above it can be seen that the year on year variability of the amount of energy seen in individual frequency components is quite large but that there are certain trends that can be observed. For example strong components occur regularly around the 8-day period and in all cases the 24-hour period features strongly. If the same analysis is applied to a ten-year data set at the same location (November 1994 to October 2004) then the periodogram in Figure 39 results. Here, the observed trends are reflected.

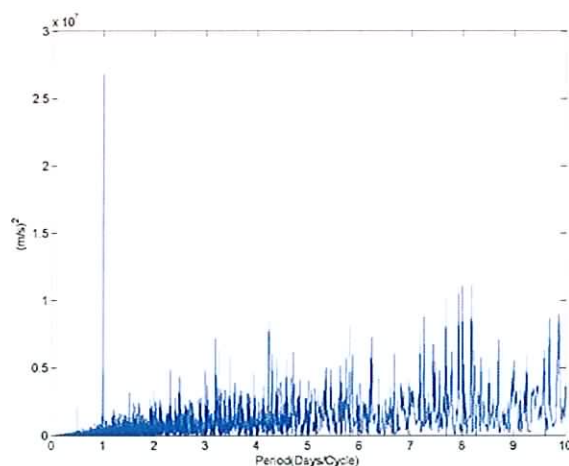


Figure 39: Periodogram of normalised data from Nov. 94 to Oct. 04

Figure 40 and Figure 41 extends this analysis to the Valentia site. In these plots a very clear pattern can be seen with very strong frequency components seen at the 24-hour



and 12-hour period in all years. This trend is again reflected in the periodogram of the ten-year data set from Valentia (November 1994 to October 2004) as shown in Figure 42.

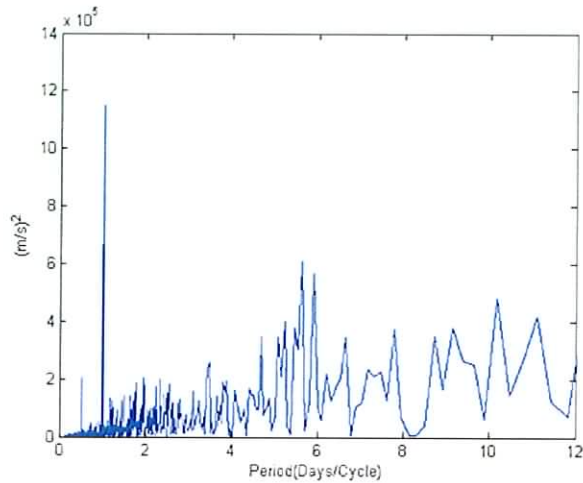


Figure 40: Periodogram of normalised Valentia data from Nov. 94 to Oct. 95

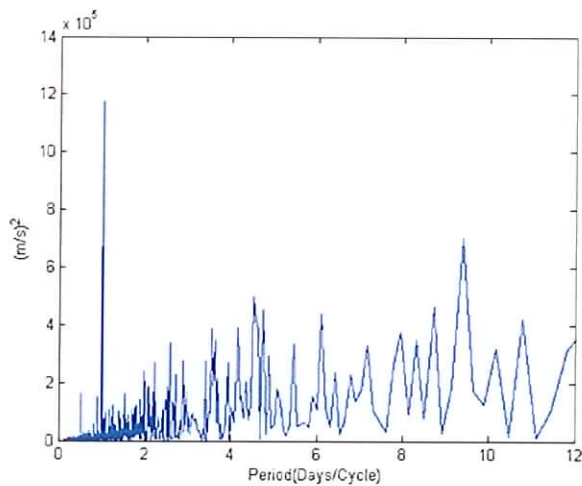


Figure 41: Periodogram of normalised Valentia data from Nov. 95 to Oct. 96

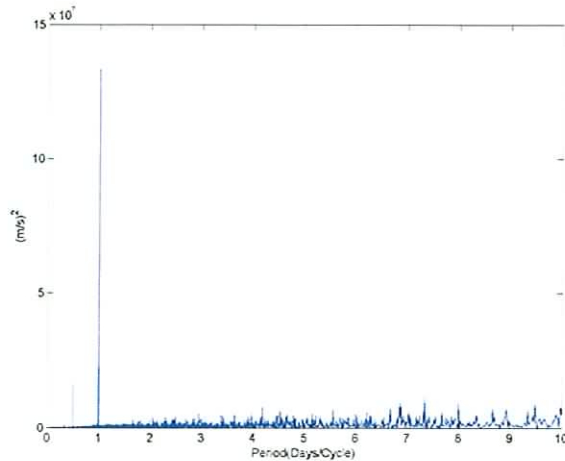


Figure 42: Periodogram of normalised Valentia data from Nov. 99 to Oct. 04

From Figure 39 and Figure 42 it can be seen that over the ten-year period the consistency of the diurnal pattern results in the amplitude of the frequencies that form this pattern dominate the frequency spectrum. In the periodogram that is based on individual years there are strong frequency components around the 11 day, 7 day and 4 day period elements. These elements are driven by the synoptic patterns caused by the flow of areas of relatively high and low pressure passing across the country that had occurred that year. But as the synoptic patterns vary from year to years the periods and amplitudes of these components change from year to year and therefore there overall importance is reduced. In terms of characterising the wind regime at a particular site it can be established that in any year the diurnal pattern will result in strong frequency components principally at the 24-hour and 12-hour period and that the synoptic patterns will result in strong frequency components around the 11 day, 7 day and 4 day periods but that exact frequency of these component can not be predicted.

### 5.3 WIND PRODUCTION DATA

The production data that was made available is from six wind farms details of which are given in Table 27.

Table 27: Wind farm information

Location	Capacity (MW)	Turbine Type
Cullagh, Co. Donegal	11.88	660kW Vestas
Coreen, Co. Cavan	3	1.5 MW G.E.
Kingsmountain, Co. Sligo	25	2.5 MW Nordex
Cronlaght, Co. Donegal	1.98	n/a
Carnsore, Co. Wexford	11.9	850 kW Vestas
Snogborough, Co. Cavan	13.5	1.5 MW G.E.

The main reason for analysing these wind power series is to investigate whether the frequency components that have been seen in the wind speed series are reflected in the wind power series. In Figure 43 the duration of the record from each site is shown.

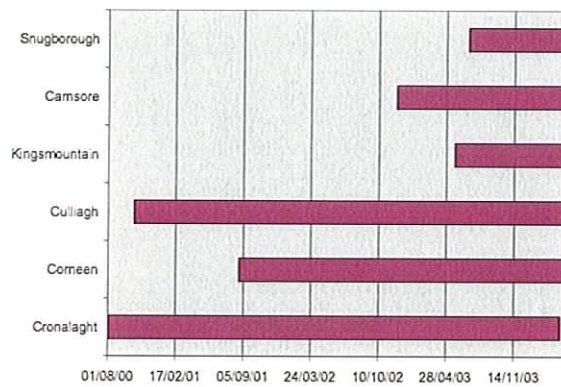


Figure 43: Duration of the available wind power series

To investigate the degree to which the diurnal pattern that was seen in the wind speed data was reflected in the wind power data, the data from each site was summed so that the total energy production in each hour of the day over the course of the available record was found. These sets of 24 values were then divided by the number of days in the record to give the average hourly production of each site and then the total average over the twenty four hour period was subtracted from each hour to zero centre the calculated values to allow for comparison. The results of this process are shown in Figure 44

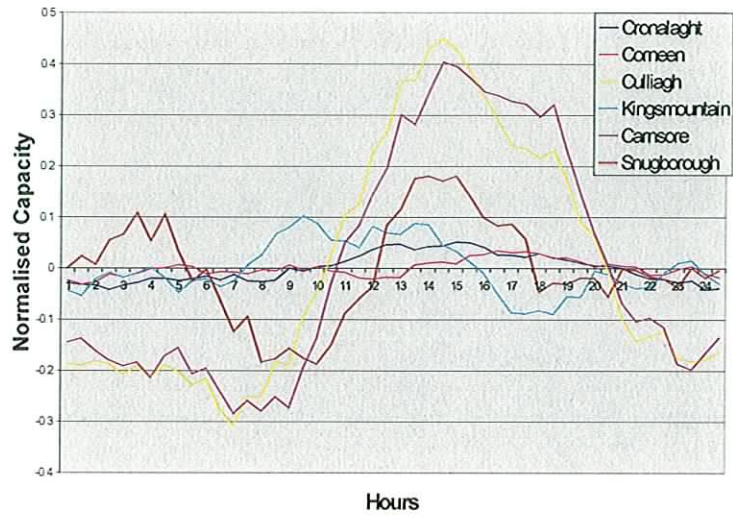


Figure 44: Diurnal patterns in wind production data

From Figure 44 it can be seen that a clear diurnal pattern exists at the six sites but the relative scale of this pattern can not be read from Figure 44 as the values have not been normalised in terms of the relative capacity of the different sites.

## 5.4 CONCLUSION

Various aspects of the wind speed data that was acquired from six Met Eireann weather stations has been investigated including the annual variation from the overall mean, the formulation and calculation of a seasonality indicator, the relative variability and the strength of the cross correlation that exist between the six sites. Also the periodicity was investigated using both the auto-correlation and the Fourier transform. From this analysis the effect of the diurnal and synoptic patterns on the frequency spectrum was noted. The presence and consistency of the diurnal pattern were further shown when recorded wind power series from six Airtricity wind farms were examined to see if this pattern was present in this data. From these observations the key points that any wind capacity model should be able to encompass were determined, such the inter-annual mean and standard deviation, the annual and diurnal pattern and the inter-site correlation relationship.

## 6 TIME SERIES METHODS

### 6.1 INTRODUCTION

In Chapter 5 the statistical properties of a wind speed data set acquired from Met Eireann was investigated. This data set is intended to be the basis of a wind capacity model which will be able to generate  $n$  years of hourly wind energy estimates which can in turn be combined with a Monte Carlo based adequacy indices calculation. This process can be divided into two sections: the generation of  $n$  years of wind speed estimates and the application of these wind speed estimates to form wind energy estimates. In this chapter the use of time series modelling to implement the first of these sections is discussed. This modelling method will be extended to all six Met Eireann wind speed records. The resulting wind speed estimates are compared to the original recorded series in terms of their statistical properties and probability distributions. Also the need to insure that the simulated wind speed estimates have the same correlation coefficient matrix as the recorded data is addressed.

### 6.2 INTRODUCTION TO TIMES SERIES MODELS

Time series are generally used to describe, explain, predict and control a data set [57]. In many cases recorded values of a variable are used as a basis of a time series model so that future values of the variable can be predicted. One of the most simplistic stochastic processes that can be applied as a time series model is that of a random draw.

$$x(t) = z(t) \tag{6.2.1}$$

where  $z(t)$  is a random draw from a distribution of specified mean and variance and  $t$  is a discrete time variable.

It follows that the mean of the process will be constant and the auto-covariance function will be zero for all values of lag greater than one and therefore is also time invariant.

When the mean and auto-covariance function of a process are both time invariant the resulting time series is said to be second order stationary.

Generally a time series can be considered to be stationary if there is no systematic change in the mean of the series, if there is no systematic change in variance and if periodic variations have been removed. By definition a series is said to be strictly stationary if the joint distribution (i.e. the combined distribution of the time series and a lagged version of itself of the time series) is time invariant. This means that a shift in the time origin has no effect on the joint distribution. Second order stationarity is a similar definition but only considers the first two moments of the joint distribution.

Another example of a straightforward time series model is a random walk, which can be defined as in Equation (6.2.2)

$$x(t) = x(t-1) + z(t) \quad (6.2.2)$$

where  $z(t)$  is a random draw from a distribution of mean ( $\mu$ ) and variance ( $\sigma_z^2$ )

At  $t=0$   $x(1)=z(1)$

and

$$x(t) = \sum_i^t z(i) \quad (6.2.3)$$

Therefore the mean of the series can be calculated as the expectation of the series and the variance of the series can be calculated as the expectation of the square of the series minus the mean.

$$E(x) = \frac{\sum_{i=1}^t \sum_{i=1}^t z(i)}{t} = t\mu \quad (6.2.4)$$

Similarly

$$Var(x) = \frac{\sum_{i=1}^t \left[ \sum_{i=1}^t z(i) - \mu \right]^2}{t} = t\sigma_z^2 \quad (6.2.5)$$

As the mean and variance are dependent on time the process is non-stationary. A moving average process of order  $q$  (i.e. MA( $q$ )) can be defined as

$$x(t) = \beta_0 z(t) + \beta_1 z(t-1) + \dots + \beta_q z(t-q) \quad (6.2.6)$$

where  $z(t)$  is a random draw from a distribution of mean zero and variance ( $\sigma_z^2$ )

$\{\beta_i\}$  are the parameters of the model

The mean and variance can again be found as the expectation of the series and the variance of the series can be calculated as the expectation of the square of the series minus the mean.

$$E(x) = \frac{\sum_{i=0}^t (\beta_0 z(i) + \beta_1 z(i-1) + \dots + \beta_q z(i-q))}{t} = 0 \quad (6.2.7)$$

$$Var(x) = \frac{\sum_{i=1}^t ((\beta_0 z(i) + \beta_1 z(i-1) + \dots + \beta_q z(i-q)) - \mu)^2}{t} = \sigma_z^2 \sum_{i=0}^q (\beta_i)^2 \quad (6.2.8)$$

Therefore the second moment is time invariant and the moving average model is second order stationary. The auto-covariance function can be shown to be dependent on the values of  $\{\beta_i\}$  values for lag less than or equal to the order of the model and all other values are zero. The auto-correlation function is derived from the auto-covariance function. With a value of one for zero lag the auto-correlation function will reduce to zero for values of lag greater than the order of the model.

The auto-regressive process of the order  $p$  (i.e. AR( $p$ )) can be defined as in Equation (6.2.9).

$$x(t) = \alpha_1 x(t-1) + \alpha_2 x(t-2) + \dots + \alpha_p x(t-p) + z(t) \quad (6.2.9)$$

In this way the current value of  $x$  is proportional to past values of  $x$  plus a random number  $z$  whose source distribution has a mean  $\mu$  and variance  $\sigma^2$ . This equation can be rewritten using the backward shift operator  $B$  as in Equation (6.2.10).

$$(1 - \alpha_1 B - \dots - \alpha_p B^p)x(t) = z(t) \quad (6.2.10)$$

It has been shown by [57] that AR models will be stationary when the roots of the Equation (6.2.11) lie outside the unit circle.

$$\phi(B) = 1 - \alpha_1 B - \dots - \alpha_p B^p = 0 \quad (6.2.11)$$

By combining a moving average and auto-regressive, a model of the form in Equation (6.2.12) can be formed.

$$x(t) = \alpha_1 x(t-1) + \dots + \alpha_p x(t-p) + z(t) + \beta_1 z(t-1) + \dots + \beta_q z(t-q) \quad (6.2.12)$$

This type of model are termed auto-regressive moving average of order (p,q) i.e. ARMA(p,q). Using the backward shift operator this equation can be written as in Equation(6.2.13).

$$\phi(B)X(t) = \theta(B)z(t) \quad (6.2.13)$$

where

$$\phi(B) = 1 - \alpha_1 B - \dots - \alpha_p B^p \quad (6.2.14)$$

and

$$\theta(B) = 1 + \beta_1 B + \dots + \beta_q B^q \quad (6.2.15)$$

As discussed above the moving average section of the model is second order stationary regardless of the parameter values chosen and the auto-regressive section of the model will be second order stationary if the roots of  $\phi(B)$  lie outside the unit circle. The importance of ARMA models is that a stationary time series can often be described by a lower order ARMA model than by a pure MA or AR model.



Deciding which of these model types to apply in different situations can be a difficult problem. It is suggested in [57] that a good indication of the type of model to apply is a plot of the auto-correlation function or correlogram. If the correlogram of a time series tends to alternate with successive observations, then the time series will also alternate on different sides of the overall mean. A non-stationary time series will result in a correlogram where values only trend to zero at large lag values. This is because an observation on one side of the overall mean trend to be followed by a large number of further observations on the same side of the overall mean because of the trend in the time series. If a time series contains a periodic variation, then the correlogram will also show an oscillation over the same period. By comparing the correlogram of an observed time series to the theoretical correlogram of a MA, AR and ARMA model the appropriate model type can be chosen. The correlogram of a MA model will cut off at a lag  $q$ , while an AR model will produce a correlogram formed from exponentially damped sinusoids. The ARMA model will be a mixture of these two elements and will tend to attenuate slowly rather than cut off.

Once the type of model to be used is established the parameters of the model and the order of the model need to be determined. For an AR model of order  $p$  the parameters of the model can be fitted using a least squares method by minimising the sum of squared residuals as shown in Equation (6.2.16) with respect to  $\alpha_1 \dots \alpha_p$

$$S = \sum_{t=p+1}^N [x(t) - \alpha_1 x(t-1) - \dots - \alpha_p x(t-p)]^2 \quad (6.2.16)$$

To find the best order of the model one approach is to fit an AR model of successively higher order and then plot the residual sum of squares for each order of the model against the order of the model. From this plot the order of model where the improvement from increasing the order of the model saturates can be seen. Estimating the parameters of a MA model requires an iterative process, as the residual sum of squares of a MA model is not a quadratic function of the parameters. Initial values of the parameter are chosen and then the resulting residual sum of squared errors calculated. Further values of the parameter are chosen so as to minimise the residual sum of squared errors. The order of a MA model can normally be determined from the

correlogram of the time series being modelled as the cut off lag of the correlogram indicates the appropriate order of the model.

Estimating the parameters of an ARMA model is similar to estimating the parameters of an MA model in that an iterative process is used to find the parameters that minimise the residual sum of squares. The order of an ARMA model can be chosen in a similar way to an AR model in that the order of the model is successively increased and the benefit gained on each increase in order is used to determine if the added complexity of increasing the order is worthwhile. Once a model has been fitted the question of how well the model represents the derived data is addressed by comparing the model and the observed correlogram and by analysis of the residuals. If the model is well fitted to the data then the residuals will be random and relatively small. The structure of an ARMA model is intuitively appealing to form the basis of wind series models as the current value is influenced by one or more previous values combined with a noise term. But as has been discussed above the ARMA model can only be applied to stationary series and as has been shown in Section 5.2 the wind series data from the Met Eireann stations has shown itself to be unstationary, as both the mean and the variance of the data from all the sites displays a clear trend over the course of a year and also the diurnal pattern represents a strong periodic element in the data. Therefore before the wind series can be modelled using an ARMA model these artefacts of the data must be addressed.

### **6.3 *PURPOSED DEVELOPMENT OF WIND MODELS***

The implementation of this model is split into three sections. The objective of the first section is to normalise the variance and mean of the wind speeds in the data and in this way remove the annual trend from the data. This process can also be seen as a filtering process where the low frequency elements in the data are greatly reduced making the rest of the spectrum more easily investigated. The second divides the recorded wind series into periodic and stochastic elements. This essentially involves removing the diurnal pattern from the normalised data. In the third section the stochastic elements are modelled using an ARMA model. This is then used to generate iterations of the modelled stochastic process, which in turn are recombined with the periodic elements and then denormalised. The objective of this process is to form possible wind series that could occur at the site where the original is recorded. To illustrate the proposed method

it is applied to wind data recorded from Malin Head from October 1995 to October 1996. The recorded data is plotted in Figure 45. In Figure 46 a plot of the probability density function as calculated directly for the wind data is shown. Also the Weibull distribution that was fitted to the data using maximum likelihood estimates to a confidence interval of 95%, the result of this was a Weibull distribution with a scale parameter of 0.0299 and a shape parameter of 2.1712 are also shown in Figure 46.

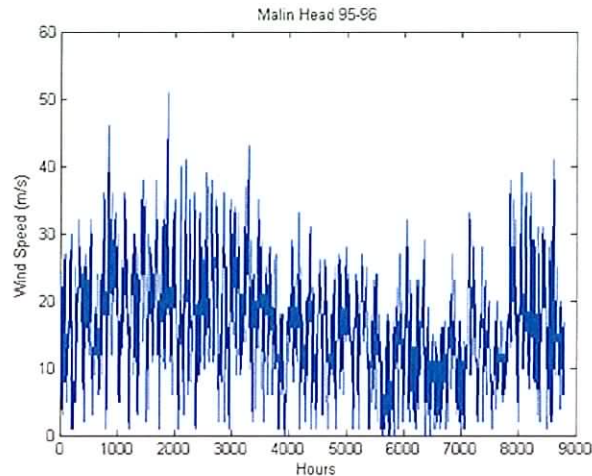


Figure 45: Plot of the original recorded wind speed

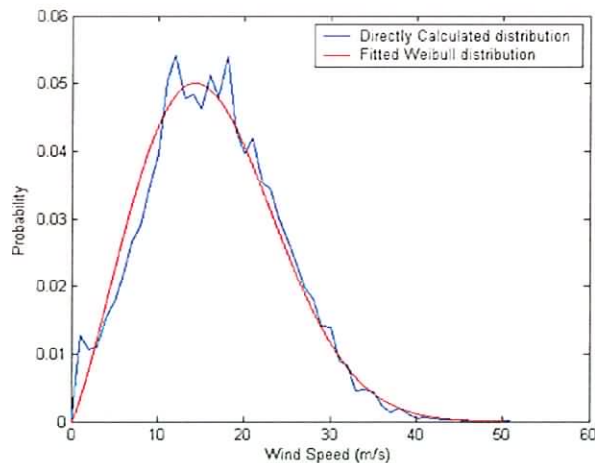


Figure 46: Probability density function of data

### 6.3.1 Data Normalisation

The implementation of the first section is straightforward. The data is divided into appropriate sections i.e. weeks or months. The mean of each section is calculated and then subtracted from the data in each section so the data becomes zero centred. When this is done the standard deviation of each of the sections is calculated and the normalised data is found by dividing each section by its standard deviation. In Figure 47 the normalised version of the original data is shown. In the example shown below the recorded data was split into month long sections the resulting calculated values of standard deviation are shown in Table 28.

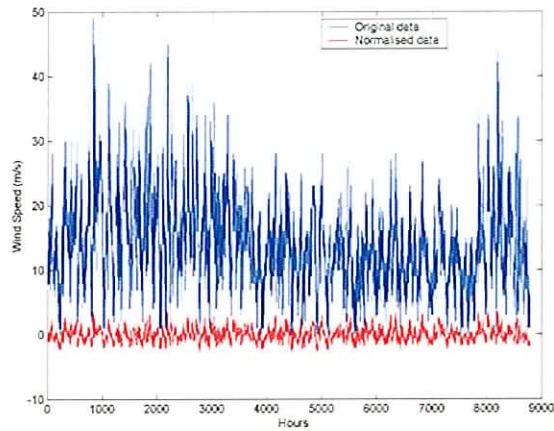


Figure 47: Normalised version of the original data

Month	Mean	Standard Deviation	Month	Mean	Standard Deviation
January	11.36	4.12	July	5.91	3.38
February	9.97	3.91	August	5.91	2.91
March	10.33	3.94	September	6.75	3.34
April	8.211	3.52	October	7.71	3.52
May	7.97	3.12	November	8.42	3.40
June	8.38	2.56	December	10.67	4.38

Table 28: Calculated statistical data

### 6.3.2 Separating the Data Components

The objective of the second section to divide the recorded wind series into periodic and stochastic elements, this can be implemented by a number of different methods. In the following sections a number of these methods are discussed.

### 6.3.2.1 Time domain removal of dominant elements over total sample

In the first of these the Fourier transform of the wind series is taken and a periodogram calculated as the square of the modulus of the discrete Fourier transform. The dominant frequency components are highlighted by the periodogram and these correspond to strong periodic elements within the wind series. Figure 48 shows the periodogram of the sample data. From this plot it can be seen that there are strong peaks occurring at approximately the nine and six day interval and to a lesser degree at the three-day interval.

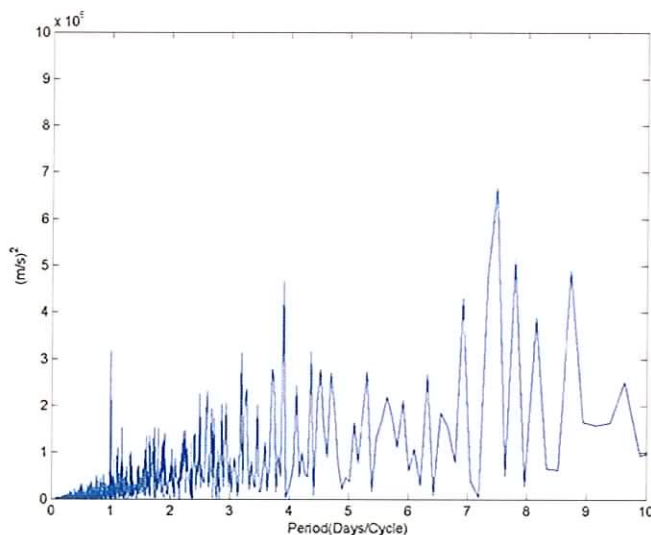
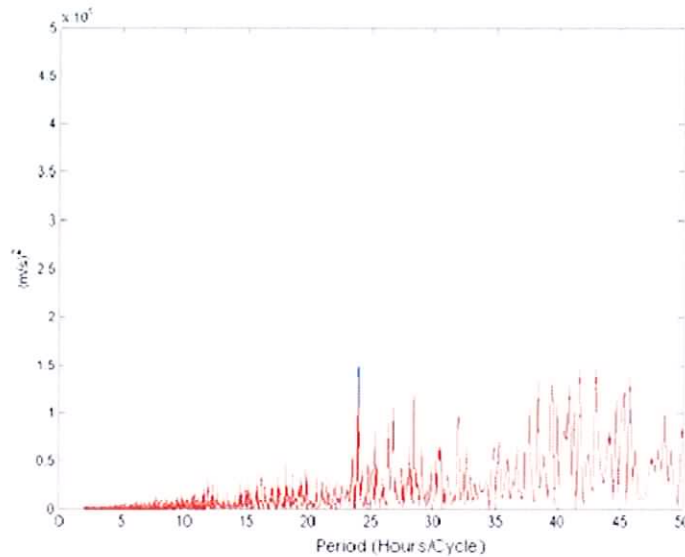


Figure 48: Periodogram of sample data

These elements can be removed by using the corresponding frequency to calculate the time interval equivalent to one period. Then a set of average values is found in the wind series based on the derived time interval and this set of values is subtracted from the recorded series periodically. While this process has the effect of reducing the periodicity found at the target frequency, because the set of averages is based on the full series length, the calculated average values are small relative to the values in the normalised series. Therefore the effect on the periodogram is limited as shown in Figure 49 and in

Figure 50 a closer view of the target frequency is shown. It can be seen that the power seen at the 24 hour/cycle interval has been reduced from approximately  $2.03 \times 10^7$  to  $1.41 \times 10^7$  (m/s)<sup>2</sup>.



**Figure 49: Effect of method on the periodogram**

To improve performance the series can be split into sections. The length of the sections was determined so that the number of sections and the number of periods of the target frequencies in each section are as similar as possible. For example the largest peak in Figure 49 occurs at 24 hours/cycle. This results, for the length of the sample data set in 20 sections with 19 periods per section each period is 24 samples long giving a total sample length of slightly less than one-year. The effect of this change is to increase the value of the averages being subtracted and so increases the level of reduction at the target frequency.

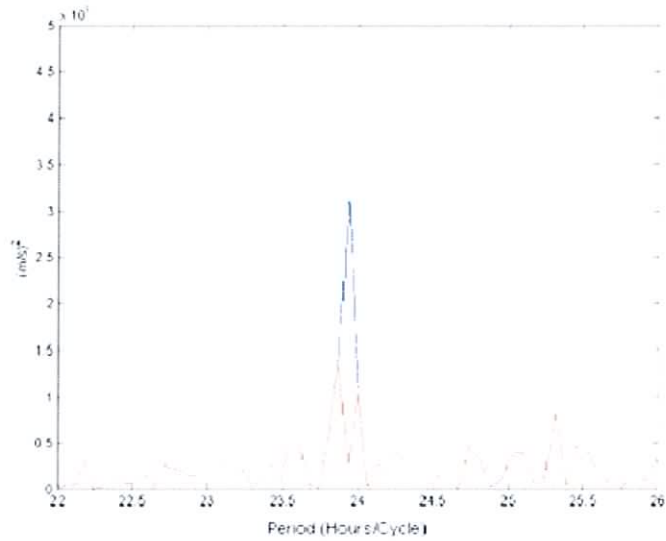


Figure 50: Closer view on the target frequency

The results of applying the above method at a 24 hours/cycles interval are shown in Figure 51 where calculated average terms that are subtracted from the original series.

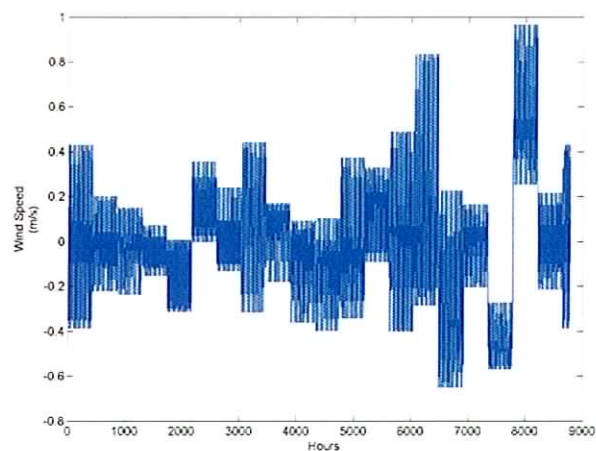


Figure 51: Average terms

The effect this has on the periodogram is shown Figure 52. It can be seen that the peak on the periodogram corresponding to the 24-hours/cycle interval has been reduced. From Figure 53 it can be seen that the level of reduction was from approximately  $2.03 \times 10^7$  to  $1.47 \times 10^6$  ( $\text{m}^2/\text{s}^2$ ). Also there is an increase in the values found at the harmonics of the target frequency. This is caused by mismatches between the average and the time

period in each case. In Figure 54 the waveforms show a sample of the periodic average values and the remaining stochastic wind series.

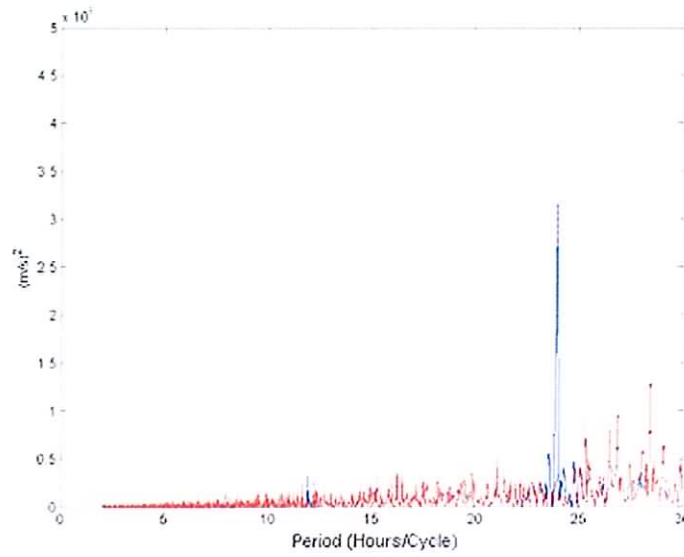


Figure 52: Resulting periodogram after averaging method was applied

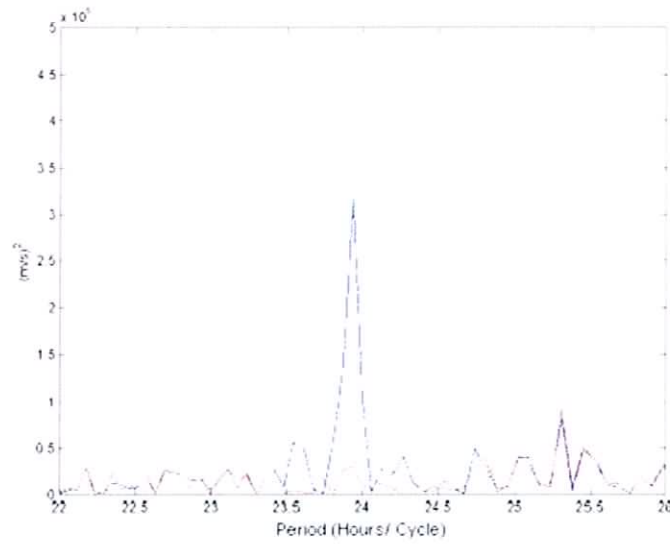


Figure 53: A closer view of the resulting periodogram after averaging method was applied



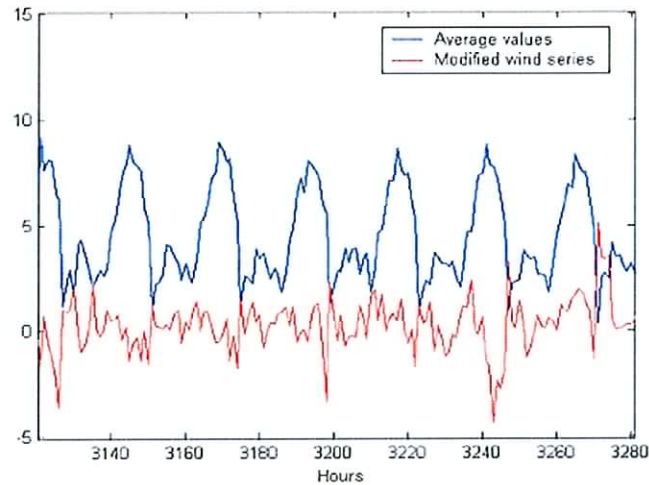


Figure 54: Plot of the resulting series after averaging method was applied

While this method has shown some good results, more direct methods have been investigated using the Fourier transform of the series that has already been calculated to find the frequencies that relate to high levels of periodicity in the wind series.

### 6.3.2.2 Time domain removal of dominant elements by frequent analysis

If the complex Fourier coefficient of the frequency corresponding to the 24 hours/period element is removed from the calculated series (with its conjugate) and are stored in another array of the same size and in the same position, then the inverse Fourier transform of a series will restore just this periodic element in the form of a sine wave. This can then be subtracted in the time domain from the original series. The effect of this method is to reduce the peak that is seen in the periodogram at 24 hours as shown in Figure 55. From Figure 56 it can be seen that the level of reduction was from approximately  $2.03 \times 10^7$  to  $1.56 \times 10^7$  (m/s)<sup>2</sup>.

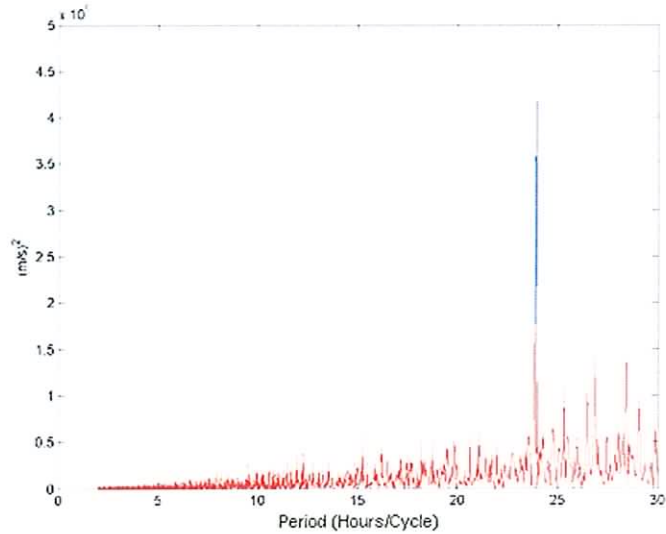


Figure 55: Level of reduction seen in the dominant peak

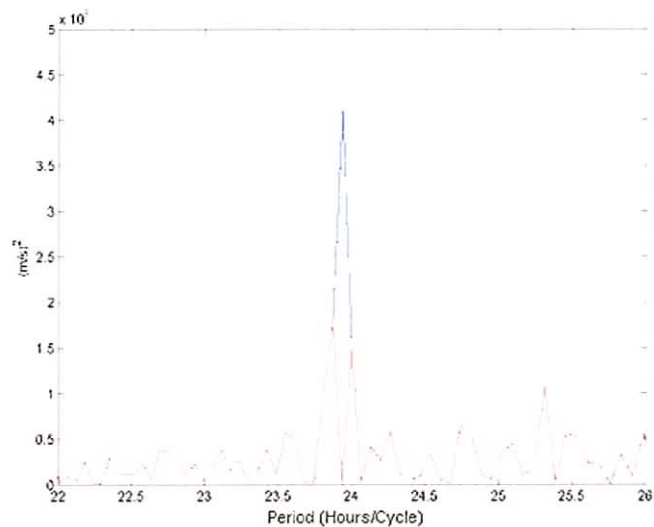


Figure 56: Closer view of the level of reduction seen in the dominant peak

Due to the properties of applying the discrete Fourier transform, all of the energy that occurs at a single frequency in the time domain signal does not occur at a single frequency in the frequency domain. Instead some energy is spread among the frequency bins surrounding the actual frequency. In order then to improve the performance of the method described above, a range of values centred on the dominant frequency were used as the basis of the second array. Also, instead of subtracting the inverse Fourier transform of the constructed second array, the inverse Fourier transform of the original array minus the second was used. The increased effect of this method has is shown in

Figure 57 and more closely in Figure 58 where it can be seen that the 24 hour/period peak has been reduced to approximately  $2.03 \times 10^7$  to  $3.65 \times 10^6$  (m/s)<sup>2</sup>.

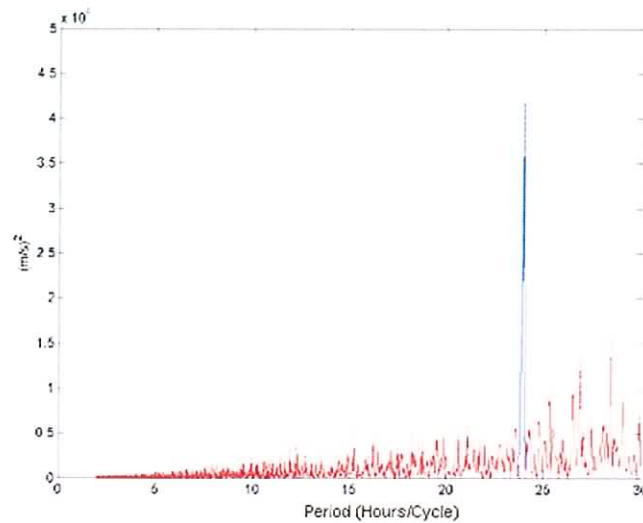


Figure 57: Resulting periodogram after Fourier method was applied

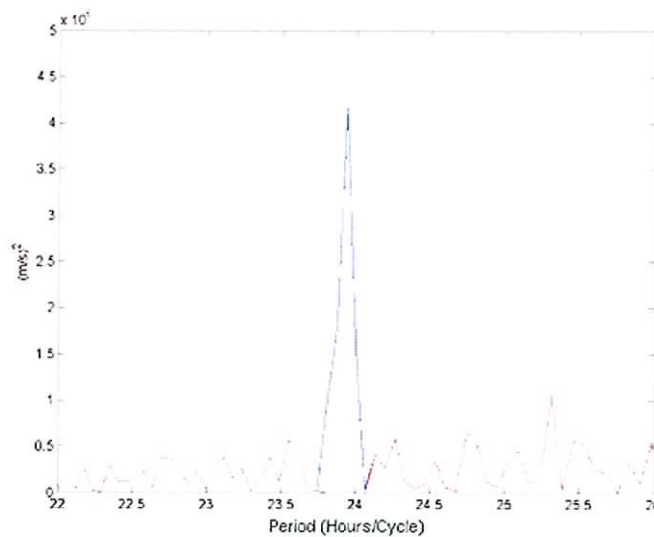


Figure 58: Closer view of the periodogram after Fourier method was applied

These methods offer a way to separate the elements found in the recorded wind series into two sub-series containing periodic and stochastic elements. Once the diurnal pattern was removed from the time series the remainder of the original series is considered to be the stochastic elements.

### 6.3.3 Modelling Stochastic Elements

The effect of normalising and separating the periodic elements associated with the diurnal pattern on the correlogram of the data is shown in Figure 59. From this figure the non-stationary aspects of the original time series can be seen in the auto correlation. The correlogram of the normalised data shows that the removal of the seasonal trend in the data improves the auto correlation function above the original by increasing the rate at which the values of correlation approach zero. In the final correlogram the ripple effect caused by the periodicity of the diurnal pattern with peaks seen at integrals of twenty-four lag seen the previous two has been reduced.

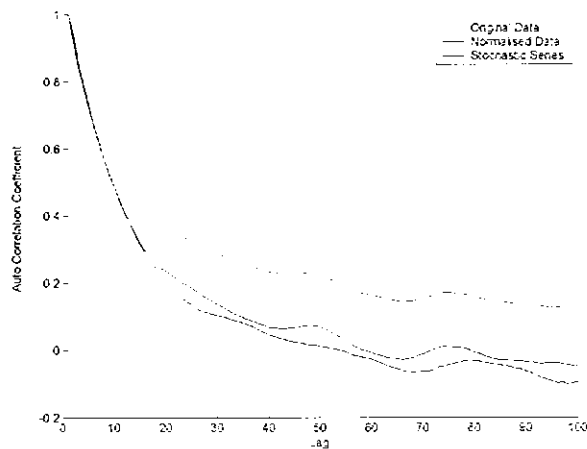


Figure 59: Comparison of auto correlation functions

An ARMA time series model is applied to the stochastic series so that different iterations of the underlying process can be found. The process applied to fit the model is as described in [57] that uses the assumption that a stationary stochastic process can be modelled by a model of the order ARMA ( $n, n-1$ ). Then by taking an initial value of  $n=2$  a minimisation procedure is applied to derive the model parameter such that the residual sum squares will be a minimum. The value of  $n$  is incremented and process repeated, to investigate if increasing the order of the model has improved performance.

The F-criterion statistical test is applied. This test is based on the Fisher-Snedecor distribution [33], which results from the ratio of two Chi-squared distributions. To perform the F-test first the F-statistic is calculated as given in Equation (6.3.1).

$$F = \frac{RSS(n, n-1) - RSS(n+1, n)}{2} \div \frac{RSS(n+1, n)}{N-r} \quad (6.3.1)$$

where  $RSS(n, n-1)$  and  $RSS(n+1, n)$  are the residual sum of squares of the models

$N$  is the number of observations

$$r = 2n + 2$$

The value of the F-statistic calculated is compared to the value found at  $F_p(2, N-r)$ , which the F distribution with degrees of freedom of 2 and  $N-r$  at a probability of  $p$ . The degree of significance chosen was 95% so that  $p$  was set to 0.05. Therefore if the value of the F-statistic calculated was greater than  $F_{0.05}(2, N-r)$ , the improvement in the model performance (i.e. the reduction in the residual sum of squares) is as great or greater than the reduction of the residual sum of squares that would have arise by chance for 95% of the time.

In this way the test is considered to be passed then the increase in order was warranted and the process is repeated. If the value of the F-statistic calculated was less than  $F_{0.05}(2, N-r)$  then the improvement seen from the last iteration is not enough to warrant the added complication of increasing the order of the model. Therefore the model formed by the previous iteration is chosen. This procedure was applied to the stochastic elements derived above, the results of which can be seen in the derived ARMA model given in Equation (6.3.2).

$$y(t) = 0.76932y(t-1) - 0.0034015y(t-2) + z(t) - 0.083248z(t-1) \quad (6.3.2)$$

A full set of the derived ARMA models is detailed in Appendix F. Once the model has been fitted to the data it is important to check its appropriateness. To do this the correlogram of the observed data and that of data generated by the model can be compared. In Figure 60 these autocorrelations are shown and from this figure it can be seen that the two autocorrelations are quite similar.

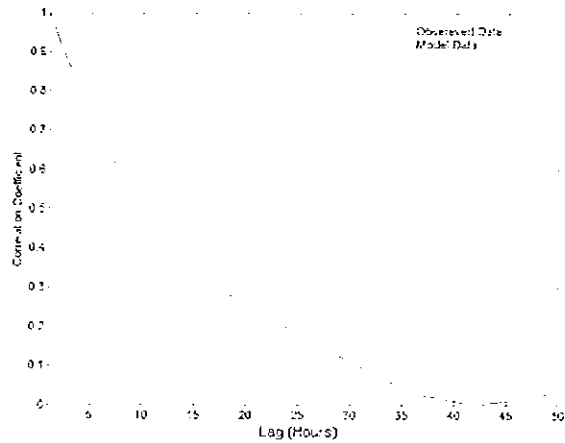


Figure 60: Comparison of observed and model generated auto-correlation functions

Also if the model is a good fit for the data, then the residuals are independent and normally distributed. In Figure 61 the distribution of the residuals is shown and can be seen to be of normal form.

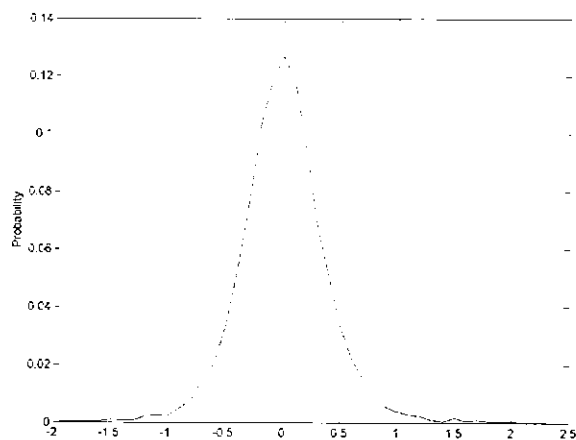


Figure 61: Probability distribution of the residuals

To assess if the residuals are independent their auto-correlation function can be calculated. The calculated values should be small if the residuals are independent. To quantify how small the auto-correlations should be is quite difficult. In [57] it is suggested that a range of  $\pm 2/\sqrt{N}$  be used as a guide level to correlations that significantly differ from zero. However if a small number of the auto-correlation coefficients are marginally greater than this level and there is no clear physical meaning

for their occurrence, then there is not enough evidence to reject the model. In Figure 62 the auto-correlations of the residuals are shown. It can be seen that only five out of the first fifty auto-correlation coefficients are marginally greater than suggested range therefore the independence of the residuals can be safely assumed.

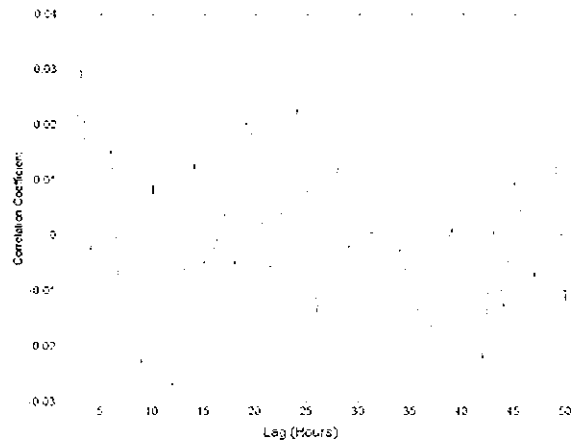


Figure 62: Correlogram of the residuals

#### 6.3.4 Generation Of Simulated Series

With the ARMA model of the stochastic elements in place  $n$  iterations of the stochastic element can be generated. In order to use these different stochastic series as the basis for wind speed predictions the periodic elements that had been removed from the normalised series using the methods outlined in Section 6.3.2 are added to the stochastic series. These combined stochastic and periodic elements then need to be denormalised. To do this the series is again broken into appropriate sections and then multiplied by an appropriate variance value and added to an appropriate mean level. Assuming the length chosen for the section is equal to a month then the ten year data set available for each site offers ten different possible values for the mean and variance for each month. If the data set were much longer it would be possible to form a joint distribution of mean wind speed and variance for the months and use random draws from this distribution to determine the level of mean and variance to denormalised to. But in this case it was necessary to assume that the recorded levels of mean and variance are equally probable, and the level of mean and variance to denormalise to in each month was chosen by a

randomly drawing from the recorded levels. In this way  $n$  series of wind speed series can be formed.

#### 6.4 SIMULATED WIND SPEED SERIES

In order to test the ability of the developed modelling methods to generate wind series that are representative of the data on which they are based, a set of data for each of the six sites was generated of the same length as the recorded wind series. The same set of statistical data that was calculated for the recorded data in Section 5.2 is calculated for the simulated series to allow for comparisons to be drawn. In Table 29 the annual mean wind speed of the recorded and simulated are detailed.

Table 29: Comparison of recorded and simulated series annual mean wind speed

Year	Belmullet		Clones		Knock	
	Recorded	Simulated	Recorded	Simulated	Recorded	Simulated
1994	7.30	7.38	4.22	4.23	N/A	N/A
1995	6.63	6.67	3.62	3.59	N/A	N/A
1996	6.86	6.85	3.72	3.77	4.95	5.06
1997	7.02	7.06	4.34	4.35	5.14	5.18
1998	7.34	7.49	4.39	4.45	5.34	5.42
1999	7.30	7.33	4.17	4.18	5.06	5.08
2000	5.65	5.63	3.96	3.98	4.92	4.98
2001	6.76	6.81	4.11	4.14	5.07	5.12
2002	6.25	6.35	4.03	4.10	4.93	5.03
2003	6.58	6.58	4.05	4.06	5.02	5.02
Year	Malin Head		Shannon		Valentia	
	Recorded	Simulated	Recorded	Simulated	Recorded	Simulated
1994	8.52	8.66	4.80	4.94	4.82	4.79
1995	8.15	8.17	4.50	4.55	4.61	4.52
1996	7.88	7.92	4.51	4.67	4.26	4.21
1997	8.23	8.30	4.66	4.75	4.62	4.54
1998	8.49	8.57	4.89	4.97	4.81	4.76
1999	8.05	8.04	4.52	4.65	4.93	4.87
2000	7.87	7.92	4.45	4.52	4.55	4.52
2001	7.71	7.74	4.63	4.70	4.92	4.90
2002	7.56	7.60	4.63	4.75	4.74	4.69
2003	7.74	7.81	4.82	4.94	4.86	4.78

The inter-annual variation from the long-term mean of the recorded series was investigated in Section 5.2. This procedure has been repeated with the simulated data. In Figure 63 the mean inter-annual variation for both the recorded and simulated wind



series are shown. From this figure it can be seen that the two sets of data show good agreement in the mean inter-annual variation for each of the sites.

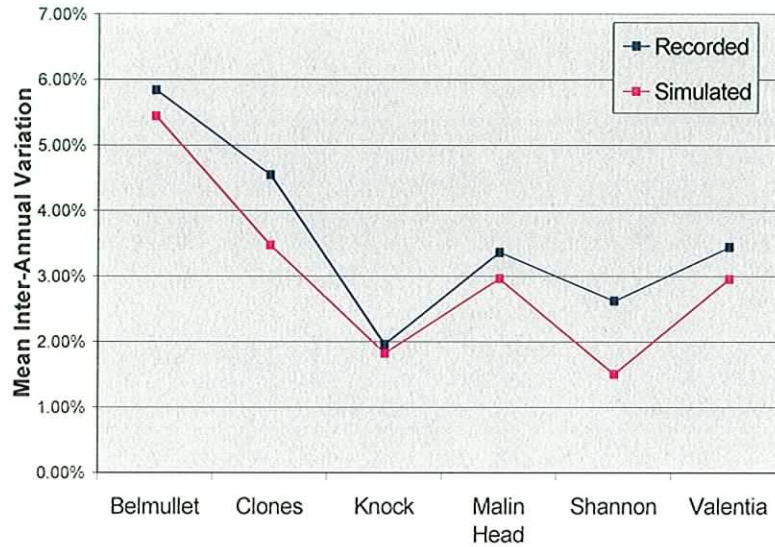


Figure 63: Comparison of recorded and simulated series inter-annual

Another important aspect in characterising a wind regime is the degree it is affected by a seasonal variation. To investigate this an index was introduced in Section 5.2, which was formulated by calculating the maximum monthly variation between winter and summer. This index is expressed as a percentage of the maximum monthly mean for that year. This index was calculated for the simulated data set. In Figure 64 the mean values of the seasonality indicator for the six sites (both simulated and recorded) are plotted. From these results good agreement between the simulated and recorded data can be seen.

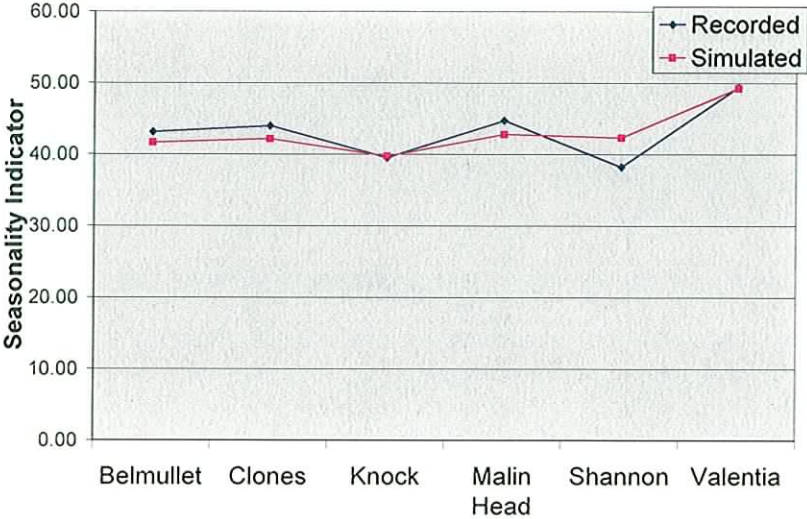


Figure 64: Comparison of recorded and simulated series seasonal indicator

In Table 30 the standard deviation of the simulated and recorded data is detailed. In this table the standard deviation has been normalised by dividing by the mean for the same period. This normalised standard deviation gives an impression of the degree of variability that exists in the data from Table 30. The values of normalised standard deviation seen in the recorded data is consistent with that found in the simulated data.

Table 30: Comparison of recorded and simulated series standard deviations

	Belmullet		Clones		Knock	
	Recorded	Simulated	Recorded	Simulated	Recorded	Simulated
	0.48	0.56	0.65	0.61	N/A	0.57
	0.49	0.56	0.68	0.62	N/A	0.56
	0.55	0.57	0.67	0.60	0.54	0.56
	0.51	0.58	0.52	0.59	0.51	0.57
	0.51	0.54	0.54	0.58	0.53	0.61
	0.53	0.55	0.56	0.56	0.57	0.56
	0.58	0.54	0.57	0.60	0.52	0.62
	0.55	0.55	0.55	0.58	0.54	0.57
	0.55	0.61	0.52	0.57	0.50	0.56
	0.51	0.55	0.52	0.55	0.50	0.58
Average	0.53	0.56	0.58	0.59	0.53	0.58
	Malin Head		Shannon		Valentia	
	Recorded	Simulated	Recorded	Simulated	Recorded	Simulated
	0.49	0.58	0.57	0.56	0.67	0.65
	0.48	0.55	0.60	0.61	0.65	0.67
	0.53	0.55	1.08	0.57	0.77	0.62
	0.47	0.57	1.02	0.62	0.63	0.70
	0.47	0.53	0.57	0.62	0.60	0.61
	0.57	0.54	0.63	0.59	0.64	0.63
	0.49	0.53	0.59	0.61	0.65	0.58
	0.52	0.55	0.62	0.62	0.63	0.62
	0.52	0.54	0.54	0.62	0.57	0.59
	0.48	0.57	0.57	0.58	0.60	0.63
Average	0.50	0.55	0.64	0.60	0.64	0.63

In Figure 65 the probability distribution from the simulated data for the Malin Head site is shown, as is the probability distribution from the recorded data from the Malin Head. The two distributions are similar with the distribution from the recorded data oscillating around the distribution from the simulated data. Similar results were observed when the probability distributions from the other sites were compared.

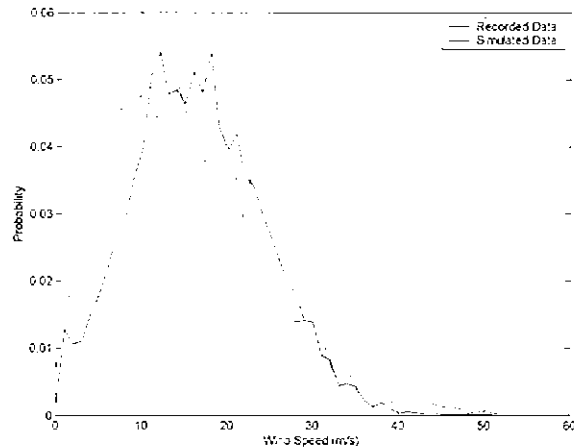


Figure 65: Comparison of recorded and simulated series periodograms

## 6.5 INTER SITE CORRELATION

It was important when extending the model to multiple sites to maintain the cross correlation relationships that have been observed in the recorded data. To an extent this is achieved by recombining the ARMA model generated series with the periodic elements. In Equation (6.2.12) the structure of the ARMA model is given. From this formulation it can be seen that the ARMA model is driven by the value of the random value chosen in each hour. If the correlation relationship between the random numbers that drive the six ARMA models based on the Met Eireann data can be manipulated then the correlation relationship of the series generated by the ARMA models can be chosen to match the relationship seen in the recorded data. Therefore it is required that the random series which drives the ARMA models have a correlation matrix so that the resulting values generated by the ARMA models will have the same correlation matrix as the residual data from the six sites. In [58] the question of simulating wind speeds at several wind farms taking into account the correlations observed between them is addressed by two methods.

In the first method the simulation of multivariate distributions with a given correlations is solved by generating a vector of independent variables  $z$ , a second set of variables  $y$  can be formed by applying the transformation  $y = Lz + \mu_y$  where  $L$  is the lower triangular matrix such that  $LL^T$  equals the required covariance matrix and  $\mu_y$  are the mean values of  $y$ . The second method is based on conditional probabilities. The joint

distribution function of a set of recorded dependent variables  $z$  can be expressed through the conditional distributions:

$$F(z) = F_1(z_1), F_2(z_2 | z_1 = z_1^0) \dots F_n(z_n | z_1 = z_1^0, \dots, z_{n-1} = z_{n-1}^0) \quad (6.5.1)$$

where  $F_1(z_1)$  is distribution function of the variable  $y_1$ ,  $F_2(z_2 | z_1 = z_1^0)$  is the distribution function of the variable  $z_2$ , conditioned by the variable  $z_1$ , etc. A new vector  $z$  can be generated by using  $n$  random numbers to sample the conditional distributions.

Each of these methods use a specified covariance or correlation relationship to generate wind speed data with the same relationship, whereas the problem being addressed here requires that the correlation relationship in the random series results in the values generated by the ARMA models having the same correlation relationship in the recorded data. To address it was decided to develop a method that would produce the required correlation relationship between the random series. Therefore the correlation relationship of values generated by the AMRA models are tuned as required. To do this the assignment detailed in Equation (6.5.2) is used to specify the seed values  $y = (y_1, y_2, \dots, y_n)^T$ .

$$\begin{bmatrix} y_1 \\ y_2 \\ \cdot \\ \cdot \\ y_n \end{bmatrix} = \begin{bmatrix} a_{11} & a_{12} & \cdot & \cdot & a_{1n} \\ a_{21} & a_{22} & \cdot & \cdot & a_{2n} \\ \cdot & \cdot & \cdot & \cdot & \cdot \\ \cdot & \cdot & \cdot & \cdot & \cdot \\ a_{n1} & a_{n2} & \cdot & \cdot & a_{nn} \end{bmatrix} \begin{bmatrix} y_1 \\ y_2 \\ y_3 \\ \cdot \\ y_n \end{bmatrix} + \begin{bmatrix} b_{1,r1} \\ b_{2,r2} \\ b_{3,r3} \\ \cdot \\ b_{n,rn} \end{bmatrix} \quad (6.5.2)$$

where  $a_{ij}=a_{ji}$  for  $i,j=1:n$ ,  $a_{ij}=0$  where  $i=j$  and  $r$  is a normally distributed random number with a mean of zero and a variance of one. The  $a$  and  $b$  terms in Equation (6.5.2) can be used to adjust the correlation matrix of the generated  $y$  terms to the required values. For example if the pair of terms  $(a_{12} \ a_{21})$  are increased relative to the other terms in the matrix then the correlation seen between  $y_1$  and  $y_2$  will increase, similarly if  $(a_{12} \ a_{21})$  is decreased then the correlation seen between  $y_1$  and  $y_2$  will decrease. The interdependent nature of the cross correlation relationship between the different sites means that the process of choosing the  $a$  and  $b$  terms becomes an iterative optimisation process, such

as the Newton method, where the difference between the recorded correlation matrix and that seen between the ARMA generated series is minimised by the selection of the  $a$  and  $b$  parameters. In Table 31 the average correlation matrix from the residuals of the data recorded is compared to the average correlation matrix from the series generated by the ARMA models over a ten-year sample. From this table good agreement between the average correlation matrices of both the recorded and simulated series can be seen. In Figure 66 the correlation coefficients calculated over the length of the data set between Belmullet and Clones are compared to the correlation coefficients found between simulated data based on these two sites. From this figure it can be seen that the range of inter-annual variation in the correlation of the recorded data is matched well by the simulated data.

Table 31: Comparison of recorded and simulated series correlation coefficient matrices

Recorded	Belmullet	Clones	Knock	Malin Head	Valentia	Shannon
Belmullet	1.00	0.60	0.72	0.57	0.57	0.58
Clones	0.60	1.00	0.75	0.66	0.52	0.64
Knock	0.72	0.75	1.00	0.60	0.61	0.72
Malin Head	0.57	0.66	0.60	1.00	0.39	0.48
Valentia	0.57	0.52	0.61	0.39	1.00	0.71
Shannon	0.58	0.64	0.72	0.48	0.71	1.00
Simulated	Belmullet	Clones	Knock	Malin Head	Valentia	Shannon
Belmullet	1.00	0.61	0.74	0.59	0.60	0.62
Clones	0.61	1.00	0.76	0.67	0.58	0.62
Knock	0.74	0.76	1.00	0.61	0.67	0.72
Malin Head	0.59	0.67	0.61	1.00	0.35	0.46
Valentia	0.60	0.58	0.67	0.35	1.00	0.74
Shannon	0.62	0.62	0.72	0.46	0.74	1.00

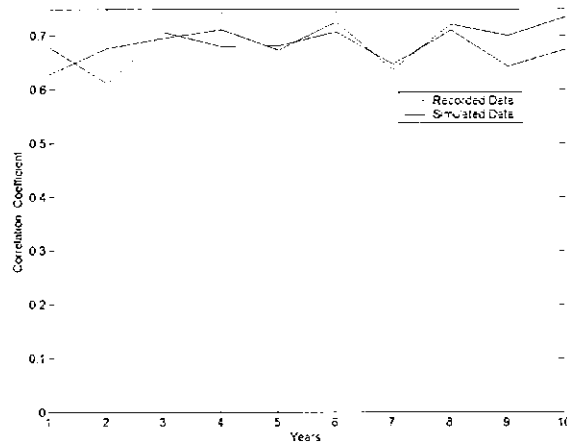


Figure 66: Comparison of recorded and simulated inter-annual variation in correlation coefficient

## 6.6 CONCLUSION

A modelling method was developed which allows of the generation of simulated wind series based on observed data. This method involves the normalisation of the recorded series and the separation of the periodic and stochastic elements of the normalised series. A number of approaches were developed for the calculation of the periodic elements of the wind series and the performance of each was investigated. The use of time series modelling of the stochastic elements of the normalised series was investigated. The result of which was a time series modelling method that once fitted to a series would allow for the generation of  $n$  iterations of the original series. By reversing the separation and denormalisation process the time series model can form the basis for generating multiple simulated wind series. The simulated wind speed series that were generated when this modelling method was applied to the six Met Eireann wind speed records show good agreement with the original series. Comparisons were drawn in terms of mean and variance measured over different time scales and also in terms of the probability distribution. A method has been developed to enforce the correlation coefficient matrix found in the data on to the simulated data. The results of applying this method have been shown to reflect well both the long-term averages and the inter-annual variations found in the recorded data as shown in Table 31.

## **7 EVALUATION AND APPLICATION OF WIND SPEED MODELS**

### **7.1 INTRODUCTION**

The modelling methods for wind speed series that were developed in Chapter 6 allow for the generation of  $n$  years of wind speed estimates. The wind speed estimates will be used as a basis for the generation of hourly wind power estimates for the generation system of the R.O.I. To do this the wind speed series needs to be converted to wind power series and then a methodology developed to scale and combine these six wind power estimates to form the best possible estimates for the hourly system-wide wind power. These hourly wind power estimates are applied to Monte Carlo adequacy calculations. Different aspects of the wind capacity model are investigated using case studies.

### **7.2 WIND SPEED TO WIND POWER CONVERSION**

In converting from wind speed to wind power there are three factors to be taken into consideration. Firstly before the wind speeds can be converted to wind power a height adjustment must be made. This is to account for the records on which the wind speeds are based being recorded at a lower height than is typical for the hub of a wind turbine. Secondly the geographical distribution of wind capacity and the association of wind capacity to the simulated wind speed series. Thirdly the nature of the PV wind turbine model that is to be used.

#### **7.2.1 Wind Height Adjustment**

For a given location at increasing heights the wind speeds that will be recorded will tend increase this is due the reduced effect of friction with the terrain. This effect is known as vertical wind shear, which will increase with the roughness of the surface terrain. The European wind atlas project has developed a standard for roughness classification. In Table 32 the details for this standard are given. Included in this table a is term known as



roughness length, which is defined as the height above ground where the effect of the terrain on the wind speed is theoretically zero.

Table 32: Roughness length classification definitions

Roughness Class	Roughness Length (m)	Landscape Type
0	0.0002	Water surface
0.5	0.0024	Open terrain with a smooth surface
1	0.03	Open agricultural area without fences or hedgerows
1.5	0.055	Agricultural area with low hedgerows
2	0.1	Agricultural area with high hedgerows and sparse buildings
2.5	0.2	Agricultural area with high hedgerows and many buildings
3	0.4	Villages, small town and forests and very uneven terrain
3.5	0.8	Larger cities with tall buildings
4	1.6	Very large cities with tall buildings and skyscrapers

Two principle methods of adjusting wind speed records height are the power law wind profile and the logarithmic wind profile. The logarithmic wind profile under neutral conditions is given in Equation (7.2.1).

$$U(z_1) = U(z_2) \frac{\ln\left(\frac{z_1}{z_0}\right)}{\ln\left(\frac{z_2}{z_0}\right)} \tag{7.2.1}$$

where  $z_0$  is the roughness length at that location

$U(z_1)$  and  $U(z_2)$  are wind speeds at the original and required height respectively

The power law is a more empirical approach and is given in Equation (7.2.2)

$$U(z_1) = U(z_2) \left( \frac{z_2}{z_1} \right)^p \quad (7.2.2)$$

A typically  $p$  is set equal to  $1/7$ . This is equivalent to the logarithmic wind profile where  $p = 1/\ln(10/z_0)$  and  $z_0$  assumed to be equal to 0.01 meters. Both of these methods allow wind records to be adjusted for typical meteorological recording heights for 10 m up to the hub height required. With these method established the height to which the meteorological data should be adjusted to is determined. For example the hub height at Corneen is 64.5 m while at Culligh it is 45 m. To address this problem it was decided to scale all the meteorological records so that the mean long-term wind speed is 8.5 m/s. In this way there is no need to specify a particular hub height. Under the current market structures and at the present state of technology, a mean wind speed of 8.5 m/s represents the minimum mean wind speed required at a site in order to make the development of a wind farm economically viable.

### **7.2.2 Association Of Wind Capacity To Wind Speed Series**

With this wind height correction in place the next question to be addressed is the capacity that should be associated with each of the available wind series. To do this the country was divided into four regions as shown in Figure 67, which is courtesy of Sustainable Energy Ireland. This figure also shows the location of the six Met Eireann weather stations and the completed wind farm projects as of August 2004.

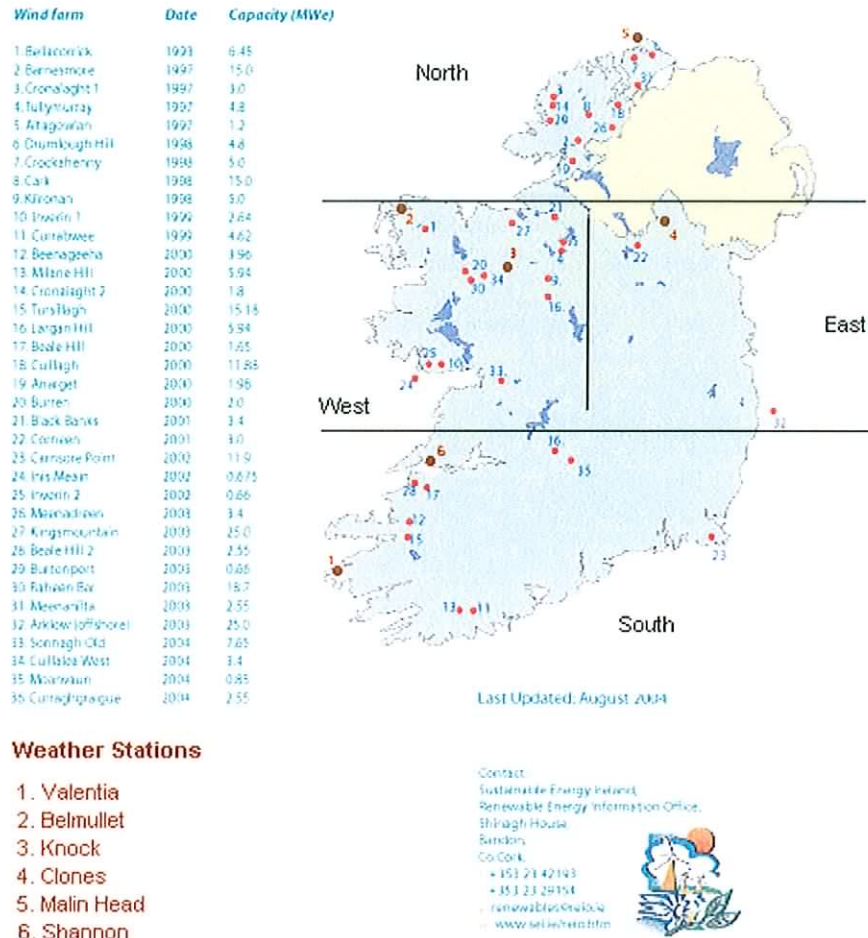


Figure 67: Map of the regional divides and the location of each of the weather stations courtesy of Sustainable Energy Ireland

The country was divided into four regions and in this way the proportion of current developed level of wind capacity that occur in each of the regions was be calculated. Using the assumption that future developments will occurs in the same pattern then for the total level of wind capacity predicted in the [59] the amount of capacity that will occur in each region can be calculated. Where there are two weather stations in a region the predicted wind capacity level is divided evenly between them. In Table 33 the level of wind capacity growth predicted in [59] is given with the break down of the resulting level of wind capacity that is associated with each of the weather stations.

Table 33: Breakdown of predicted wind capacity associated with each weather station

Year		2005	2006	2007	2008	2009	2010	2011
Region	Weather Sataion							
East	Clones	92	101	106	110	114	119	123
West	Belmullet	144	158	165	172	179	186	192
	Knock	144	158	165	172	179	186	192
North	Malin Head	214	235	245	255	266	276	286
South	Shannon	81	89	93	97	100	104	108
	Valentia	81	89	93	97	100	104	108
	Total	756	831	866	902	938	974	1010

### 7.2.3 Wind Turbine Model

The wind series could now be converted into wind power series using a typical PV characteristic for a wind turbine. In [60] a method is detailed to generate a normalised PV characteristic for a wind turbine given cut-in, rated and cut-out wind speed that can then be scaled to the required capacity. In Figure 68 the PV characteristic of a wind turbine with a cut in speed of 3 m/s, a rated speed of 12 m/s and cut out speed of 25 m/s is shown. This method offers an accurate way of estimating the output of a single wind turbine for a given wind series. However using this method to estimate the wind power that would arise across an entire region would ignore the effect of smoothing in time and space. In [61] a method is suggested which attempts to adjust to both of these effects. The method uses the size and the mean wind speed of the region under consideration to specify the length of a moving average filter applied to a representative wind speed series from the region. In this way the spatial memory effect of wind speed fluctuations i.e. a wind speed measured upfront in an area relative to the wind direction will be still present within the area in a time period proportional to the wind speed and the size of the area. The method also suggests forming a multi-turbine characteristic by smoothing the single wind turbine PV characteristic by combining it with a normal distribution as in Equation (7.2.3).

$$Pm_j = \sum_i P_{S(j+i)} \times ps_i \quad (7.2.3)$$

where  $Pm_j$  and  $P_{S_j}$  is the  $j^{th}$  element of adjusted wind turbine characteristic

$ps_i$  is the probability of the normal distribution at wind speed  $i$

This is done as it assumed that the actual wind speed that is seen at the individual wind turbines across a region would be normal distributed around the moving averaged value. The standard deviation of this distribution is related to the size of the region and the turbulence intensity associated with the area. Turbulence intensity is similar to roughness class but whereas roughness class considers the effect of obstacles of the terrain, turbulence intensity is related to the type terrain that underlies the region i.e. open, mountainous etc. The result of combining a normal distribution with the PV characteristic of a wind turbine is shown in Figure 68. In Figure 69 the result of applying a single turbine characteristic and the multi-turbine methods to a wind series generated using the data from the Malin Head weather station and applying it to the Northern region with a level of wind capacity set nominally to a value of 100 MW. From this figure it can be seen that the tendency to go to the maximum capacity level has been reduced and the large rapid fluctuation have been reduced.

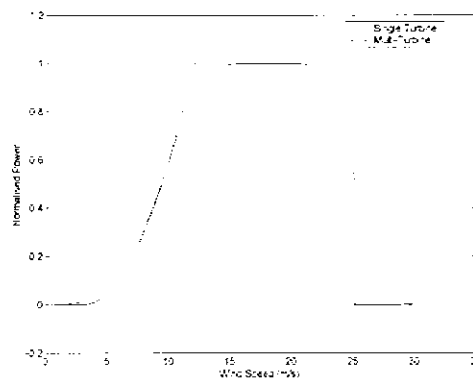


Figure 68: Contrast of single and multi-turbine PV characteristics

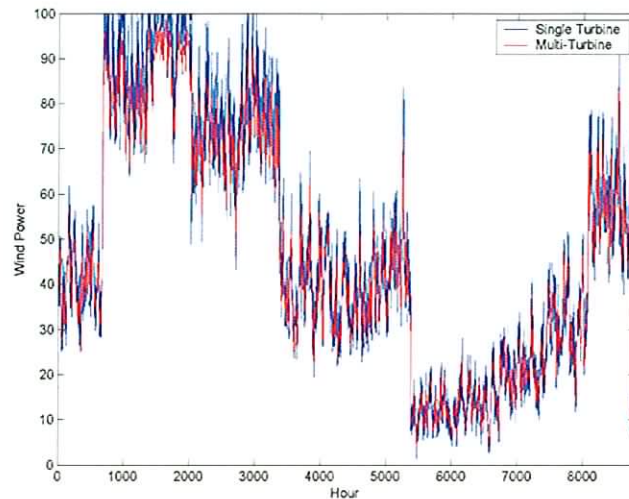


Figure 69: Contrast calculated power series using a single and multi-turbine method

With this method of converting from wind speed to wind power series in place, wind speed series based on the data from each of the six sites were generated and converted to a power series with associated capacities as outlined in Table 33. The hourly sum of these six generated wind power series is the estimated wind power output for each hour.

### ***7.3 APPLICATION OF TIME SERIES WIND CAPACITY MODEL***

The hourly wind power series generated by the developed time series method was applied to a Monte Carlo adequacy calculation by adding the capacity model to the wind power series. The calculation was then made as described in Chapter 4. This method of including wind capacity is intuitively appealing as the marginal cost of generation for wind capacity is very low assuming zero fuel cost. Therefore the wind capacity will always be dispatched before conventional generation. Applying the generated wind power series in this way to an adequacy calculation allows the developed time series method to be compared to other methods of wind capacity representation and also allows for the investigation of the effects of different aspects of the time series model on the adequacy calculation outcome.

### 7.3.1 Comparison of various wind capacity models

To compare the developed wind capacity model to the simplistic methods discussed earlier and also with results from [59], the same conditions that were applied in Chapter 4 (i.e. load and capacity growth, availability and scheduled maintenance requirement and system adequacy standard) were repeated. In Table 34 the results of this process are tabulated. Results are shown for the time series method described above. Results are also shown for the system with no wind capacity included, the results from applying the elevated FOR and Wiebull load modifier methods and also the results under the same conditions from [59]. These results are plotted in Figure 70. From this figure it can be seen that the elevated FOR appears to produce a slightly higher level of capacity margin compared to the results produced in [59], apart from 2005 and 2011.

Table 34: Result of various wind capacity models

Year	Wind Capacity	No Wind	Elev.FOR	Wiebull Load Mod.	Time Series	GAR 05-11
2005	756	-131	-67	129	112	65
2006	831	166	235	458	441	221
2007	866	262	331	561	539	281
2008	900	188	256	499	469	200
2009	938	-20	37	273	267	19
2010	974	-131	-82	156	134	-92
2011	1010	-508	-411	-133	-139	-291

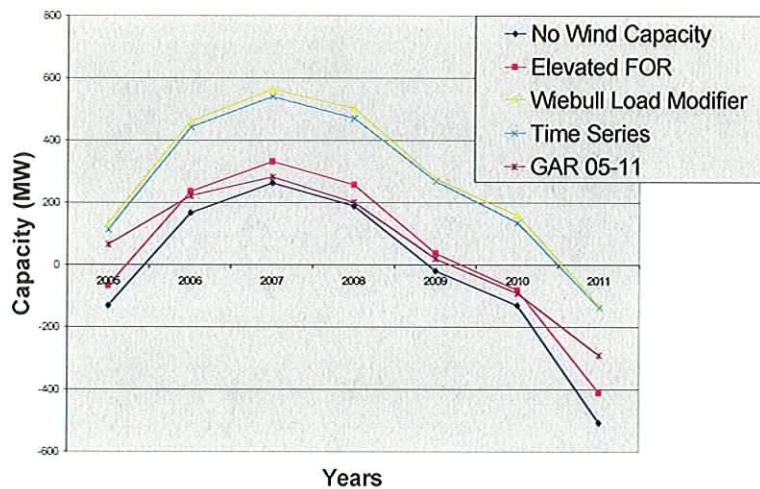


Figure 70 Plot of results from various wind capacity models

The results when wind capacity is excluded are similar to the results in [59]. Overall, when wind capacity is excluded from the calculation the capacity margin calculated is lower than in [59]. The differences observed are caused by the assumptions made to form the conventional capacity model, which, result in the values calculated for the output of conventional capacity being too high and therefore the results from all the adequacy calculations being too optimistic. This reason also explains why the Weibull load modifier and time series method both appear to exceed the results in [59]. In summary, the two main causes of the differences between the results in [59] and those for the no wind capacity and elevated FOR case are the availability values of the conventional plant and the incorporation of wind capacity. Of these, the availability data and in particular the conventional plant FOR values, are the most significant.

Comparison of the results from the time series method with to the Weibull load modifier method shows that the methods developed to incorporate the annual and diurnal variation and to impose the correlation relationships found in the recorded into the wind capacity estimates results in a reduction of the effect of the wind capacity on the generation adequacy of the system. To investigate this point further the time series model was implemented so that the correlation relationship found in the recorded wind speed data between the difference sites was not imposed on the data generated by the model and the results for the Irish system were recalculated. In Table 35 the results of this calculation are compared to the previously calculated values

From this table it can be seen that the effect of imposing the correlation relation is to reduce the impact of the wind capacity on the system adequacy. This result is consistent with the view that increasing the geographical diversity of wind capacity (i.e. reduces the degree to which the wind speeds seen at wind capacity site are correlated) will improve the impact of wind capacity on system performance.



Table 35: Comparison of results with and without correlation relationship

Year	With Correlation	No Correlation
2005	112	132
2006	441	460
2007	539	542
2008	469	495
2009	267	283
2010	134	157
2011	-139	-131

### 7.3.2 Calculation of Risk-Based Capacity Credit

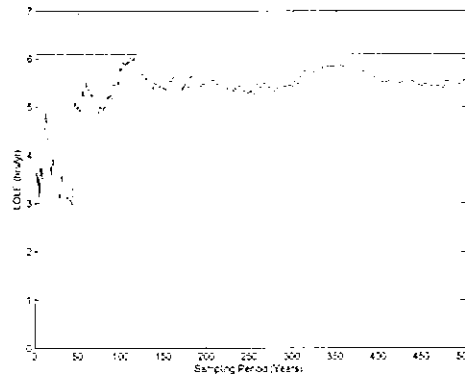
Comparison of the results when wind capacity is excluded from the calculation with the results from the other models (elevated FOR, Weibull distribution and time series) allows for the development of a risk-based credit capacity estimate. A risk-based capacity estimate indicates the potential energy production capability of the wind capacity. This relates not only to the conditions under which the wind capacity is operating but also relates to the system capacity composition, the chronological load and wind characteristics and the system adequacy standard. The risk-based capacity credit estimate can be calculated as the difference found when wind capacity is included using the various models divided by the wind capacity value for that year. In Table 36 the risk-based capacity credit found for each of the wind capacity models is shown. From this table it can be seen that the elevated FOR model results in wind capacity having a very low capacity credit with an average value of 0.08 while the Weibull load modifier method and time series methods shown similar results with average values of 0.34 and 0.29 respectively. The low value of capacity credit associated with the elevated FOR is caused by the nature of the model resulting in a very small impact on system adequacy while the other models result in a more realistic estimation of the impact of wind capacity on the system adequacy and therefore the value of risk-based capacity is more closely inline with the capacity factor that would relate to wind capacity. In this table it can be seen that year on year the risk-based capacity credit varies. This is due to the risk-based capacity credit given to the wind capacity being dependent on the circumstances of the generation system as a whole. This trend seen can be in the risk-based capacity credit over the course of the study match that seen in Tables 14 and 15.

Table 36: Risk-based capacity credit estimates calculated

Year	Elevated FOR	Wiebull Load Modifier	Time Series
2005	0.08	0.34	0.30
2006	0.08	0.35	0.29
2007	0.08	0.35	0.28
2008	0.08	0.35	0.28
2009	0.06	0.31	0.27
2010	0.05	0.29	0.26
2011	0.10	0.37	0.33
Average	0.08	0.34	0.29

### 7.3.3 Effect of inter-annual variations on LOLE calculations

The effect of inter-annual variations in loss of load expectation (LOLE) when a single year of wind data is used was investigated. To do this, several years of simulated wind energy estimates were generated. These estimates were applied to individual probabilistic LOLE calculations (i.e. the method applied in [59]). This process is repeated using a Monte Carlo calculation such that for each year simulated in the Monte Carlo calculation, a different set of wind energy estimates are generated. The nature of this type of calculation results in the most likely level of LOLE. The study was carried out on the basis of the generation system of the R.O.I. for the year 2005. In Figure 71 the results for the Monte Carlo calculation where the result tends to converge to the expected value of LOLE as the number of simulation years increases is shown. Figure 71 also shows the upper and lower bounds from the probabilistic calculation. As described above, each of these LOLE calculations is based on a single (but different) year of wind data. Whereas an LOLE value of 5.54 hours/year is calculated for the expected value (using the Monte Carlo method), the range of values for single year calculations is from 4.76 hours/year to 6.1 hours/year. Thus this result establishes the range of expected LOLE values when one year of wind data is used. Putting these results in terms of surplus capacity gives a range of values from 126 MW to 67 MW with the Monte Carlo result approximately in the middle of this range at 98 MW.



**Figure 71: Convergence path of Monte Carlo calculations including upper and lower boundaries**

The result of extending this calculation forward to include the years to 2011 is shown in Figure 72. It would be expected that the range of values resulting for single year calculations widens as the wind capacity penetration increase but this effect is not observed in Figure 72 where the range (between the upper and lower boundaries) of values stays relatively constant. The reason for this is the relatively small increase in wind capacity over the course of the study. Also the impact of any unit on the system will depend on the conditions of the system in that year. For example, as the calculated LOLE of the system approaches zero (i.e. the system has excess capacity) the impact of the addition of any unit on the system in terms of LOLE will be reduced. Likewise as the system moves away from the 8hrs/yr standard, the addition of any new unit on the system will cause the LOLE to increase. Therefore, depending on the change in system conditions from one year to the next, an increase in the wind capacity penetration could result in a decrease in the variability seen in the values of LOLE calculated.

To establish that an increase in wind capacity penetration will lead to an increase in the range of values resulting for single year calculations under constant conditions, the process was repeated for 2005 while the wind capacity penetration increased to 25% (i.e. 1702 MW). The result of this calculation is shown in Figure 73. From this figure it can be seen that, as would be expected, the level of variation seen increases as the wind penetration increases.

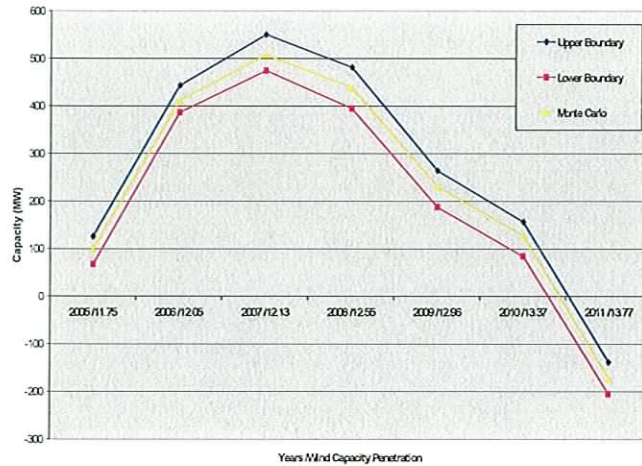


Figure 72: Results of extending calculation over the period to 2011

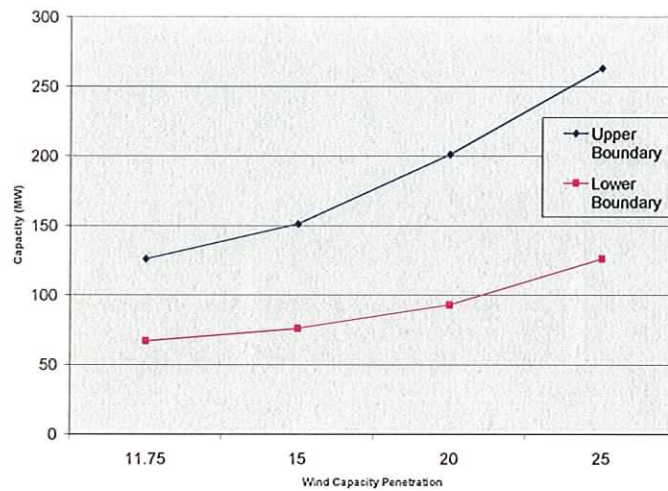


Figure 73: Result of applying increasing wind penetration under the same conditions

## 7.4 CONCLUSION

To convert the simulated wind speed series to a power series, a multi-turbine approach was adopted. This method attempts to account for the memory effect of wind speeds across a region by applying a moving average filter to the wind speed series. The length of the window is determined from the mean wind speed and the size of the region under consideration. Also the effect of the spatial wind speed distribution is included into the method by combining a typical single wind turbine characteristic with a normal distribution, the parameters of which are dependent on the terrain type and size of the

region. In order to apply this method, the four regions to which the wind speed series are being applied were defined. These regions were also used to define the proportion of the projected wind capacity that should be associated to each of the Met Eireann sites. In this way hourly wind power estimates for the generation system were calculated. These hourly wind power estimates have been then applied to a Monte Carlo adequacy assessment calculation. The degree of variance that can arise in LOLE values calculated on the basis of single year wind speed records has been investigated in the case of 2005 it was found that a range of values from 126 MW to 67 MW were calculated, but the Monte Carlo result of 98 MW represents the most probable outcome.

## 8 CONCLUSIONS AND FUTURE WORK

### 8.1 CONCLUSIONS

This thesis has reported on an investigation into generation adequacy assessment in a power system with increasing levels of wind generation. Initially the required modelling and calculations to evaluate both the LOLE and the LOEE using an analytical method were developed for the IEEE-RTS. Two maintenance scheduling techniques based on the levelised reserve and levelised risk methods, were also developed. The results gained from these calculations were then compared to previous published results. A Monte Carlo simulation of the IEEE-RTS was then developed and used to derive values for both the LOLE and the LOEE, with maintenance scheduling incorporated, agreement was achieved between the Monte Carlo and analytical techniques. The results from the analytical calculation were used as reference point for the expected results for the Monte Carlo calculations.

The methods developed were then extended to the Irish generation system. The majority of the data required to do this was available but specific data regarding individual units forced outage rates (FOR) and maintenance requirements was not available and therefore some assumptions had to be made to overcome this. Comparisons were made between the results calculated for the Irish system as part of this work and those published by the TSO in [59]. The differences between these two sets of results were due largely to the assumptions made to calculate the approximate FOR values and the wind capacity models applied. The wind capacity model applied in [59] is based on both recorded on-shore wind power series and offshore wind speed series. While initial efforts to model wind capacity used simplistic wind models, it became clear that these initial wind-modelling methods were not adequate to capture the full impact of wind capacity on the adequacy of a system. The elevated FOR method attempted to represent the generation adequacy benefit from wind capacity as the long term probability of the wind capacity operating at rated capacity. While over an extended time period a wind series can be seen to some extent as a probabilistic event, it is a broad approximation to model the hourly wind power generated across the country from over 40 wind capacity sites containing hundreds of individual wind turbines in this way. An improvement to

the basic elevated FOR method was to develop the wind capacity as a multi-state unit where the probability of the wind capacity operating at different capacity levels is included in the model. But this continues to ignore the stochastic nature of the wind series that acts as a prime mover for the wind capacity. The Weibull based load modifier method attempts to address this problem. The long-term probability is represented in this model by setting the parameters of the Weibull distribution to values relating to the wind regime of the wind capacity. The stochastic nature of the wind series is represented by taking random draws from the Weibull distribution, the resulting series converted into a wind power series. This method represents an improvement over the elevated FOR method but fails to recognise the periodic elements that exist in wind series over different time horizons. These seasonal aspects can be preserved by basing the model of wind capacity on recorded wind series as in [59] but this ignores the stochastic elements. Also there are concerns around basing the model on a single year of data as this can lead to unrepresentative results.

It was required to develop a method that would be capable of modelling the three important characteristics of wind series namely, the long term probabilistic wind speed and the shorter term periodic and stochastic elements. Also when expanding the model to include wind series for different areas, the correlations that occurs between the different locations were also taken into account. This model is able to combine the stochastic and periodic elements of a wind regime to form hourly predictions in a way that results in the long-term probability being preserved.

This modelling method was applied to the Irish system using data from six Met Eireann weather stations. Various statistical parameters of this data were investigated including the annual variation from the overall mean, calculation of a seasonality indicator, the relative variability and the strength of the cross correlation that exist between the six sites. Also the periodicity in the data was investigated using both auto-correlation analysis and the Fourier transform. From this analysis the effect of the diurnal and synoptic patterns on the frequency spectrum was observed. The presence and consistency of the diurnal pattern were further shown when recorded wind power series from six Airtricity wind farms were examined to confirm that this pattern was present in wind farm production data.

The modelling method was developed which allows for the generation of simulated wind series based on observed data. This method involves the normalisation of the recorded series and the separation of the periodic and stochastic elements of the normalised series. A number of approaches were developed for the calculation of the periodic elements of the wind series and the performance of each was investigated. The use of time series modelling of the stochastic elements of the normalised series was investigated. The result of which was a time series modelling method that once fitted to a series would allow for the generation of  $n$  iterations of the original series. By reversing the separation and denormalisation process the time series model can form the basis for generating multiple simulated wind series. The simulated wind speed series that were generated when this modelling method was applied to the six Met Eireann wind speed records show good agreement with the original series. Comparisons were drawn in terms of mean and variance measured over different time scales and also in terms of the probability distribution. A method has been developed to enforce the correlation coefficient matrix found in the data on to the simulated data. The results of applying this method have been shown to reflect well both the long-term averages and the inter-annual variations found in the recorded data

To convert the simulated wind speed series to a power series, a multi-turbine approach was implemented. This method attempts to account for the memory effect of wind speeds across a region by applying a moving average filter to the wind speed series. The length of the window is determined from the mean wind speed and the size of the region under consideration. Also the effect of the spatial wind speed distribution is included into the method by combining a typical single wind turbine characteristic with a normal distribution, the parameters of which are dependent on the terrain type and size of the region. In order to apply this method, four regions in Ireland to which the wind speed series are being applied were defined. These regions were also used to define the proportion of the projected wind capacity that should be associated to each of the Met Eireann sites. In this way  $n$  series of hourly wind power estimates for the generation system were calculated.

These  $n$  years of simulated power series can be then applied to a Monte Carlo calculation where each year of data is used to calculate LOLE under those specific conditions. The repetition of this process over  $n$  years results in the mean results from



the calculation converging to the most probable outcome. The developed model has been applied to the calculation of adequacy assessment indices in the Irish system. The results from this process show that imposing the correlation relationship that exists between wind capacity sites on to the model lead to in a reduction in the impact of wind capacity on the system adequacy. Also the model has been applied to allow for an investigation of the degree of variance that can arise in LOLE values calculated on the basis of single year of wind speed records. Results from this investigation have shown that using a single year of wind speed records can result in a wide range of calculated values, however the Monte Carlo calculation using multiple years of wind speed estimates will tend to the most probable result.

## **8.2 FUTURE WORK**

The methods that have been developed for both the conventional generation and wind capacity are constrained by the information that is available. If more detailed data was available then it would be possible to represent the operation of the system more accurately. For example if the probability of failure on start-up of the peaking units was known then it would be possible to differentiate between the operation of base and peaking capacity. Likewise the current implementation of the wind capacity model assigns the wind capacity for each region to one or two of the available wind records. While the multi-turbine method for converting from wind speed to wind power series attempts to correct for applying a single wind series to a region this type of approximation will lead to some error. This aspect could be analysed if wind speed data from the wind capacity sites were available as it could be easily incorporated into the model. Also as, off-shore wind farms are currently an area of increasing interest, an important area of future work would be to investigate the extent to which the impact of these off-shore farms on the adequacy of the generation system differs from the impact of on-shore wind farms.

**REFERENCES**

- [1.] Billinton, R. and L. Gan, "*Use of Monte Carlo Simulation In Teaching Generating Adequacy Assessment*". IEEE Transactions on Power Systems, 1991. 6(4): p. 1571-1577.
- [2.] Lyman, W.J., "*Fundamental Considerations in Preparing Master System Plan*". Electrical World, 1933. 101(24): p. 788-792.
- [3.] Benner, P.E., "*The use of the Theory of Probability to Determine Spare Capacity*". General Electric Review, 1934. 37(7): p. 345-348.
- [4.] Seelye, H.P., "*Outage Expectancy as a basis for Generator Reserve*". AIEE Transactions, 1947. 66: p. 1483-88.
- [5.] Lyman, W.J., "*Calculating Probability of Generating Capacity Outages*". AIEE Transactions, 1947. 66: p. 1471-1477.
- [6.] Calabrese, G., "*Generating Reserve Capacity Determined by the Probability Method*". AIEE Transactions, 1947. 66: p. 1439-1450.
- [7.] Loane, E.S. and C.W. Watchorn, "*Probability Methods Applied to Generator Capacity Problems of a Combined Hydro and Steam System*". AIEE Transactions, 1947. 66: p. 1645-1654.
- [8.] Halperin, H. and H.A. Alder, "*Determination of Reserve-Generating Capacity*". AIEE Transactions, 1947. 66: p. 530-544.
- [9.] Adler, H.A. and K.W. Miller, "*A new approach to Probability Problems in Electrical Engineering*". AIEE Transactions, 1946. 65: p. 630-632.
- [10.] Pitcher, W.J., et al., "*Generator Unit Size Study for the Dayton Power and Light Company*". AIEE Transactions, 1958. 77: p. 515-520.
- [11.] Brennan, M.K., C.D. Galloway, and L.K. Kirchmayor, "*Digital Computer aids Economic-Probabilistic Study of Generation Systems I*". AIEE Transactions, 1958. 77: p. 564-571.
- [12.] Limmer, H.D., "*Determination of Reserve and Interconnection Requirements*". AIEE Transactions, 1958. 77: p. 544-550.
- [13.] Miller, A.L., "*Details of Outage Probability of Calculations*". AIEE Transactions, 1958. 77: p. 551-557.
- [14.] Kirst, C. and G.J. Thomas, "*Probability Calculations for Systems Generation Reserves*". AIEE Transactions, 1958. 77: p. 515-520.

- [15.] IEEE Subcommittee on the Application of Probability Methods, "*Bibliography on the application of probability methods in power systems evaluation 1971-1977*". IEEE Transaction on Power Apparatus and Systems, 1978. **PAS-97(6)**: p. 2235-2242.
- [16.] Billinton, R., et al., "*Bibliography on the application of probability methods in power systems evaluation 1987-1991*". IEEE Transaction on Power Systems, 1994. **9(1)**: p. 41-49.
- [17.] Billinton, R., et al., "*Bibliography on the application of probability methods in power systems evaluation 1992-1996*". IEEE Transaction on Power Systems, 1999. **14(1)**: p. 51-57.
- [18.] Billinton, R., M. Fotuhi-Firuzabad, and L. Bertling, "*Bibliography on the application of probability methods in power systems evaluation 1996-1999*". IEEE Transaction on Power Systems, 2001. **16(4)**: p. 595-602.
- [19.] Billinton, R. and A. Chowdhury, "*Incorporation of wind energy conversion systems in conventional generating capacity adequacy assessment*". IEE Proceedings-C, 1992. **139(1)**.
- [20.] Castro, R. and L. Ferreira, "*Comparison between Chronological and probabilistic methods to estimate wind power capacity credit*". IEEE Transactions on Power Systems, 2001 Nov. **16(4)**.
- [21.] Billinton, R. and H. Chen, "*Assessment of risk-based capacity benefit factors associated with WECS*". IEEE Transactions on Power Systems, 1998. **13(9)**.
- [22.] Billinton, R. and H. Chen, "*Effect of Wind Turbine Parameters on the Capacity Adequacy of Generating Systems using Wind Energy*". Conference on Communication, Power and Computing WESCANEX'97 Proceedings, 1997: p. 47-52.
- [23.] Billinton, R. and G. Bai, "*Adequacy of Generation Systems Including Wind Energy*". Proceedings of the 2002 IEEE Canada Conference On Electrical & Computer Engineering, 2002.
- [24.] Milligan, M., "*Measuring wind plant capacity value*". National Renewable Energy Laboratory, Colorado, 1996.
- [25.] Milligan, M., "*Sliding Window Technique for Calculating System LOLP Contributions of Wind Power Plants*". National Renewable Energy Laboratory, Colorado, 2001.

- [26.] Milligan, M., "*Alternative wind power modelling methods using chronological and load duration curve production cost models*". National Renewable Energy Laboratory, Colorado, 1996.
- [27.] Milligan, M., C.K. Pang, and G. Tam, "*Alternative methods of modelling wind generation using production costs*". National Renewable Energy Laboratory, Colorado, 1996.
- [28.] Milligan, M., "*Variance estimates of wind plant capacity credit*". National Renewable Energy Laboratory, Colorado, 1996.
- [29.] Milligan, M., "*Wind Plant Capacity Credit Variations A Comparison of Results Using Multiyear Actual and Simulated Wind-Speed Data*". National Renewable Energy Laboratory, Colorado, 1997.
- [30.] Milligan, M. and M. Graham, "*An enumerative technique for modelling wind power variations in production costing*". National Renewable Energy Laboratory, Colorado, 1997.
- [31.] Milligan, M. and M.S. Graham, "*An enumerated probabilistic simulation technique and case study*". National Renewable Energy Laboratory, Colorado, 1996.
- [32.] Milligan, M., "*A comparison and case study of capacity credit algorithms for intermittent generators*". National Renewable Energy Laboratory, Colorado, 1997.
- [33.] Billinton, R., H. Chen, and R. Ghajar, "*Time-Series Models for Reliability Evaluation of Power Systems including Wind Energy*". *Microelectronic Reliability*, 1996. **36(9)**: p. 1253-1261.
- [34.] Milligan, M., "*Alternative Wind Power Modelling Methods Using Chronological and Load Duration Curve Production Cost Models*". National Renewable Energy Laboratory: Colorado., 1996.
- [35.] Billinton, R. and L. Gan, "*Use of Monte Carlo Simulation in Teaching Generating Capacity Adequacy Assessment*". *IEEE Transactions on Power Systems*, 1991. **6(4)**.
- [36.] Morrow, D. and G. L., "*Comparison of the Methods for Building a Capacity Model for Generating Capacity Studies*". *Communications, Computers and Power in the Modern Environment*. 1993. Canada: IEEE Conference Proceeding., 1993.

- [37.] Bhavarju, M.M., "*An Analysis of Generating Capacity Reserve Requirements*". IEEE Transactions on Power Apparatus and Systems,, 1997( PAS-93).
- [38.] Stremel, J.P. and N.S. Rau, "*The Cumulant Method of Calculating LOLP*". IEEE-PES Summer Meeting, 1979.
- [39.] Mazumdar, M., Gaver D.P. "*A Comparison of Algorithms for Computing Power Generating Systems Reliability Indices*". IEEE Transactions on Power Apparatus and Systems, 1984. **PAS-103(1)**: p. pp. 92-99.
- [40.] Allen, R.N., "*Discrete Convolution in Power System Reliability*". IEEE Transactions on Reliability of Power Supply Systems, 1981. **R-30(5)**: p. pp. 452-456.
- [41.] Sutant, D., H.R. Outhred, and Y.B. Lee, "*Probabilistic Power System Production Cost and Reliability Calculation by the Z-transform Method*". IEEE Transactions on Energy Conversion, 1989. **4(4)**: p. pp. 559-566.
- [42.] IEEE Reliability Test System Task Force, "*IEEE Reliability Test System*". IEEE Transactions on Power Apparatus and Systems, 1979. **PAS-98(6)**: p. pp. 2047-2054.
- [43.] Basaru, U. and H. Kurban., "*The Strategy for the Maintenance Scheduling of Generation Units*". Proceedings of Power Engineering, 2003 Large Engineering Systems Conference, 2003.
- [44.] Khatib, H., "*Maintenance Scheduling of Generating Facilities*". IEEE Transactions on Power Apparatus and Systems,, 1979. **PAS-98(5)**.
- [45.] Ghajar, R., R. Billinton, and H. Chen, "*A Sequential Simulation Technique for Adequacy Evaluation of Generation Systems*". IEEE Transactions on Energy Conversion, 1988. **11(4)**: p. pp. 728-734.
- [46.] Eirgrid (Transmission System Operator), "*Generation adequacy report 2005-2011*". 2004.
- [47.] Department for Communications Marine and Natural Resources, "*All-Island Energy Market Development Framework*". 2004.
- [48.] Billinton, R. and R.N. Allan, "*Reliability Evaluation of Power Systems*". 1984, New York: Plenum Press.
- [49.] Eirgrid (Transmission System Operator), "*Generation adequacy report 2004-2010*". 2003.

- [50.] IEEE Reliability Test System Task Force, "*IEEE Reliability Test System*". IEEE Transactions on Power Apparatus and Systems, 1979. PAS-98(6): p. 2047-2054.
- [51.] Ghajar, R., R. Billinton, and H. Chen, "*A Sequential Simulation Technique for Adequacy Evaluation of Generation Systems*". IEEE Transactions on Energy Conversion, 1988. 11(4): p. 728-734.
- [52.] Billinton, R. and L. Gan, "*Use of Monte Carlo Simulation in Teaching Generating Capacity Adequacy Assessment*". IEEE Transactions on Power Systems, 1991. 6(4).
- [53.] Milligan, M., "*Alternative Wind Power Modelling Methods Using Chronological and Load Duration Curve Production Cost Models*". 1996, National Renewable Energy Laboratory: Colorado.
- [54.] Jangamshetti, S.H. and V.G. Rau, "*Site Matching of Wind Turbine Generators: A Case Study*". IEEE Transactions on Energy Conversion, 1999. 14(4): p. 1537-1543.
- [55.] ESB National Grid, "*Impact of Wind Power Generation in Ireland on the Operation of Conventional Plant and the Economic Implications*". 2004.
- [56.] Coelingh, J.P., "*Geographical Dispersion of Wind Power Output in Ireland*". 1999, Irish Wind Energy Association.
- [57.] Chatfield, C., "*The Analysis of Time Series*". Fifth Edition ed. Texts in Statistical Science, ed. C. Chatfield and J.V. Zidek. 1997: Chapman and Hall.
- [58.] Feijoo, A.E., J. Cidras, and J.L.G. Dornelas, "*Wind Speed Simulation in Wind Farms for Steady-state Security Assessment of Electrical Power Systems*". IEEE Transactions on Energy Conversion, 1999. 14(4): p. pp. 1582-1588.
- [59.] Transmission System Operator Ireland, "*Generation Adequacy Report 2005-2011*". 2005.
- [60.] Billinton, R. and L.Gan, "*Wind Power Modelling And Application In Generating Adequacy Assessment*". IEEE Wescanex 93 Conference, 1993: p. pp. 100-106.
- [61.] Holttinen, H. "*A Multi-Turbine Power Curve Approach*". in *Nordic Wind Conference*. 2004. Chalmers University of Technology.

## 9 Appendix A UPEC Bristol 2004

### GENERATION ADEQUACY ASSESSMENT INCORPORATING WIND ENERGY CAPACITY

Michael F Conlon and William Carr

Dublin Institute of Technology

#### ABSTRACT

The assessment of generation adequacy in power networks which include high levels of intermittent generation capacity presents particular problems to power system planners and operators. In particular, networks with high levels of wind energy penetration require careful consideration. This paper deals with the generation adequacy assessment of the electrical network in the Republic of Ireland. In recent years, a significant level of wind generation has been added to, or is being planned for connection to the transmission and distribution networks in Ireland. The current installed wind capacity of 166MW is forecast to increase to 775MW within the next few years. This paper looks at the application of both the Loss of Load Expectation (LOLE) and Monte Carlo techniques to the generation adequacy assessment in the Irish system. The LOLE is calculated for a range of levels of wind generation capacity. The efficacy of the method of representing the wind generation as a negative load (load-modifier method) is considered. The greater flexibility in analysis of adequacy using a Monte Carlo approach is also demonstrated.

**Keywords: Generation Adequacy Assessment, Wind Energy, Reliability**

curves are formed by sorting the load by demand levels from high to low this may be done for a typical peak week and this week used to represent the whole peak period. Regardless of the load model applied in each time

#### INTRODUCTION

Estimates of the adequacy of the installed generation capacity in a power system are normally based on the calculation of the loss of load expectation (LOLE). The LOLE is a statistical measure of the likelihood of a failure of supply to match demand and is generally expressed in the number of hours that the available plant will be unable to match the load in a year [1]. The LOLE is calculated by the comparison of two models, the capacity model and the load model. There are a number of different methods for the generation of these models but in a typical calculation the capacity model will contain all the possible capacity outages in the system together with the probability of that outage level occurring. The load model can be one of two types, chronological models are based on forming a sequence of hourly load predictions for the whole year that occur in the model as they would be expected to be recorded or representative models also called load duration

period (typically an hour) the load model gives the level of capacity required by the system. The LOLE for that hour is given by the summation of probabilities that are associated with capacity outages that will lead to a capacity shortfall. Repeating this process for the duration of the load model gives the LOLE index for the system, which is typically expressed as hours/year.

The LOLE therefore attempts to calculate the expected number of hours that some degree of load shedding may be required but gives no indication of the extent to which this may be required. The loss of energy expectation (LOEE) resolves this problem. The LOEE is a similar index to the LOLE

and is formed in much the same way except that in each time period the LOEE is calculated as the summation of the capacity requirement minus the available capacity for each of the outage levels that would cause a capacity shortfall.

As a 100% reliable system is not feasible, or even possible, the results of the calculations described above are compared to an adequacy standard. These standards will vary from system to system and are generally developed on a basis of past experience. Failure to meet this standard suggests that corrective action may be needed, such as placing increased emphases on improvement of average unit availability, the development of additional capacity or by the modification of the load characteristics. The scale of any capacity development can be estimated by the peak carrying capability (PCC). This index is calculated by multiplying the load model by a scaling factor and repeating the LOLE calculation until it is within standard. The scaling factor is then multiplied by the original peak load capacity requirement. The difference between the PCC and the original peak load is an approximate value of the required addition capacity.

Wind capacity represents a particular challenge to include in LOLE calculations. Other energy limited resources should as hydro have been successfully included by the adaptation of the model framework described above [2] but the absence of any energy storage component and the high degree of variability in the source of energy has meant that, until relatively recently, wind capacity has been excluded from adequacy calculations. However, the continuing rapid growth in the use of this resource has necessitated the development of methods to investigate wind capacity impacts on system reliability. Currently in the Irish system the level of wind capacity is projected to grow to 411 MW before the end of 2004 [3]. This will represent a wind capacity penetration of approximately 7%. Under the targets set down in the EU directive on the promotion of the electricity from renewable energy [4], Ireland should by 2010 produce 13.2% of its gross electricity requirement from renewable sources. Given the extent of the wind resource that exists in Ireland and the relatively slow growth potential from other renewable sources, wind energy is expected to make up the bulk of this requirement. Current predictions estimate approximately 985 MW of wind capacity being required to meet this target, representing a wind capacity penetration of approximately 15% [3].

The only interconnection to the Irish system at transmission level is to Northern Ireland, having a transfer capacity of 300MW. This high level of isolation and the relatively small size of the Irish system have raised concerns over the costs associated with the integration of wind capacity for both the consumer, due to the cost for extra reserves being required, and for other producers in the system, due to increased number of start-ups, increased levels of ramping requirement and increased gas prices associated with CCGT units having reduced capacity factors and being irregularly loaded. This problem is compounded by the continuing deregulation, which makes future policy and trading arrangements less clear [4].

## ADEQUACY ASSESSMENT IN THE IRISH SUPPLY SYSTEM

In this section the approach taken in modelling the Irish that was take to allow the calculation of the adequacy indices is discussed. Initially wind capacity was excluded from the LOLE calculations so that the required modelling could be investigated without this complication. Two different methodologies of LOLE calculation where investigated, namely probabilistic or analytical methods and Monte Carlo methods. The analytical methods offer a computationally efficient way of calculating the LOLE for a given system while Monte Carlo methods involve a higher computational burden. The structure of the model is such that it allows for much more detailed analysis of the system's operation.

For the analytical method, the construction of the capacity and load models in the Irish system was based on the information contained in the Generation Adequacy Report [3]. This report is a public document, published by the transmission system operator (TSO) in the Republic of Ireland on an annual basis. It contains the TSO's predictions in terms of load and capacity growth and overall system availability over a seven-year period. The statement also details the existing capacity in term of individual unit capacities. The adequacy assessment predictions of the TSO over the period are outlined.

Taking in all cases the median prediction made by the TSO in the period 2004 – 2010 the total energy requirement is expected to grow from 25.1 to 31.9 (TWh) this represents an average year on year growth rate of 3.9% this accompanied by an expected growth in the peak demand from 4468 to



5589 (MW). The overall system availability is expected to improve over the period from 84.4% to 86.7% due to the replacement of older plant but concerns exist over the validity of this prediction as current system availability is well below expected levels.

In the construction of a capacity model, regardless of the method chosen, the individual unit scheduled maintenance requirement together with the individual units forced outage rates (FOR) are needed. These details were not published the GAR and would not be released by the TSO as they are considered to be commercially sensitive. Therefore it was necessary to assume a particular level for maintenance requirement for each unit and then to derive a FOR value based on the overall system availability figure the availability, maintenance and derived FOR values are shown in Table XXXX.

**Table 37: Applied system parameters**

Year	System Availability (%)	Maintenance Requirement (days)	Derived FOR (%)
2004	84.4	20	11
2005	84.4	20	11
2006	85	20	10.1
2007	86	20	9
2008	85	20	10.1
2009	86	20	9
2010	86.7	20	8.25

The maintenance requirement was scheduled on the basis of equalizing the level of reserve that would be in the system assuming that all the units were available over the whole year in this way as the system is winter peaking the majority of the maintenance was scheduled during the summer.

On the basis of these assumptions a capacity outage probability table was generated used the regression method [5]. A chronological load model was developed, based on the recorded hourly load values for the years 2000 to 2003 and the forecast load values. These load curves were normalised to the 2004 total energy requirement level and then for each of the years under investigation. Each of these load curves were scaled by the growth predicted by the TSO. Forecast load traces based on these four base years were used in the analysis so that the effect of load shape on LOLE levels could be determined.

Table 1 shows the results of this analysis for the period 2004 to 2010. Clearly these are some differences in the results for the load shapes based

on the different base years but these differences are relatively minor. Note that these results do not include the impact of forecast levels of wind generation on the system.

**Table 38: Results gained from the Irish system using analytical methods**

Year	Load '00	Load 01	Load '02	Load '03	Avg. LOLE
2004	12.4	13.5	16.0	14.4	14.1
2005	17.0	18.1	21.5	19.6	19.0
2006	26.0	27.8	32.5	30.3	29.1
2007	87.4	91.4	102.3	98.0	94.8
2008	296.5	304.9	318.8	314.6	308.6
2009	394.2	403.5	416.9	413.6	407.1
2010	564.5	574.6	584.9	582.4	576.6

In applying Monte Carlo techniques to the LOLE calculation, the load model was formed in the same manner as discussed above but the capacity model was generated by simulating the failure and repair cycle of each generation unit. To do this each generation unit was represented by a two state model comprised of an operating state and a forced outage state. The time spent in each state by each unit is such that the overall system availability will be as specified earlier. This was done by using the FOR that had been previously calculated and then by specifying a mean time to failure and mean repair times. [Did this allocation have any effect?]

Exponential probability distributions were used to represent the failure and repair times of each of the units in the Monte Carlo simulation. When this method is expanded to include all the units, the capacity of the system at any time is given by the summation of the units capacity that are in an operating state. To include scheduled maintenance into this calculation a third state is added and units were placed into and removed for this state as specified by the maintenance schedule [6].

On an hourly basis the available capacity is compared to the load level specified by the load model for that hour. When there is a shortfall in capacity the LOLE figure for that hour is incremented and in this way an annual LOLE figure is calculated. The LOEE is calculated in a

similar way except that the amount of capacity shortfall in each hour where there is a shortfall is recorded, the summation of these gives the annual LOEE estimate. For any year the results of these calculations will depend on the random draws that drive the capacity model. However, as the number of simulation years increases the mean of the individual years will tend to converge to the analytically calculated value. The results in Table 39 detail the results that were found from these calculations over a period from 2004 to 2010.

**Table 39: Results gained from the Irish system using Monte Carlo methods**

Year	Load '00	Load '01	Load '02	Load '03	Avg. LOLE
2004	12.2	12.8	16.7	14.0	13.9
2005	16.5	17.5	20.9	19.9	18.7
2006	23.3	29.0	31.6	32.3	29.1
2007	90.4	89.9	104.0	102.6	96.7
2008	300.1	309.7	316.3	313.5	309.9
2009	405.2	408.5	418.5	414.7	411.7
2010	569.5	573.1	584.7	589.1	579.1

Each iteration of the Monte Carlo calculation can be seen as one possible outcome from the year that is being modelled. The LOLE calculation calls for multiple iterations to be made depending on the level of convergence required. These iterations can be used to form a probability distribution of the calculated LOLE values. In Figure 74 data drawn for 2005 is shown both the probability distribution calculated directly from the data and an exponential distribution that was fitted to the data are shown. The exponential shape of the distribution is derived from the nature of the cumulative probability of the units in the system being on forced outage at any time i.e. the probability of a small amount of capacity being out will be high and this probability will decrease as the capacity on outage is increased. The ability to describe the LOLE as a distribution allows the calculation of a wider range of statistical data. Table 40 shows the results of these calculations applied to the distribution in Figure 74.

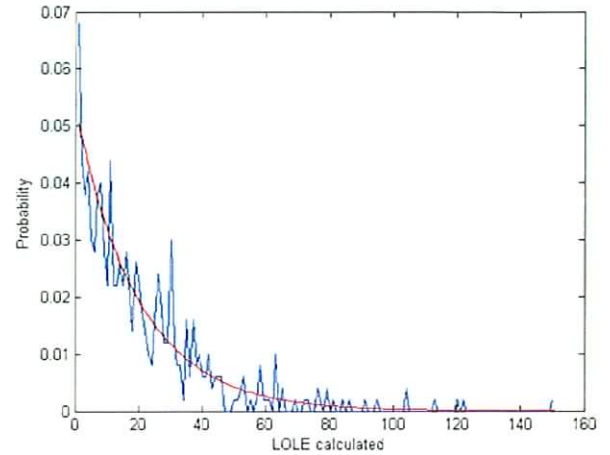


**Figure 74: LOLE probability distribution**

**Table 40: Statistics calculated of LOLE distribution**

Mean	19.7
95% C.I.	18.0
	21.5

### INCLUSION OF WIND CAPACITY IN ADEQUACY ASSESSMENT

Considerable work has been done in developing methods to include wind capacity in to LOLE calculation of adequacy. The most direct of these methods models wind capacity by considering the available wind capacity to be a single conventional lumped unit with an elevated level of FOR to account for both the forced outage and also for the probability of their being a lack of wind energy at a particular time i.e. the elevated FOR reflects the wind capacity's actual level of availability [typical reference]. The figure used for the elevated FOR is typically related to a calculated level capacity credit. The capacity credit is estimated in many different ways but one of the most straight forward and common methods is to approximate capacity credit to capacity factor, which is the ratio of average output to rated output [7]. An improvement to this technique is to represent the wind capacity as a multi-state unit. In this case the model is defined over  $n$  states. Each state describes a possible capacity level of the unit and the probability of the unit being in that state. In this way the possibility of the wind capacity operating at de-rated levels is accounted for in the LOLE calculation.

These models can be applied as either supply side units or as load modifiers. To include them as supply side models they are folded into the capacity model in the same way as conventional units. The ability to include them as load modifiers depends on the type of load model being used. If a load duration curve is being used, a wind capacity modified load duration curve can be determined by combining the original load duration curve with the capacity and probability of each state in the unit model the capacity and probability of each state in the unit model. If a chronological load curve is being used then these types of models are not applicable as load modifiers, but this type of load model does give the opportunity to include in the model some of the important chronological aspects associated with wind capacity e.g. the degree of correlation between fluctuations in the available wind capacity and the load level on a daily and seasonal basis.

The type of chronological wind capacity model used will depend on the information available. If only an estimate of the mean and variance of the wind series at a location is known then the wind can be modelled by the construction of a Weibull distribution on these parameters [8] and then taking random draws from the constructed distribution to form a hourly wind series. This series can be passed through the model of the wind turbine, which defines the relationship between wind speed and power output. If the mean and variance are known multiple sites then a distribution can be generated for each of them and the total capacity divided among them. While this process will capture the stochastic element that drives the wind capacity but it will ignore the chronological aspects mentioned earlier.

Current methods used in the assessment of adequacy in the Irish system use recorded power series from wind farms that are currently operating both onshore and offshore to form a combined power series that can be scaled to any level of wind capacity. This series is then applied as a load modifier to the load curve. The method has the advantages that as power series are being used the effects of forced outages and maintenance requirements do not need to be dealt with separately. Also the smoothing effects on the power series of spatial separation of wind turbines on

wind farms and the dispersed geographical location of wind farms are included in the model.

A contrast can be drawn between the last two types of model outlined. Each of these methods present ways to capture one of two important properties of wind, i.e. the first captures the stochastic elements while the second captures the periodic elements and preserves the chronological relationship to the load.

## RESULTS FOR THE IRISH SYSTEM

The results presented in this section attempt to highlight the degree to which the three wind capacity modelling methods described above compare. The results presented for the method employed by the TSO are garnered from the GAR 04-10, the specific assumptions made in calculating these results such as load and capacity growth and overall system availability where recreated in calculating results from the other wind modelling methods.

In applying the elevated FOR method a level of FOR had to be chosen that would be representative of the capacity factor of all the installed wind capacity to do the level suggested in [4] was applied. In this report power outputs from 18 existing on-shore farms were combined with offshore recorded wind series converted to power series in a 67% on-shore to 33% offshore split. The overall capacity factor was calculated to be 34.7%.

The application of the Weibull based load modifier method suggests that the mean and variance of the wind at different locations be known and that the parameters of the wind turbines used at these locations also be known. As this information was not available it was necessary to assume a set of generic wind turbine characteristics therefore values of 4, 12 and 20 m/s were chosen for cut in, rated and cut out wind speeds cut in and cut out speeds are half and double this value respectively. It was decided that in order to give a fair comparison of the methods the characteristics of the wind series used to drive the turbine model would be chosen so that the average capacity factor over a one year period would be 34.7% approx. therefore a mean wind speed of 8.15 m/s and a variance of 6 m/s were used

The calculations were made in two ways the first considered the wind capacity as a single lumped

unit and the second with the capacity split equally among ten units in this way the effect of dividing the capacity among increasing numbers of smaller units was investigated for both methods.

The results of these calculations are presented in Table 41 and plotted in Figure 75. It was felt that not all of the disparity between the calculated results and those found in the [4] are due to the wind model applied and that some of the approximations necessary to make the calculations cause differences, especially in the earlier years. But if the results from the GAR 04-10 are taken as a reference then both of the other methods initially underestimate the contribution from wind capacity but as the wind penetration increases through the years, so does the contribution attributed to wind capacity. It is clear then that these methods are unable to model the tendency of wind capacity's contribution to system adequacy to saturate as penetration increases [9].

Table 41: Results from different wind models

Year	Elevated FOR		Load Modifier		Results for [4]
	1 unit	10 units	1 unit	10 units	
2004	10.3	6.9	7.1	6.0	3.8
2005	14.2	6.8	7.4	5.2	2.7
2006	21.8	9.7	10.8	7.4	11.2
2007	70.1	39.7	34.2	23.7	72.1
2008	224.3	110.7	121.7	86.5	184.7
2009	295.5	138.9	151.5	106.2	322.9
2010	416.4	192.3	216.7	146.2	621.9

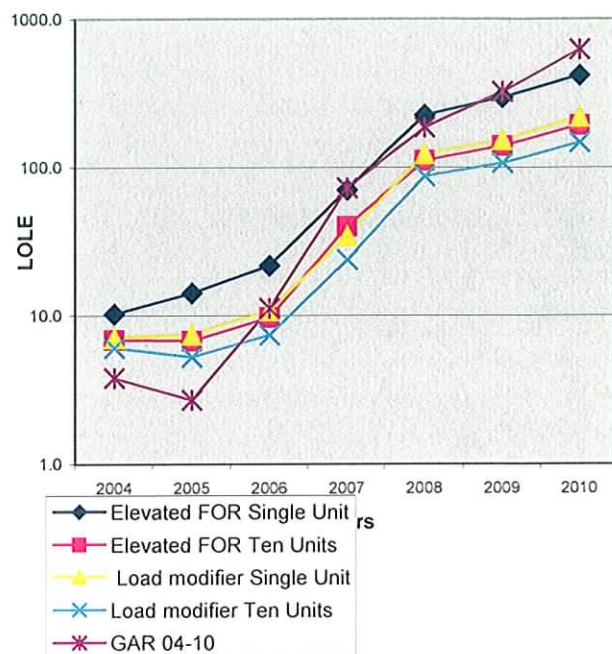


Figure 75: Plot of the result detailed in Table 3

### CONCLUSION

It has been possible by making some necessary assumptions to implement the models necessary to calculate the adequacy indices of the Irish system. This modelling has then allowed for the testing and comparison of different types of wind capacity models. It is clear that the wind modelling methods applied in this paper were not adequate to capture the full impact of wind capacity on the adequacy of a system, in order to do this it would be necessary to form a model that will combine the ability to capture both the stochastic and periodic elements of the wind resource. One way to attempt this would be to use combined power series formulated by the TSO to generate  $n$  years of simulated data that has the same statistical properties as the original. These  $n$  years of simulated power series are then applied to a Monte Carlo calculation where each year of data is used to calculate LOLE under specific conditions the repetition of this process over  $n$  years results in the mean results from the calculation converging to the most probable outcome. More rigorous still would be to model the wind series that drive the power series individually then scheduling maintenance and simulating forced outages as is done for conventional units, wind turbine models would be used to convert the wind series to power series

which could be summed and then applied as a load modifier to the LOLE calculation. While this work is outside of the scope of this paper they are considered as being areas of future work.

### REFERENCES

1. Billinton R., Allen R.N 'Reliability Evaluation of Power System' Plenum Publishing, 1996
2. Billinton R., Cheung L.C.H. 'Load modification: a unified approach for generating-capacity reliability evaluation and production-cost modelling' IEEE Proceeding, Vol. 134, Pt. C No. 4 July 1987
3. Transmission System Operator Ireland 'Generation adequacy report 2004-2010' Nov. 2003
4. Transmission System Operator Ireland 'Impact of Wind Power Generation in Ireland on the Operation of Conventional Plant and the Economic Implications' Feb. 2004
5. Morrow D., Gan L. "Comparison of methods for building a capacity model in generation capacity adequacy studies" Communications, Computers and Power in the Modern Environment.' Conference Proceedings IEEE, 1993
6. Billinton R., Gan L. 'Use of Monte Carlo Simulation in Teaching Generation Capacity Adequacy Assessment' IEEE Transactions on Power Systems Vol. 6 No.4 Nov. 1991
7. Milligan M.R. 'Measuring Wind Plant Capacity Value' NREL/TP-441-20493 Golden, Colorado: National Renewable Energy Laboratory 1996
8. Jangamshetti S. H., Rau Dr. V. G. 'Site Matching of Wind Turbine Generators: A Case Study' IEEE Transaction on Energy Conversion Vol. 14 No. 4 Dec 1999
9. Castro R. M. G. Ferreira L. A. 'A Comparison between Chronological and Probabilistic Methods to Estimate Wind Power Capacity Credit' IEEE Transactions on Power systems Vol. 16 No. 4 Nov. 2001

### AUTHOR'S ADDRESS

School of Control Systems and Electrical Engineering  
Dublin Institute of Technology,  
Kevin Street,  
Dublin 8,  
Ireland.  
william.carr1@student.dit.ie

## 10 Appendix B UPEC Cork 2005

### SIMULATION OF WIND SPEED RECORDS FOR USE IN GENERATION ADEQUACY ASSESSMENT CALCULATION

William Carr and Michael F Conlon

School of Control Systems and Electrical Engineering,  
Dublin Institute of Technology, Ireland

#### ABSTRACT

The incorporation of high levels of wind energy penetration into generation adequacy assessment calculations presents a set of unique challenges due to the variable nature of wind resources. In this paper a method of generating simulated wind series from a recorded wind series is presented. The recorded wind speed data is first normalised. Using the Fourier transform, the frequency content of the normalised data is analysed. The results of this analysis are used to split the normalised data into two time series. The first time series corresponds to strong frequency components that represent recurring periodicity in the data. The second time series corresponds to more stochastic elements in the data that are modeled using an auto-regressive moving average (ARMA) model. This method is applied to the generation of wind series based on recorded data from six weather stations in Ireland. The variation in the results of adequacy calculations for the Irish supply system is then investigated by means of a Monte Carlo simulation.

Keywords: Generation Adequacy, Wind Energy, Time Series Modelling

#### INTRODUCTION

The question of including wind capacity into generation adequacy assessment calculations has led to the development of a variety of different wind capacity models. The most direct of these methods represents the wind capacity by considering the available capacity to be a single conventional lumped generation unit with an elevated level of forced outage rate (FOR) to account for both forced outage and also for the probability of their being a lack of wind energy at a particular time, i.e. the elevated FOR reflects the wind capacity's actual level of availability. The value used for the elevated FOR is typically related to a calculated level of capacity credit. The capacity credit can be estimated in many different ways. One of the simplest methods is to equate capacity credit to

capacity factor (ratio of average output to rated output) [1].

An improvement to this technique is to represent the wind capacity as a multi-state unit [2] of  $n$  states. Each state describes a possible capacity level of the unit. The model defines the probability of the unit being in each state. In this way, the possibility of the wind capacity operating at a de-rated level is accounted for in any generation adequacy calculation. Both of these models consider wind capacity from a probabilistic perspective. However, these methods do not incorporate the important chronological aspects associated with wind capacity e.g. the degree of correlation between fluctuations in the available wind capacity and the load level on a daily and seasonal basis. If the adequacy assessment calculation being considered uses a chronological load curve, then the opportunity exists to include these chronological aspects of wind capacity behaviour also.

The type of chronological model used will depend on the information available. If only an estimate of the mean and variance of the wind series at a location is known then the wind can be modelled by the construction of an appropriate probability distribution (e.g. a Weibull

distribution). By taking random draws from the constructed distribution, an hourly wind series can be formed. This series can be applied to the capacity model of the wind turbine (which relates output power to wind speed) being investigated and hence a time series of power generation can be calculated. If the mean and variance are known for multiple sites, then a distribution can be generated for each site and the total capacity for all sites can be determined. An important feature of this method is that it will capture the stochastic nature of wind but it will ignore the chronological aspects mentioned earlier.

If a recorded wind series is available from a site, then a scalable power series can be generated by applying an appropriate turbine power/wind speed curve [3] and in this way all the chronological elements are preserved. However, any generation adequacy calculation based on this model will not take the stochastic nature of the wind into account. If wind series are available from a variety of locations, then this method can be expanded to include such data.

Both methods present ways to capture one of two important properties of wind i.e. the first captures the stochastic while the second preserves the chronological relationship to the load. In order to capture both properties, one method that has been suggested involves applying a sliding window technique [4,5] to the recorded time series. In this method, for every hour, a window of specified length is centred on the recorded value for that hour. An equivalent forced outage rate is generated which is given by:

$$FOR = 1 - \frac{E}{P_{Rated} \times D} \quad (1)$$

Where  $E$  is the total energy output recorded during the interval of the window,  $P_{Rated}$  is the rated output of the wind capacity and  $D$  is the duration of the window width. The equivalent forced outage rate based on the capacity level recorded for that hour is used in the generation of the capacity outage probability table. One extension to this technique is to allow the wind to be represented by the multi-state method. To do this, the sliding window is reformed into a relative frequency distribution where each state is represented by a row in the distribution, which contains a capacity level and a relative frequency that can be convolved into the capacity outage table.

The size of the sliding window used will have a large impact on the nature of the model. If the sliding window is reduced to a width of one time interval, then the results would be the same as the method based on a recorded wind series discussed earlier, while if the sliding window is extended to the length of the whole year then the results

would be same as directly convolving the wind capacity to the capacity outage probability table with a forced outage based on the capacity factor.

Another widely accepted method normalises a recorded wind series by subtracting the hourly mean values from it and dividing the result by hourly variance values [6]. The normalised data is then modelled by a time series model, such as an Auto-Regressive Moving Average (ARMA). The results drawn from the model are then denormalised to create a simulated wind series. An extension to this method has been developed that takes the Fast Fourier Transform (FFT) of the recorded wind series in order to identify the periodic elements in the data. Strong periodic elements are removed from the data using an averaging technique and the residual data is then modelled by an ARMA model. The results drawn from the model are then added to the periodic element to generate the simulated wind series [7]. The simulated wind series generated by these methods can be used to create power series as discussed above. Simulated power series can be generated which can then be applied to a Monte Carlo-based adequacy calculation where each year of data is used to calculate the loss of load expectation (LOLE) under specific conditions. The repetition of this process over multiple years results in the average results from the calculation converging to the most probable outcome [8,9]. This technique can be extended to data from a number of locations and, in doing this, another important property of wind capacity, which effects the generation system can be investigated. This property is the level of correlation between the site locations. A low degree of correlation between two sites means that the output levels of the two sites are rarely similar. Therefore if a series of locations are uncorrelated the impact of the variability seen at each of the site will be minimised from a system perspective, i.e. the net output from all locations will approach a mean value. The converse is true for highly correlated sites [10]. It is important that the method chosen to generate the simulation wind series preserves the correlative aspects of the wind series

## OUTLINE OF THE PURPOSED MODEL

The wind modelling method purposed is built on the assumption that wind can be characterised by its periodic and stochastic elements [11]. The implementation of this model is split into three sections. The objective of the first section is to normalise the mean and variance of the wind speeds in the data. The second splits the recorded wind series into periodic and stochastic elements. In the third section the stochastic elements are modelled using an ARMA model. This is then used to generate iterations of the modelled stochastic process, which in turn are recombined

with the periodic elements and then denormalised. The objective of this process is to form possible wind series that could occur at the site where the original is recorded. To illustrate the proposed method it will be applied to data taken from the Malin Head weather station in the Republic of Ireland. A data set for this site consisting of ten years of hourly wind speed records extending from November 1994 to October 2004 was used. A sample of the year of data is plotted in Figure 76.

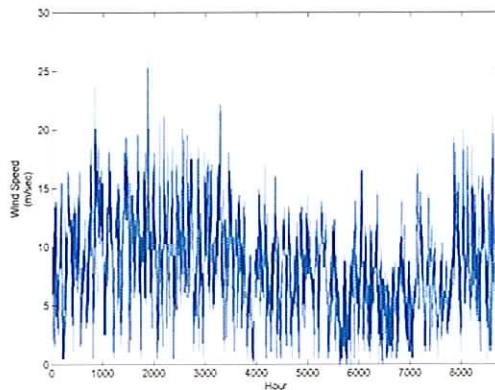


Figure 76: Malin Head data from Oct. '03 to Nov. '04

To implement the first section, the data is divided into weeks and the mean and variance of each of the sections is calculated. The normalised data of each section is found by subtracting the mean and dividing by the variance. Figure 77 shows the normalised version of the original data. The Fourier Transform of the normalised series is determined and a periodogram is calculated (the square of the modulus of the discrete Fourier transform). The dominant frequency components are highlighted by the periodogram and these correspond to strong periodic elements within the wind series. Figure 78 shows the periodogram of the sample data. From this plot it can be seen that there are clear peaks that correspond to diurnal and synoptic pattern as noted in [12]. It was found from analysis of the other years of data available that the diurnal peak is consistently present on a year on year basis while the synoptic peaks are also present in each year of data. However, the frequency at which they occur changes from year to year and for this reason the synoptic pattern found in one year could not be used as a basis for developing multiple simulated wind series.

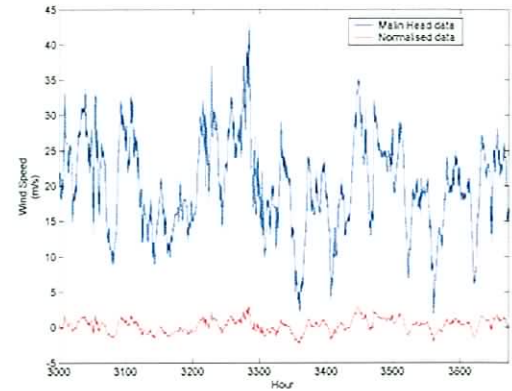


Figure 77: Comparison of original to normalised data

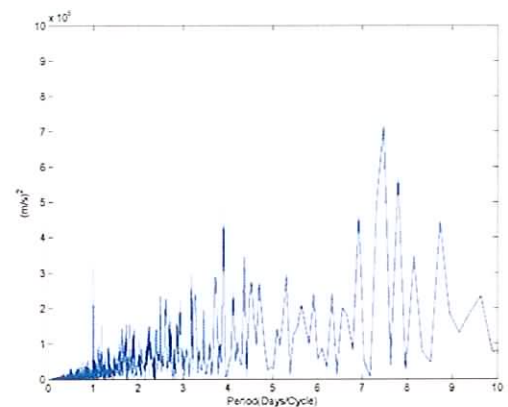
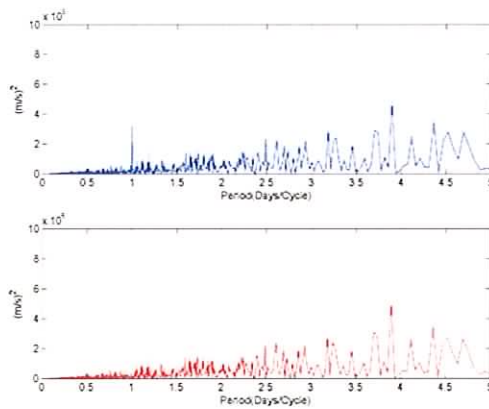


Figure 78: Periodogram of normalised data

The diurnal pattern can be removed by using the corresponding frequency to calculate the time interval equivalent to one period. A set of average values is then found in the wind series based on the derived time interval and this set of values is subtracted from the recorded series periodically. While this process has the effect of reducing the periodicity found at the target frequency, because the set of averages is based on the whole series length, the calculated average values are relatively small. To improve the performance, the series can be split into sections. The length of the sections was determined so that the number of sections and the number of periods of the target frequencies in each section are as similar as possible. For example the diurnal pattern results in approximately 19 sections with 19 periods per section. Each period is 24 samples long giving a total sample length of slightly less than



one year. The effect of this change is to increase the value of the averages being subtracted and so increases the level of reduction at the target frequency. The effect this has on the periodogram is shown Figure 79. It can be seen that the peak on the periodogram corresponding to the 24-hour/cycle interval has been reduced. At the end of this process the normalised version of the original series has been split into two sub-series, one containing the periodic element of the series relating to the diurnal pattern in the data and the second containing the more stochastic elements in the series.



**Figure 79: Contrast of periodogram before and after diurnal pattern is removed**

An ARMA time series model is applied to the stochastic series so that different iterations of the underlying process can be found. The form of an ARMA model is given in (2) below [13]. From this equation it can be seen that there are two components. The first set of terms is the weighted sum of the previous values and the second is the weighted sum of the current and previously drawn random values.

$$y(t) = a_1y(t-1) + a_2y(t-2) + \dots + a_ny(t-n) + z(t) - b_1z(t-1) - b_2z(t-2) - \dots - b_mz(t-m) \quad (2)$$

In (2), the order of the model is ARMA (n, m). The parameters  $a$  and  $b$  are the autoregressive and moving average parameters respectively and  $z$  are random draw numbers with zero mean and a specified variance. The process applied to fit the model is as described in [3]. This method uses the assumption that wind is a stationary stochastic process that defines the order of the model as being ARMA (n, n-1). By taking an initial value of  $n=2$ , a minimisation procedure is applied to derive the model parameters such that the residual

sum of squares will be a minimum. The value of  $n$  is incremented and process repeated, to investigate if increasing the order of the model has improved performance. The F-criterion statistical test is applied. This test is based on the Fisher-Snedecor distribution that tests whether two observed samples have the same variance [14]. If the test is passed, then the increase in order was warranted and the process is repeated. If not, then the improvement seen from the last iteration is not enough to warrant the added complication of increasing the order of the model. Therefore the model formed by the previous iteration is chosen. This procedure was applied to the series of stochastic elements derived above from the Malin Head data and the results of the ARMA model are given in (3). Figure 80 shows the stochastic series and a series generated from the ARMA model.

$$y(t) = 0.83607y(t-1) + 0.089018y(t-2) + z(t) - 0.0077328z(t-1) \quad (3)$$

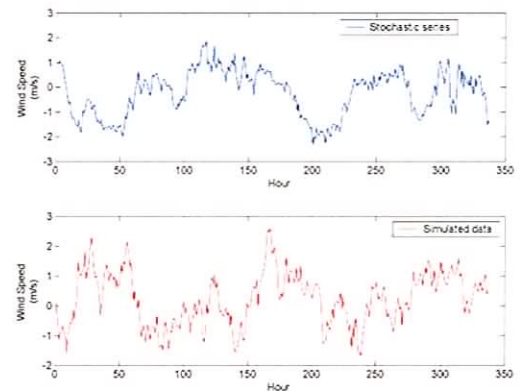


**Figure 80: Comparison of stochastic series to simulated data**

### APPLICATION OF MODEL TO GENERATION ADEQUACY CALCULATIONS

The model outlined above allows for the development of multiple years of simulated wind data for a single or multiple years of recorded data. Under ideal conditions, applying this model to generation adequacy calculations would use recorded wind series from each wind farm site in Ireland to form hourly estimates of the wind power. The generated wind speed estimates would then be converted to power estimates using turbine power/wind speed characteristics. However, a complete data set is not available. Rather, ten-year hourly wind records from six Met Eireann weather stations (Belmullet, Malin Head, Shannon, Clones, Knock and Valentia) are used. The records from Shannon, Clones, Knock

and Valentia were recorded at 10m while the record from Malin Head was recorded at 22m and the record from Belmullet was recorded at 12m. As the records are at heights below the normal hub height for a wind turbine, the data needed to be scaled. Currently in Ireland the typical mean wind speed required at an economically viable site is approximately 8.5 m/s. Therefore it was decided to scale all the data so that the mean wind speed matches this level. In order to relate an appropriate level of wind capacity to each of the records, the existing wind capacity was divided on a regional basis as shown in Figure 81.

**Table 42a: Breakdown to projected wind capacity on a regional basis (2004-2007)**

	Site	Year			
		'04	'05	'06	'07
North	Malin	65.1	214	235.3	245.2
South	Valentia	24.6	80.9	89.0	92.7
South	Shannon	24.6	80.9	89.0	92.7
West	Belmullet	43.8	144	158.2	164.9
West	Knock	43.8	144	158.2	164.9
East	Clones	28.0	92.1	101.3	105.5
	<b>Total</b>	<b>161.4</b>	<b>756</b>	<b>831.0</b>	<b>866.0</b>

**Table 1b: Breakdown to projected wind capacity on a regional basis (2008-2011)**

	Site	Year			
		2008	2009	2010	2011
North	Malin	255.4	265.6	275.8	286
South	Valentia	96.6	100.4	104.3	108.1
South	Shannon	96.6	100.4	104.3	108.1
West	Belmullet	171.8	178.6	185.5	192.3
West	Knock	171.8	178.6	185.5	192.3
East	Clones	109.9	114.3	118.7	123.1
	<b>Total</b>	<b>902</b>	<b>938</b>	<b>974</b>	<b>1010</b>

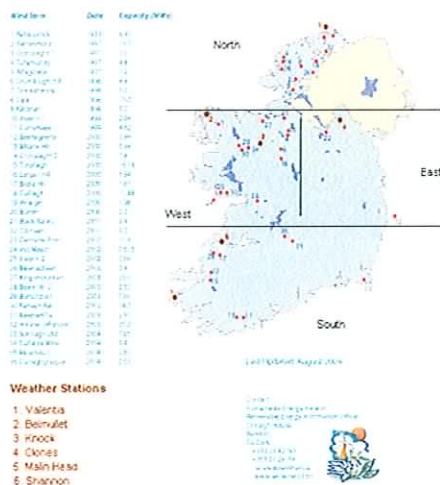


**Figure 81: Regional division of wind capacity (Image courtesy of SEI www.sei.ie)**

The breakdown in terms of the projected wind capacity that is associated with each of the records is detailed in Table 42. The projected levels of wind capacity are based on figures published by the Eirgrid (the Irish TSO) in the current Generation Adequacy Report [15] these figures are derived from committed wind projects and also from renewable energy production targets. With this application of the model in place, the adequacy assessment indices of the system could be calculated using the assumptions and methods developed in [16]. One of the first areas to be investigated was the effect of inter-annual variations on loss of load expectation (LOLE) based on a single year of wind data. To do this, several years of simulated wind energy estimates were generated. These estimates were applied to individual probabilistic LOLE calculations and the results recorded. This process is repeated using a Monte Carlo calculation such that for each year simulated in the Monte Carlo calculation, a different set of wind energy estimates are generated. The nature of this type of calculation results in the most likely level of LOLE. A study was carried out basis on the Irish generation system for the year 2005. The estimates used system parameters such as the total energy requirement, generation capacity and availability are based on the median levels predicted in [15]. Figure 82 shows the results for the Monte Carlo calculation where the result tends to converge to the expected value of LOLE as the number of simulation years increases. Figure 82 also shows the upper and lower bounds from the probabilistic calculation. As described above, each of these LOLE calculations are based on a single (but different) year of wind data. Whereas an LOLE value of 3 hours/year is calculated for the expected value (using the Monte Carlo method), the range of values for single year calculations is from 2.2 hours/year to 3.6 hours/year. Thus this result establishes

the range of expected LOLE values when one year of wind data is used.

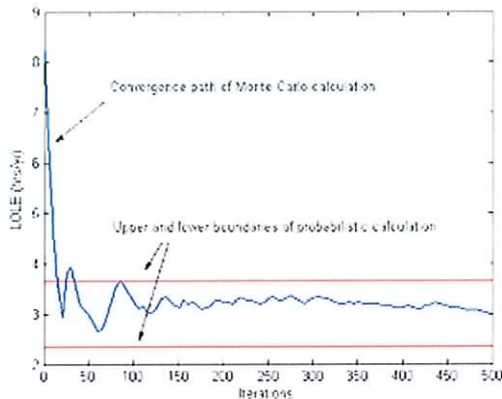


**Figure 82: Result of Monte Carlo and probabilistic calculation**

### CONCLUSION

A model has been developed that allows for the generation of multiple years of simulated wind speed data based on single or multiple year records. Using data from six weather stations in Ireland, this model has been applied to the calculation of adequacy assessment indices and allowed for an investigation of the degree of variance that can arise in LOLE values calculated on the basis of single year wind speed records. Future analysis will deal with an investigation of the validation of the data generated using the model described above. This will be carried out by comparison with source wind data using statistical indices and the typical auto- and cross-correlations measured. This validation will also be made by comparison of the generated power series to recorded wind power series from wind farms, using the statistical indices and typical auto and cross-correlation values.

### REFERENCES

1. Milligan M. "Measuring wind plant capacity" January 1996, National Renewable Energy Laboratory, Colorado U.S.A NREL/TP-441-20493
2. Billinton R, Cheung L.C.H. "Load modification: a unified approach for generation-capacity reliability evaluation and production-cost modelling" IEEE proceedings Volume: 134, Pt. C, No. 4, July 1987
3. Billinton R., Chowdhury A.A. "Incorporation of wind energy conversion systems in conventional generating capacity adequacy assessment" IEEE proceedings-C Volume: 139, No. 1, January 1992
4. Milligan M. "A chronological reliability model to assess operating reserve allocation to wind power plants" Proceedings of the 2001 European wind energy conference, July 2001, Copenhagen, Denmark. NREL/CP-500-30490.
5. Milligan M. A Sliding Window Technique for Calculating System LOLP Contributions of Wind Power Plants. Proceedings of the Wind Power 2001 Conference. 2001. Washington, D.C.: American Wind Energy Association. NREL/CP-500-30363.
6. Billinton R., Chen H., Ghajar R "Time series models for reliability evaluation of power systems including wind energy" Microelectronic Reliability Volume. 36 No. 9 pp 1253-1261
7. Kennedy S., Rogers P. "A Probabilistic Model for Simulating Long-Term Wind-Power Output" Wind engineering Volume: 27, No.3, 2003 Pages 167-181.
8. Billinton R., Chen H. "Assessment of risk-based capacity benefit factors associated with wind energy conversion systems" IEEE Transactions on Power Systems Volume: 13, No. 3 August 1998.
9. Billinton R., Gan L. "Use of Monte Carlo simulation in teaching generation capacity adequacy assessment" Transactions on Power Systems Volume: 6, No. 4, Nov. 1991
10. Milligan M., Artig R. "Reliability benefit of dispersed wind resource development" Proceeding of Wind Power '98 California U.S.A. 1998 NREL/CP-500-24314.
11. Kennedy S., Rodgers P. " A probabilistic model for simulating long term wind-power output" Wind Engineering Vol. 27, No.3, 2003
12. Eggleston E. D., Clark R. N. "Wind Speed Power Spectrum Analysis for Bushland Texas, USA" Wind Engineering. Vol. 24 No. 1 2000
13. Chatfield C. "The analysis of time series, an introduction" Fifth edition, Chapman and Hall
14. Billinton R., Chen H., Ghajar R. "Time-series models for reliability evaluation of power systems including wind energy" Microelectronics and reliability Vol. 36 No.9 Sept. 1996
15. Transmission System Operator Ireland ' Generation Adequacy Report 2004-2010' Nov. 2004
16. Conlon M., W. Carr "Generation adequacy assessment incorporating wind energy capacity" Proceeding of UPEC 2004 Vol. 2, pp 1014-1018

AUTHORS' ADDRESS

School of Control Systems and Electrical  
Engineering  
Dublin Institute of Technology,

Kevin Street,  
Dublin 8,  
Ireland.  
william.carr1@student.dit.ie

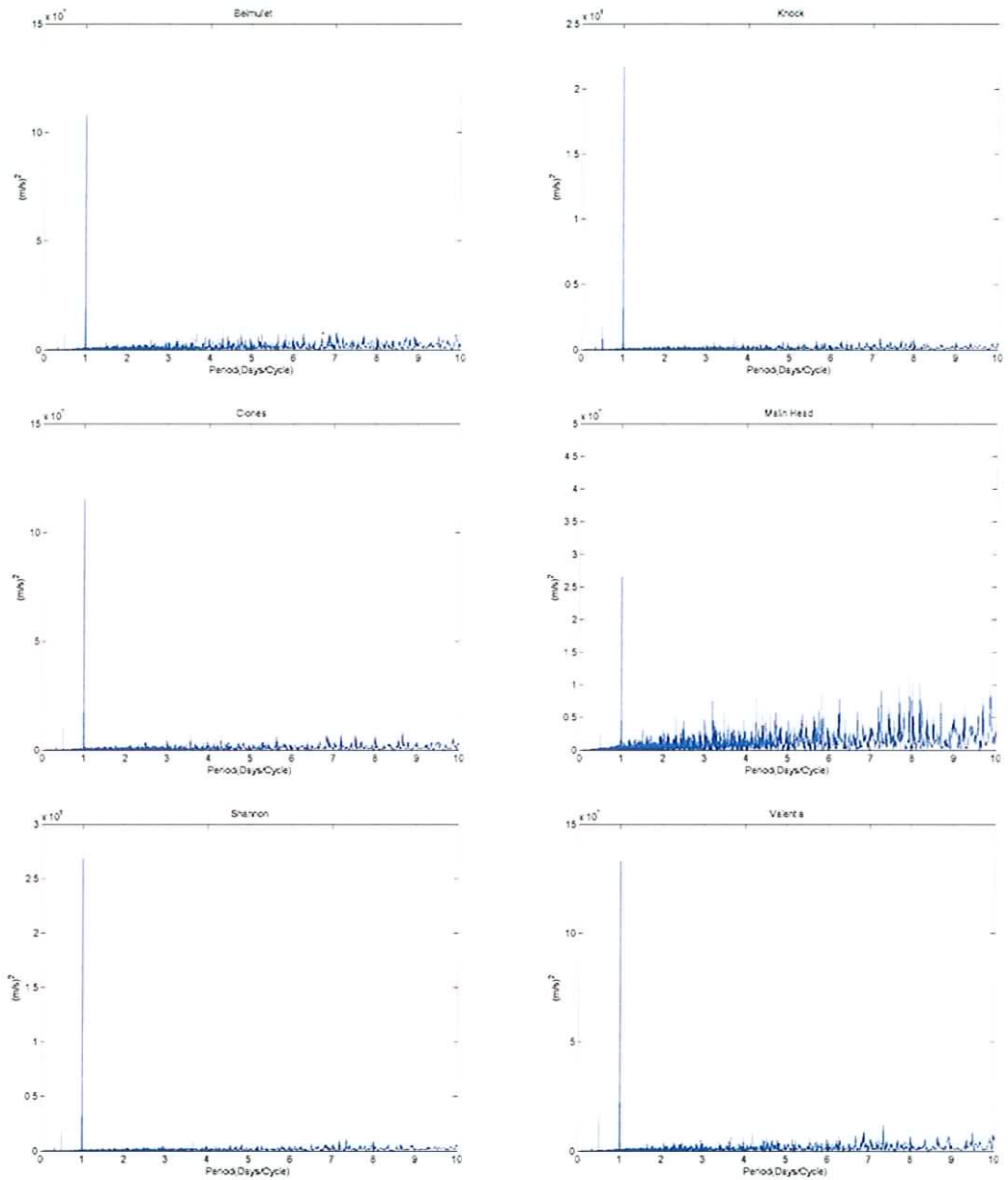
## 11 Appendix C: Generation Capacity Predictions 2005-

Station	Unit	Fuel Type	2005	2006	2007	2008
Moneypoint	MP1	Coal/HFO	287.5	287.5	287.5	282.5
	MP2	Coal/HFO	287.5	287.5	282.5	282.5
	MP3	Coal/HFO	287.5	282.5	282.5	282.5
Poolbeg	PB1	Gas/HFO	109.5	109.5	109.5	109.5
	PB2	Gas/HFO	109.5	109.5	109.5	109.5
	PB3	Gas/HFO	242	242	242	242
	PBC	Gas/HFO	460	460	460	460
Aghada	AD1	Gas	258	258	258	258
	AT1	Gas/DO	90	90	90	90
	AT2	Gas/DO	90	90	90	90
	AT4	Gas/DO	90	90	90	90
Aughinish Alumina	SK3	Gas/DO	75	75	75	75
	SK4	Gas/DO	75	75	75	75
Huntstown	HN0,HN1	Gas/DO	343	343	343	343
Huntstown 2	HN2, HN3	Gas/DO	0	0	400	400
Marina	MRT	Gas/DO	112	112	112	112
North Wall	NW4	Gas/DO	163	163	163	163
	NW5	Gas/DO	109	109	109	109
Tynagh	TY	Gas/DO	0	382	382	382
Dublin Bay	DB1	Gas	409	409	409	409
Great Island	GI1	HFO	54	54	54	54
	GI2	HFO	54	54	54	54
	GI3	HFO	108	108	108	108
Tarbert	TB1	HFO	54	54	54	54
	TB2	HFO	54	54	54	54
	TB3	HFO	241	241	241	241
	TB4	HFO	241	241	241	241
Bellacorrick	BK1	Peat	0	0	0	0
	BK2	Peat	0	0	0	0
Edenderry	ED1	Peat	118	118	118	118
Lough Ree Power	LR4	Peat	91	91	91	91
West Offaly Power	WO4	Peat	137	137	137	137
NIE Contract			0	0	0	0
Aghada PCP	AP5	DO	51	51	0	0
Tawnaghmore APC	TP1	DO	51	51	0	0
Rhode APC1	RP1	DO	51	51	0	0
Rhode APC2	RP2	DO	51	51	0	0
Ardnacrusha Hydro	AA 1-4	Hydo	89	89	89	89
Erne Hydro	ER 1-4	Hydo	65	65	65	65
Lee Hydro	LE 1-3	Hydo	27	27	27	27
Liffy Hydro	LE 1-4	Hydo	38	38	38	38
Turlough Hill	TH 1-4	Hydo	292	292	292	292
<b>Total Base</b>			<b>5464.5</b>	<b>5841.5</b>	<b>6032.5</b>	<b>6027.5</b>
Hydro			22	23	24	25
Biomass			28	32	36	40
CHP			152	162	172	182
SSG			9	9	9	9
<b>Total</b>			<b>5675.5</b>	<b>6067.5</b>	<b>6273.5</b>	<b>6283.5</b>
Renewable - Wind			756	831	866	902
<b>Total</b>			<b>6431.5</b>	<b>6898.5</b>	<b>7139.5</b>	<b>7185.5</b>

## APPENDICES

Station	Unit	Fuel Type	2009	2010	2011
<b>Moneypoint</b>	MP1	Coal/HFO	282.5	281.5	281.5
	MP2	Coal/HFO	282.5	281.5	281.5
	MP3	Coal/HFO	282.5	281.5	281.5
<b>Poolbeg</b>	PB1	Gas/HFO	109.5	109.5	109.5
	PB2	Gas/HFO	109.5	109.5	109.5
	PB3	Gas/HFO	242	242	242
	PBC	Gas/HFO	460	460	460
<b>Aghada</b>	AD1	Gas	258	258	258
	AT1	Gas/DO	90	90	90
	AT2	Gas/DO	90	90	90
	AT4	Gas/DO	90	90	90
<b>Aughinish Alumina</b>	SK3	Gas/DO	75	75	75
	SK4	Gas/DO	75	75	75
<b>Huntstown</b>	HN0,HN1	Gas/DO	343	343	343
<b>Huntstown 2</b>	HN2, HN3	Gas/DO	400	400	400
<b>Marina</b>	MRT	Gas/DO	112	112	112
<b>North Wall</b>	NW4	Gas/DO	163	163	163
	NW5	Gas/DO	109	109	109
<b>Tynagh</b>	TY	Gas/DO	382	382	382
<b>Dublin Bay</b>	DB1	Gas	409	409	409
<b>Great Island</b>	GI1	HFO	54	54	54
	GI2	HFO	54	54	54
	GI3	HFO	108	108	108
<b>Tarbert</b>	TB1	HFO	54	54	54
	TB2	HFO	54	54	54
	TB3	HFO	241	241	241
	TB4	HFO	241	241	241
<b>Bellacorrick</b>	BK1	Peat	0	0	0
	BK2	Peat	0	0	0
<b>Edenderry</b>	ED1	Peat	118	118	118
<b>Lough Ree Power</b>	LR4	Peat	91	91	91
<b>West Offaly Power</b>	WO4	Peat	137	137	137
<b>NIE Contract</b>			0	0	0
<b>Aghada PCP</b>	AP5	DO	0	0	0
<b>Tawnaghmore APC</b>	TP1	DO	0	0	0
<b>Rhode APC1</b>	RP1	DO	0	0	0
<b>Rhode APC2</b>	RP2	DO	0	0	0
<b>Ardnacrusha Hydro</b>	AA 1-4	Hydo	89	89	89
<b>Erne Hydro</b>	ER 1-4	Hydo	65	65	65
<b>Lee Hydro</b>	LE 1-3	Hydo	27	27	27
<b>Liffy Hydro</b>	LE 1-4	Hydo	38	38	38
<b>Turlough Hill</b>	TH 1-4	Hydo	292	292	292
<b>Total Base</b>			6027.5	6024.5	6024.5
<b>Hydro</b>			26	27	28
<b>Biomass</b>			44	48	52
<b>CHP</b>			192	202	212
<b>SSG</b>			9	9	9
<b>Total</b>			6298.5	6310.5	6325.5
<b>Renewable - Wind</b>			938	974	1010
<b>Total</b>			7236.5	7284.5	7335.5

## 12 Appendix D: Ten-Year Periodograms of Normalised Data



### 13 Appendix E: Fitted ARMA models

Given below are the ARMA models that were fitted to the normalised data from each of the six Met Eireann sites.

Belmullet  $\Rightarrow y(t) = 0.99333y(t-1) - 0.062605y(t-2) + z(t) - 0.11807z(t-1)$

Clones  $\Rightarrow y(t) = 1.3009y(t-1) - 0.35773y(t-2) + z(t) - 0.4992z(t-1)$

Knock  $\Rightarrow y(t) = 0.89452y(t-1) - 0.0095491y(t-2) + z(t) - 0.034579z(t-1)$

Malin Head  $\Rightarrow y(t) = 0.80254y(t-1) - 0.10389y(t-2) + z(t) - 0.064358z(t-1)$

Shannon  $\Rightarrow y(t) = 1.0309y(t-1) - 0.11418y(t-2) + z(t) - 0.202z(t-1)$

Valentia  $\Rightarrow y(t) = 0.86759y(t-1) - 0.055488y(t-2) + z(t) - 0.17157z(t-1)$